AD_____

# CHARACTERIZATION BY NMR AND FLUORESCENCE SPECTROSCOPY OF DIFFERENCES IN THE CONFORMATION OF NON-AGED AND AGED ORGANOPHOSPHORYL CONJUGATES OF AChE

Annual Summary Report

Y. ASHANI[1]
I. SILMAN[2]

September 1985

Supported by

U.S. Army Medical Research and Development Command
Fort Detrick, Frederick, Maryland 21701-5012

Grant No. DAMD17-83-G-9548

Israel Institure for Biological Research[1]
P.O.Box 19, Ness-Ziona
70450 ISRAEL

and

The Weizmann Institute of Science[2], Rehovot
76100 ISRAEL





The findings in this report are not to be construed as an official Department of the Army position unless so designated by other authorized documents.

# REPORT DOCUMENTATION PAGE

READ INSTRUCTIONS BEFORE COMPLETING FORM

| | |
|---|---|
| 1. REPORT NUMBER | 2. GOVT ACCESSION NO. / 3. RECIPIENT'S CATALOG NUMBER |
| 4. TITLE (and Subtitle): CHARACTERIZATION OF NMR AND FLUORESCENCE SPECTROSCOPY OF DIFFERENCES IN THE CONFORMATION OF NON-AGED AND AGED ORGANOPHOSPHORYL CONJUGATES OF AChE | 5. TYPE OF REPORT & PERIOD COVERED: Annual Summary Report<br>6. PERFORMING ORG. REPORT NUMBER |
| 7. AUTHOR(s): Y. Ashani and I. Silman | 8. CONTRACT OR GRANT NUMBER(s): DAMD17-83-G-9548 |
| 9. PERFORMING ORGANIZATION NAME AND ADDRESS: Israel Institute for Biological Research, P.O.B.19 Ness-Ziona 70450, Israel, and the Weizmann Inst. of Science, Rehovot 76100, Israel. | 10. PROGRAM ELEMENT, PROJECT, TASK AREA & WORK UNIT NUMBERS: 61102A<br>3M161102BS10<br>EM 477 |
| 11. CONTROLLING OFFICE NAME AND ADDRESS: US Army Medical Research and Development Command, Fort Detrick, Frederick, MD 21701-5012. | 12. REPORT DATE: September 85<br>13. NUMBER OF PAGES: 82 |
| 14. MONITORING AGENCY NAME & ADDRESS (if different from Controlling Office) | 15. SECURITY CLASS. (of this report): Unclassified<br>15a. DECLASSIFICATION/DOWNGRADING SCHEDULE |

16. DISTRIBUTION STATEMENT (of this Report)

Approved for public release; distribution unlimited

17. DISTRIBUTION STATEMENT (of the abstract entered in Block 20, if different from Report)

18. SUPPLEMENTARY NOTES

19. KEY WORDS (Continue on reverse side if necessary and identify by block number)

Organophosphate, Acetylcholinesterase, Chymotrypsin, Inhibition, Reactivation, Aging, $^{31}$P-nmr spectroscopy, Fluorescence spectroscopy, Pyrenebutyl label, Dansyl label, CPL.

20. ABSTRACT (Continue on reverse side if necessary and identify by block number)

The objective of this project is to detect and characterize, by nmr and fluorescence spectroscopy, differences in the conformation of non-aged and aged organophosphoryl (OP) conjugates of acetylcholinesterase (AChE) and α-chymotrypsin (α-Cht). Two series of novel fluorescent OP inhibitors were prepared, containing either pyrenebutyl or dansylaminoethyl moieties; these inhibitors were used to obtain homologous pairs of non-aged and aged phosphorylated conjugates of

DD FORM 1 JAN 73 1473 EDITION OF 1 NOV 65 IS OBSOLETE

SECURITY CLASSIFICATION OF THIS PAGE (When Data Entered)

AChE and α-Cht. The techniques employed to characterize these conjugates, and to detect differences between homologous aged and non-aged conjugates, included kinetic measurements of inhibition, reactivation, and aging, $^{31}$P-nmr spectroscopy, steady-state and time-resolved fluorescence spectroscopy, and circu-larly polarized luminescence (CPL). The main findings and principal conclusions are summarized below.

a. The same aged form of the OP-Cht conjugate is obtained, irrespective of the residue ($Cl^-$, p-nitrophenoxy, pinacolyl) which is removed from the phosphorus atom concomitantly with the aging process. In addition, we have preliminary evidence suggesting that when aging involves removal of an alkyl group, this process may be accompanied by alkylation of an adjacent amino acid residue. We have further established that the aged OP-Cht conjugate is formally a diester of phosphoric acid containing a P-$O^-$ bond.

b. In both the dansyl- and pyrene-OP conjugates of AChE and in the pyrene-OP conjugates of Cht, the orientation of the fluorophore with respect to the polypeptide is different in the aged conjugate from its orientation in the corresponding non-aged conjugate. The interaction of the dansyl moiety with the polypeptide chain of AChE is stronger in the aged than in the non-aged conjugate, as is the case for the aged and non-aged pyrene-containing α-Cht conjugates.

c. During the period of research covered by this report, two unexpected observations were made:

   1. In contrast to α-Cht, AChE was found to possess a second binding site (in addition to the catalytic site) for pyrenebutyl-OP inhibitors that also contain a pinacolyl substituent. Binding to this second site is non-covalent.

   2. Concentrated solutions of pyrenebutyl-OP-Cht conjugates (>0.1 mg/ml) form photo-dimers (excimers).

AD_____

# CHARACTERIZATION BY NMR AND FLUORESCENCE SPECTROSCOPY OF DIFFERENCES IN THE CONFORMATION OF NON-AGED AND AGED ORGANOPHOSPHORYL CONJUGATES OF AChE

Annual Summary Report

Y. ASHANI[1]
I. SILMAN[2]

September 1985

Supported by

U.S. Army Medical Research and Development Command
Fort Detrick, Frederick, Maryland 21701-5012

Grant No. DAMD17-83-G-9548

Israel Institure for Biological Research[1]
P.O.Box 19, Ness-Ziona
70450 ISRAEL

and

The Weizmann Institute of Science[2], Rehovot
76100 ISRAEL

## SUMMARY

The objective of this project is to detect and characterize, by nmr and fluorescence spectroscopy, differences in the conformation of non-aged and aged organophosphoryl (OP) conjugates of acetylcholinesterase (AChE) and α-chymotrypsin (α-Cht). Two series of novel fluorescent OP inhibitors were prepared, containing either pyrenebutyl or dansylaminoethyl moieties; these inhibitors were used to obtain homologous pairs of non-aged and aged phosphorylated conjugates of AChE and α-Cht. The techniques employed to characterize these conjugates, and to detect differences between homologous aged and non-aged conjugates, included kinetic measurements of inhibition, reactivation, and aging, $^{31}$P-nmr spectroscopy, steady-state and time-resolved fluorescence spectroscopy, and circularly polarized luminescence (CPL). The main findings and principal conclusions are summarized below.

a. The same aged form of the OP-Cht conjugate is obtained, irrespective of the residue ($Cl^-$, p-nitrophenoxy, pinacolyl) which is removed from the phosphorus atom concomitantly with the aging process. In addition, we have preliminary evidence suggesting that when aging involves removal of an alkyl group, this process may be accompanied by alkylation of an adjacent amino acid residue. We have further established that the aged OP-Cht conjugate is formally a diester of phosphoric acid containing a $P\text{-}O^-$ bond.

b. In both the dansyl- and pyrene-OP conjugates of AChE and in the pyrene-OP conjugates of Cht, the orientation of the fluorophore with respect to the polypeptide is different in the aged conjugate from its orientation in the corresponding non-aged conjugate. The interaction of the dansyl moiety with the polypeptide chain of AChE is stronger in the aged than in the non-aged conjugate, as is the case for the aged and non-aged pyrene-containing α-Cht conjugates.

c. During the period of research covered by this report, two unexpected observations were made:

   1. In contrast to α-Cht, AChE was found to possess a second binding site (in addition to the catalytic site) for pyrenebutyl-OP inhibitors that also contain a pinacolyl substituent. Binding to this second site is non-covalent.

   2. Concentrated solutions of pyrenebutyl-OP-Cht conjugates (>0.1 mg/ml) form photo-dimers (excimers).

FOREWORD

Citations of commercial organizations and trade names in this report do not constitute an official Department of the Army endorsement or approval of the products or services of these organizations.

This work has been conducted with the collaboration of J. Grunwald, E. Haas, Y. Segall, E. Shirin and N. Steinberg.

TABLE OF CONTENTS

## OBJECTIVES

### 1. General

The objective of this study is to detect and characterize, by nmr and fluorescence spectroscopy, differences in the conformation of non-aged and aged organophosphoryl (OP) conjugates of acetylcholinesterase (AChE) and α-chymotrypsin (α-Cht) which might help to explain the unexpected resistance of the aged forms to commonly used reactivators.

### 2. Studies with new pyrene- and dansyl-containing OP inhibitors.

In our first Annual Report (1), we described the preparation and characterization of non-aged and aged forms of α-Cht which were obtained by using pyrenebutyl-O-P(O)-$(OC_2H_5)F$ (PBEPF) and pyrenebutyl O-$P(O)Cl_2$ (PBPDC), respectively. We also used these two inhibitors to obtain the corresponding conjugates of AChE (2).

During the period covered by this report (September 1984-August 1985), we synthesized eight new OP fluorescent ligands containing either pyrenebutyl or dansylaminoethyl residues. The new fluorescent OP compounds were examined in the following studies:

a. Inhibition potency towards AChE and α-Cht.

b. Reactivation and aging of the corresponding phosphorylated enzymes.

c. Large-scale preparation of stoichiometric aged and non-aged fluorescent OP conjugates of AChE and Cht, followed by estimation of specificity of binding and stoichiometry.

d. Characterization of the new pyrene-containing OP conjugates of α-Cht by $^{31}P$-nmr spectroscopy.

e. Characterization of the new dansyl- and pyrene-containing OP conjugates of AChE and α-Cht by optical spectroscopy.

## BACKGROUND

Irrespective of the mechanism of aging, it is usually accepted that the common denominator in this process is the net loss of an alkyl or alkoxy group from the enzyme-bound OP moiety. This loss is depicted in Scheme I. This scheme implies that aging is associated with the introduction of a formal negative charge into the active site of the inhibited enzyme.

$$EH + XP(O)R(OR') \xrightarrow{-HX} \underset{\text{inhibited enzyme}}{E\text{-}P(O)R(OR')} \xrightarrow{-R'} \underset{\text{aged enzyme}}{E\text{-}P(O)R(O^-)}$$

where: R = alkyl, aryl, alkyloxy or aryloxy
R'= alkyl, aryl
X = $F^-$, $Cl^-$, p-nitrophenoxy, dialkylaminoethanethiol.

Scheme I

The observation that phosphoric ester dihalides of the general formula $(RO)POCl_2$ immediately produce a non-reactivatable enzyme (2,3) substantiates the hypothesis that aging involves formation of a negatively charged oxygen atom at the active site. Nevertheless, no direct evidence was reported, until the activation of this project in 1983, to confirm the presence of $P\text{-}O^-$ in the active site of the aged form of the OP conjugate of any serine hydrolase. Only recently, Van der Drift (4) demonstrated, by comparative $^{31}P$-nmr spectroscopy, the presence of $P\text{-}O^-$ in the aged conjugate of α-Cht which had been inhibited by diisopropylfluorophosphate (DFP).

In our proposal, we suggested studying the aging process in OP conjugates of α-Cht in parallel to OP conjugates of AChE, since α-Cht is a well-characterized enzyme whose sequence and 3-dimensional structure have been fully worked out. Furthermore, it is commercially available in highly purified form in large quantities, allowing preparation of OP-Cht conjugates at millimolar concentrations. This permits not only fluorescence studies but also $^{31}P$-nmr spectroscopy. Such data can thus be meaningfully correlated with the structural data, this approach, we hope, will lead to detailed understanding of the aging process at the molecular level.

In view of the above, it was envisaged that by performing $^{31}P$-nmr spectroscopy in parallel to fluorescence measurements of the same batch of the OP-Cht conjugates, we might achieve the following goals:

a. To substantiate the hypothesis that phosphoric acid derivatives of mono- (PBEPF) and dihalide (PBPDC) esters provide the corresponding non-aged and aged conjugates, respectively.

b. To permit a parallel study of OP conjugates of α-Cht and AChE with respect to the aging process, by employing the same alkyl halide phosphates for the inhibition of both enzymes.

c. To provide direct evidence concerning the nature of the substituents attached to the P atom in the non-aged and aged conjugates of α-Cht.

d. To provide evidence, by use of optical spectroscopic techniques, of putative conformational differences between aged and non-aged fluorescent OP conjugates of α-Cht, which might explain the resistance of the aged conjugates to reactivation.

e. To validate the applicability of the use of mono- and dihalide phosphates as a general preparative approach for the introduction of different fluorophores in or near the active site of non-aged and aged conjugates of AChE.

As stated in our first Annual Report (1), the $^{31}$P-nmr spectroscopy results along with the reactivation data strongly support the hypothesis that the aged form of phosphorylated α-Cht contains a P-O$^-$ bond. Thus the dihalide pyrenebutyl-O-P(O)$Cl_2$, is a suitable inhibitor for producing the aged inhibited conjugate. From the fluorescence spectroscopy data, it can be stated that the non-aged conjugate, pyrenebutyl-O-P(O) ($OC_2H_5$)Cht, differs in conformation from the aged form, pyrenebutyl-O-P(O)(OH)Cht. For the latter, the interaction of the fluorophore with the protein backbone appears to be stronger than for the non-aged species.

Fluorescent probes are used to investigate parameters such as environment, conformation, shape, rotational freedom and proximity of sites on macromolecules. In our studies, we decided to use pyrene as the fluorescent probe (see Table 1 for the detailed structures). This fluorophore has proved valuable because its excitation wavelength is well separated from the protein absorption band and because of its high quantum yield and its long radiative lifetime (5). In our comparative studies on aged and non-aged conjugates of AChE containing this fluorophore, we were able to take advantage of these properties in several ways:

a. We utilized fluorescence decay measurements to show that differences in relative quantum yield between aged and non-aged conjugates may be ascribed to dynamic quenching (2).

b. We were able, using time-resolved anisotropy, to show that there is little overall difference in the shape of the protein molecule in the aged and non-aged conjugates, although the peripheral site ligand propidium may induce shape changes in both conjugates (unpublished results).

c. Utilizing circularly polarized luminescence (CPL), we were able to clearly demonstrate a change in the environment of the pyrene in the active site of both aged and non-aged conjugates induced by propidium (6).

d. Using collisional quenching by external quenching agents, we were able to demonstrate reduced accessibility of the pyrene chromophore to an external quencher in the aged conjugates relative to the non-aged conjugates (2).

In view of the above, we initiated this project by utilizing the pyrene-containing ligands PBPDC and PBEPF to obtain the aged and non-aged forms of α-Cht, respectively (1). The pyrene moiety is, however, relatively insensitive to the polarity of its environment with respect to both its absorption and emission wavelengths. Indeed, in the pyrenebutyl OP-Cht (1) and OP-AChE (2) conjugates which we have studied so far, no difference was detected between the aged and non-aged conjugates with respect to their absorption and emission maxima. It seemed, worthwhile therefore, to expand this study to include an environmentally sensitive chromophore. One commonly used environmentally sensitive probe is the dansyl moiety. Indeed, Epstein et al. (7) have prepared a dansyl-containing organophosphonate and utilized it as a sensitive probe for ligand-induced conformational changes in Torpedo AChE.

The aged forms of either AChE (2) or α-Cht (1) which we studied initially were obtained by instantaneous aging resulting from the rapid hydrolysis of the second chlorine atom as depicted in Scheme II.

$$EH + \text{pyrenebutyl-O-P(O)Cl}_2 \longrightarrow \text{pyrenebutyl-O-P(O)(E)Cl}$$

$$\xrightarrow[\text{hydrolysis}]{\text{rapid}} \text{pyrenebutyl-O-P(O)(E)OH}$$

aged form

Scheme II

In order to establish whether a change in fluorescence or nmr spectra also parallels the dynamic aging (or dealkylation process), we proposed to prepare fluorescent OP ligands containing pinacolyl or p-nitrophenyl (pNP) groups. This rationale was based on the observation that both aryl and alkyl-contain-ing OP conjugates of either α-Cht or AChE undergo progressive aging by releasing phenol analogs (8,9,10) or losing an alkyl group (10). Thus, we hoped to compare aged conjugates, which were obtained from different non-aged forms by either gradual (Scheme I) or instantaneous (Scheme II) conversion of the non-aged conjugates, and thereby to substantiate the hypothesis that the same aged enzyme is obtained irrespective of the mechanism of aging.

In view of the above, and after establishing the principal experimental lines (1), we synthesized new series of fluorescent OP inhibitors (for structure details see Table 1) containing either the pyrene or dansyl moieties. Pinacolyl and pNP substituents were utilized for the gradual conversion of the non-aged form to the aged conjugate (dynamic aging). These ligands were used to prepare and study, by $^{31}$P-nmr and optical spectroscopy, differences between the aged and non-aged forms of OP conjugates of either AChE or α-Cht.

## TECHNICAL APPROACH

### 1. Preparation of fluorescent ligands

Table 1 lists the names and structures of the various OP ligands employed so far in this project.

Table 1: Structures and names of OP ligands

| Compound | Name | Chemical structure |
|---|---|---|
| 1 | Paraoxon | $(C_2H_5O)_2P(O)(pNP)$[a] |
| 2 | DEPC | $(C_2H_5O)_2P(O)Cl$ |
| 3 | DEPF | $(C_2H_5O)_2P(O)F$ |
| 4 | EPDC | $(C_2H_5O)P(O)Cl_2$ |
| 5 | DFP | $(isoPrO)_2P(O)F$ |
| 6 | PBEPF | Pyrenebutyl-O-P(O)$(OC_2H_5)F$[b] |
| 7 | PBEPC | Pyrenebutyl-O-P(O)$(OC_2H_5)Cl$ |
| 8 | PBPDC | Pyrenebutyl-O-P(O)$Cl_2$ |
| 9 | PB(pNP)PC | Pyrenebutyl-O-P(O)(pNP)Cl |
| 10 | PB$(pNP)_2$P | Pyrenebutyl-O-P(O)$(pNP)_2$ |
| 11 | PBPinPC[c] | Pyrenebutyl-O-P(O)(OPin)Cl |
| 12 | PBPinPF | Pyrenebutyl-O-P(O)(OPin)F |
| 13 | PBDEP | Pyrenebutyl-O-P(O)$(OC_2H_5)_2$ |
| 14 | DAEPF | Dansyl-$NHCH_2CH_2$-O-P(O)$(OC_2H_5)F$[d] |
| 15 | DPinPO | Dansyl-$NCH_2CH_2$-OP(O)(OPin) |
| 16 | DDEP | Dansyl-$NHCH_2CH_2$-O-P(O)$(OC_2H_5)_2$ |

a. pNP = 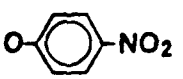

b. Pyrenebutyl = 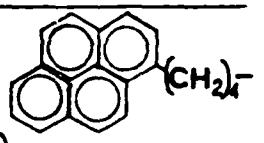

c. Pin = $-CH(CH_3)C(CH_3)_3$

d. Dansyl = 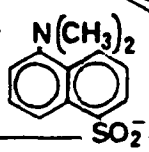

Compounds 1, 2, 4 and 5 were obtained from Aldrich Co. (2 and 4 were redistilled, whereas 1 and 5 were used as obtained). Compounds 3 and 6-8 were prepared according to procedures published by us (2). The fluorescent ligands 9-16 were prepared as described below:

The starting materials were purchased from Aldrich Corp. and purified either by distillation or recrystallization before use. The pNP containing fluorescent ligands were prepared according to the general synthesis route shown in Scheme III.

a. 1-pyrenebutanol + $(pNP)P(O)Cl_2$ → pyrenebutyl-O-P(O)(pNP)Cl

9, PB(pNP)PC

b. pyrenebutyl-O-$P(O)Cl_2$ + 2 pNP → pyrenebutyl-O-P(O)$(pNP)_2$

10, $PB(pNP)_2P$

where: pNP: 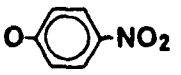 1-pyrenebutyl: 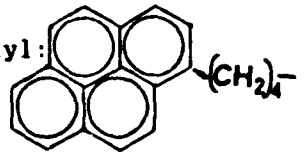

Scheme III

Pyrenebutyl (pNP) phosphorochloridate [9, PB(pNP)PC]

A cold solution (~3°C) of 1-pyrenebutanol (2) (2.3 g, 8.4 mmoles) in 10 ml dry dioxane was added dropwise to a stirred solution of $(pNP)P(O)Cl_2$ (2.15g, 8.4 mmoles) in 2 ml of cold dry dioxane. After 24 hrs, the solvent was evaporated under reduced pressure (25°C, 0.001 mm Hg) and the residue triturated with n-hexane. The insoluble material was removed by filtration. Yellow crystals (100 mg) were precipitated at 4°C (mp 98-99°C).

$^{31}P$-nmr (relative to $H_3PO_4$): $\delta$, -1.8 ppm ($C_6H_6$)
Mass spectrometry (EI): 493 ($M^+$,5%), 256 ($C_{20}H_{16}^+$, 100%), 215 ($C_{16}H_9CH_2^+$, 60%).

Pyrenebutyl bis (pNP) phosphate [10, $PB(pNP)_2P$]

A mixture of pyrenebutyl-O-$P(O)Cl_2$ (2) (3.9 g, 0.01 mole) and sodium p-nitrophenolate (4.83 g, 0.03 mole) was refluxed in 60 ml dry benzene for 2 hrs. Diethylether (100 ml) was added to the cooled mixture, followed by filtration and removal of the precipitate. A viscous red crude product was obtained after removal of the solvent under reduced pressure. The oil was redissolved in $CH_2Cl_2$, extracted twice with 10% aqueous NaOH (5°C), followed by stripping off the $CH_2Cl_2$ solution. Pure 10 was obtained as a viscous yellow oil.

$^{31}P$-nmr (relative to $H_3PO_4$): $\delta$, -13.40 ppm ($CH_2Cl_2$)

Mass spectrometry (EI): 596 ($M^+$, 8%), 340 [M-pyrenebutyl]$^+$, 15%), 256 ($C_{20}H_{16}^+$, 100%), 215 ($C_{16}H_9CH_2^+$, 60%)

Anal clcd. for $C_{32}H_{25}N_2O_8P$: C, 64.43; H, 4.19; N, 4.70
Found : C, 64.15; H, 4.22; N, 4.79

Pinacolyl-containing pyrenebutyl-OP ligands were prepared by the synthesis route depicted in Scheme IV:

$$\text{Pin-O-P(O)Cl}_2 + \text{pyrenebutanol} \rightarrow \underset{\underline{11},\ \underline{\text{PBPinPC}}}{\text{pyrenebutyl-O-P(O)(OPin)Cl}}$$

$$\underset{\underline{11}}{\text{PBPinPC}} + SbF_3 \rightarrow \underset{\underline{12},\ \underline{\text{PBPinPF}}}{\text{pyrenebutyl-O-P(O)(OPin)F}}$$

Scheme IV

Pyrenebutyl pinacolyl phosphorochloridate [11, PBPinPC]

A solution of pyrenebutanol (1.1 g, 4 mmole) and triethylamine (0.4 g, 4 mmole) in 4 ml dry dioxane was added dropwise to a stirred solution of pinacolyl phosphorodichloridate (2.3 g, 13.2 mmole) in 8 ml dioxane at room temperature. After 2 hrs, the reaction mixture was filtered and the solvent and excess of unreacted material were evaporated under reduced pressure (25°C, 0.001 mm Hg). The residue recrystallized from n-hexane to produce 1.2 g of pure 11 (mp 97-99°C).

$^{31}$P-nmr (relative to $H_3PO_4$): δ, 3.38; 3.25 ppm (dioxane) (diastereoisomers)

Mass spectrometry (EI): 456 ($M^+$, 28%), 256 ($C_{20}H_{16}^+$, 30%), 215 ($C_{16}H_9CH_2^+$, 100%)

Anal. Clcd. for $C_{26}H_{30}ClO_3P$: C, 68.42; H, 6.58, Cl, 7.68
Found: C, 68.70; H, 6.71; Cl, 7.60

Pyrenebutyl pinacolyl phosphorofluoridate [12, PBPinPF]

The foregoing chloridate 11 (0.5 g, 1.1 mmole) and dry $SbF_3$ (0.25 g, 1.4 mmole) were stirred for 12 days at room temperature in 10 ml of dry ether-$CH_2Cl_2$ (1:1). The solid was removed by centrifugation, and the solvent was then removed under reduced pressure. The residue was recrystallized from n-hexane to give 100 mg of 12 (mp 162-165°C).

$^{31}$P nmr (relative to $H_3PO_4$): δ,12.03 ($CH_2Cl_2$) (dd, diastereoisomers); $J_{P-F}$=974 HZ.

Mass spectrometry (EI): 440 ($M^+$, 10%), 256 ($C_{20}H_{16}^+$, 100%), 215 ($C_{16}H_9CH_2^+$, 100%).

Pyrenebutyl diethylphosphate [13, PBDEP]

O,O-Diethylphosphorochloridate (8.0 g, 47 mmole) in dry dioxane was added dropwise to a stirred solution of pyrenebutanol (5.8 g, 21 mmole) and triethylamine (4.74 g, 47 mmole) in 20 ml dioxane at room temperature. The mixture was stirred for 12 days. The precipitated solid was removed by filtration and dried under reduced pressure (25°C, 0.001 mm Hg).

The residue was redissolved in benzene and extracted with 10% aqueous NaOH at 5°C. After removal of benzene under reduced pressure, 13 was recrystallized from n-hexane at -70°C (mp 35-38°C).

$^{31}$P-nmr (relative to $H_3PO_4$): δ, -0.70 ($C_6H_6$).
Mass spectrometry (EI) : 410, ($M^+$, 25%), 256 ($C_{20}H_{16}^+$, 43%), 215 ($C_{16}H_9CH_2^+$, 100%).

The three dansyl-containing ligands 14-16 were prepared accordinge to Scheme V.

a. Dansyl$NHCH_2CH_2OH$ + $C_2H_5OP(O)F_2$ → dansyl-$NHCH_2CH_2O$-$P(O)(OC_2H_5)F$

14, DAEPF

b. Dansyl$NHCH_2CH_2OH$ + $PinOP(O)Cl_2$ → dansyl-$NCH_2CH_2$-$OP(O)(OPin)$

15, DPinPO

c. Dansyl$NHCH_2CH_2OH$ + $(C_2H_5O)_2P(O)Cl$ → dansyl-$NHCH_2CH_2$-$OP(O)(OC_2H_5)_2$

16, DDEP.

Dansyl: 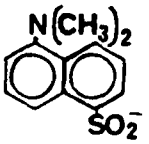


Pin: $-CH(CH_3)C(CH_3)_3$

Scheme V

Dansylaminoethyl ethyl phosphorofluoridate (14, DAEPF)

A mixture of dansylaminoethanol (11) (1.8 g, 6.2 mmole) and triethylamine (1.25 g, 12.4 mmole) in 10 ml dry $CH_2Cl_2$ was added dropwise to a stirred solution of ethyl difluorophosphate in 5 ml $CH_2Cl_2$ at -40°C. The temperature was raised to 12°C and stirring continued for 6 hrs at room temperature. After evaporating the volatile constituents under reduced pressure, the residue was eluted through a silica column with dioxane to provide 1.1 g of 14 as a yellow-green viscous oil.

$^1$H-nmr ($CDCl_3$, relative to TMS): δ, 7.80 ppm (6H, m), 5.87(1H, t, J = 6.3 Hz, NH), 4.12 (4H, m), 3.22 (2H, four lines; triplet after NH irradiation) 2.88 (6H, S), 1.33 (3H, d.triplet, $J_{P-H}$ = 0.9 Hz).

$^{31}$P-nmr (relative to $H_3PO_4$): δ, -9.51 ppm ($CDCl_3$) ($J_{P-F}$ = 983.5 Hz).

Mass spectrometry (EI): 404($M^+$, 20%), 384 [$(M-HF)^+$, 25%]
276 [(dansylaminoethyl-H)$^+$, 60%]

170 ( 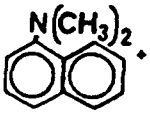 , 100%)

Anal. clcd. for $C_{16}H_{22}N_2O_5PF$: C, 47.52; H, 5.44
Found : C, 47.40; H, 5.62

1-N-Dansyl 2-pinacolyl-1,3,2-azaoxaphospholane 2-oxide [15, DPinPO]

A solution of dansylaminoethanol (11) (1.75 g, 6 mmole) and triethylamine (0.7 g, 7 mmole) in 6 ml dry dioxane was added dropwise to a solution of pinacolyldichlorophosphate (4.2 g, 19 mmole) in 3 ml dioxane. The mixture was stirred for 8 hrs at room temperature, the volatile constituents were removed under reduced pressure (30°C, 0.001 mm Hg), and the residue was dissolved in $CH_2Cl_2$. The dichloromethylene solution was chromatographed on a silica column (eluted with $CH_2Cl_2$) and the main fraction was collected and dried under reduced pressure. Compound 15 was obtained as yellow crystals (0.3 g, mp 150-160°C).

$^1$H-nmr ($CDCl_3$, relative to TMS): $\delta$, 7.90 ppm (6H, m), 4.65 (1H, m), 420 (2H, m), 3.68 (1H, m), 3.39 (1H, m), 2.88 (6H, s), 2.46 (3H, two doublets, diastereo-isomers), 1.04 (9H, two singlets).

$^{31}$P nmr (relative to $H_3PO_4$): $\delta$, 7.42 ppm (2 singlets, J = 8.3 Hz) ($CH_2Cl_2$)

Mass spectrometry (CI): 441(20%,$[M+1]^+$, 440 ($M^+$, 40.%),
356 [(M-pinacolyl)$^+$, 42%],
276 [(dansylaminoethyl-H)$^+$, 45%]

169 ( 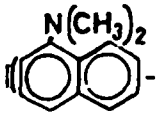 , 100%).

Dansyl diethylphosphate [16, DDEP]

Freshly distilled diethylchlorophosphate (5.2 g, 30 mmole) was added dropwise to a stirred solution of dansylaminoethanol (11) (4.4 g, 15 mmole) and triethylamine (3.0 g, 30 mmole) in 90 ml $CH_2Cl_2$ and the mixture was stirred at room temperature for 48 hrs. The precipitate was filtered off and the filtrate was evaporated to dryness under reduced pressure (25°C, 0.001 mm Hg). The residue was triturated with EtAc, filtered and evaporated under reduced pressure as above. Final purification was carried out by dissolving the residue in $C_6H_6$, followed by extraction of the organic phase with aqueous $Na_2CO_3$. The benzene was dried ($Na_2SO_4$) and evaporated to yield 3.2 g of 16 as a green oil.

$^{31}$P-nmr (relative to $H_3PO_4$): $\delta$, -1.50 ppm ($C_6H_6$.

Mass-spectrometry (EI):
430 ($M^+$, 12%), 276 [(dansylaminoethyl -H)$^+$, 18%],

169 [( 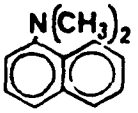 -H)$^+$, 100%]

2. Enzyme assays

AChE activity was assayed spectrophotometrically by the method of Ellman et al. (12) and α-Cht activity was monitored by the pH-stat procedure of Cunningham and Brown (13). Acetylthiocholine (0.5 mM) and N-acetyl-L-tyrosine ethyl ester (ATEE, 4 mM) were employed as substrates for AChE and α-Cht assays, respectively.

3. Enzyme source

a. AChE

The 11S form of AChE was purified from the electric organ of the electric eel according to a procedure developed in our laboratory (14). Two minor modifications were introduced: Tissue homogenization was carried out in half the original volume, i.e., 1.25 ml/gr, and the tryptic digestion time was shortened to 1 hr. The specific activity of the enzyme obtained was 5000-6000 units/$A_{280}$ under the assay conditions employed (0.5 mM acetylthiocholine iodide-0.33 mM dithiobis-nitrobenzoate [DTNB]-0.01% gelatine, 0.1 M Tris, pH 7, at 23°C).

b. α-Cht

3x crystallized and lyophilized type II (salt-free) α-Cht from bovine pancreas was purchased from Sigma Corp. Active-site concentrations of solutions of such α-Cht preparations were determined by use of cinnamoyl imidazole according to Schonbaum et al. (15). The concentrations found were 85% of the theoretical value, assuming a molecular weight of 25,000.

4. Preparation of OP-enzyme conjugates

a. AChE

The preparation of the OP-AChE conjugates was carried out in accordance with previously published procedures (2). Coupling of either PBPinPF (12) or PBPinPC (11) to AChE was accomplished by the addition of a 3.5-fold molar excess of inhibitor ($10^{-2}$ M in acetonitrile) to an AChE solution (~1 μM active-site concentration in 0.01 M phosphate buffer, pH 7.0, containing 0.1 M NaCl) at room temperature. The final

concentration of acetonitrile in the inhibition mixture was 1%. The inhibition of AChE activity was monitored by the Ellman procedure (12). When enzyme activity had been reduced to 10-40% of its original value, the conjugate was passed through a Bio-Gel P-4 column and was eluted in the void volume (monitored at 280 nm). The peak fraction was either dialyzed and used immediately or lyophilized and stored dessicated at -20°C. In the latter case, dialysis was carried out before use.

The dansyl conjugates obtained from DAEPF (14) and DPinPO (15) were prepared similarly except that the inhibitor was incubated in phosphate buffer (1:1, pH 7.0) for 1 min prior to its portionwise addition to the enzyme solution. This was done in order to ensure hydrolysis of P-Cl compounds which were apparently present as minor components (see Results and Discussion). The molar excess of the dansyl-OP inhibitor in the inhibition mixture was 7-fold.

In separate control experiments, AChE samples were first pre-incubated with non-fluorescent active-site-directed AChE inhibitors such as paraoxon (1) or DEPF (3) at ~2 μM for 10 min at 25°C. This treatment inhibited >99.5% of AChE activity. These control samples were then treated with the fluorescent OP inhibitor and gel-filtered as described above.

In order to verify the nature of the inhibited enzyme (whether aged or reactivatable), a solution of the OP-inhibited enzyme was diluted 100-fold into a buffer solution (0.01 M phosphate containing 0.1 M NaCl and 0.01% gelatine) either in the presence (induced reactivation) or absence (spontaneous reactivation) of 1 mM of the specific reactivator 1-methyl -2-hydroximinomethyl-pyridinium iodide (2-PAM) (10). Enzyme activity of these solutions was assayed at fixed intervals after the initiation of reactivation.

Table 2 lists the names and structures of the various OP-AChE conjugates used in this study:

Table 2: Structure of OP-AChE conjugates, RO-P(O)(R')-AChE

| Conjugate | Inhibitor[a] | R | R' | Status[b] |
|---|---|---|---|---|
| DEP-AChE | Paraoxon (1) | $C_2H_5$ | $OC_2H_5$ | Non-aged |
| DEP-AChE | DEPF (3) | $C_2H_5$ | $OC_2H_5$ | Non-aged |
| PBEP-AChE | PBEPC (7) | Pyrenebutyl[a] | $OC_2H_5$ | Non-aged |
| PBP-AChE | PBPDC (8) | Pyrenebutyl | OH | Aged |
| PBP-AChE | PBPinPF (12) | Pyrenebutyl | OH | Aged |
| PBP-AChE | PBPinPC (11) | Pyrenebutyl | OH | Aged |
| DAEP-AChE | DAEPF (14) | Dansyl$NHCH_2CH_2$[a] | $OC_2H_5$ | Non-aged[c] |
| DAP-AChE | DPinPO (15) | Dansyl$NHCH_2CH_2$ | OH | Aged |

a. See Table 1 for molecular structure.
b. Non-aged = reactivatable. Aged = not reactivatable.
c. A small fraction could not be reactivated

b. α-Cht.

Large quantities of the OP-Cht conjugate (200-400 mg per batch) were obtained by dropwise addition (over periods of 30-60 min) of a concentrated solution of either paraoxon (1), DEPC (2), DEPF (3), EPDC (4) or DFP (5) (0.01-0.1 M), in acetonitrile, to a stirred solution of 5-10 mg/ml α-Cht in double-distilled (dd) water at room temperature. A pH of 7.4 was maintained during the inhibition period by adjusting with a dilute NaOH solution. In the case of PBEPF (6), PBPDC (8), PB(pNP)PC (9), $PB(pNP)_2P$ (10) PBPinPC (11) and PBPinPF (12), inhibition was carried out in dilute solutions of both α-Cht (0.5-1 mg/ml) and the inhibitors (0.2-1 mM) because of the limited solubility of the pyrene OP ligands in water. The amount of organic solvent in the final inhibition medium did not exceed 10%. The decrease in activity was monitored until >90% and >98% of the initial enzyme activity were inhibited by the pyrene-containing OP ligands and the non-fluorescent inhibitors, respectively. Depending on the inhibitor employed, a 1.2-5 molar excess of inhibitor was required so as to produce the above-mentioned levels of inhibition over periods ranging between 1-4 hrs at room temperature, except for paraoxon, PB(pNP)PC and $PB(pNP)_2P$, for which 20 hrs at 4°C were required to complete inhibition.

The solution of the inhibited enzyme was then lyophilized, redissolved in 4 ml of double-distilled (dd) water and loaded onto a Sephadex G-10 column (60 x 2.5 cm). The column was

eluted with dd water at a flow rate of 1.5 ml/min. The main fractions (2 ml each) containing the protein (identified at 278 nm) were pooled and relyophilized. The dry OP-Cht conjugates were kept over dessicant at -22°C until used for either $^{31}$P-nmr or optical spectroscopy studies. Occasionally samples were dialyzed against either dd water or buffered solutions for 24 hrs at 4°C so as to remove traces of free or hydrolyzed ligands. For the optical spectroscopy measurements, the small residual activity of OP-Cht conjugates was completely inactivated by DFP followed by dialysis and lyophilization. Dialysis was carried out in dialysis tubes (flat width 10 mm, Thomas Scientific) with an MW cut-off of 12,000.

In control experiments, α-Cht was first preincubated with the specific nonfluorescent α-Cht active-site inhibitor DFP (5). This treatment inhibited >99.5% of α-Cht activity. These control samples were then treated with the fluorescent OP inhibitor, gel-filtered and lyophilized as described above.

Table 3 lists the names and structures of the various OP-Cht conjugates used in this study.

Table 3: Structure of OP-Cht conjugates, RO-P(O)R'-Cht

| | | RO-P(O)(R')-Cht | | |
|---|---|---|---|---|
| Conjugate | Inhibitor[a] | R | R' | Status[b] |
| DEP-Cht | Paraoxon (1) | $C_2H_5$ | $OC_2H_5$ | Non-aged |
| DEP-Cht | DEPF (3) | $C_2H_5$ | $OC_2H_5$ | Non-aged |
| EP-Cht | EPDC (4) | $C_2H_5$ | OH | Aged |
| DIP-Cht | DFP (5) | $CH(CH_3)_2$ | $OCH(CH_3)_2$ | Partially aged |
| PBEP-Cht | PBEPF (6) | Pyrenebutyl[a] | $OC_2H_5$ | Non-aged |
| PBP-Cht | PBPDC (8) | Pyrenebutyl | OH | Aged |
| PBP-Cht | PB(pNP)PC (9) | Pyrenebutyl | OH | Aged |
| PBP-Cht | $PB(pNP)_2P$ (10) | Pyrenebutyl | OH | Aged |
| PBPinP-Cht | PBPinPC (11) | Pyrenebutyl | OPin[a] | Partially aged |
| PBPinP-Cht | PBPinPF (12) | Pyrenebutyl | OPin | Partially aged |

a. See Table 1 for molecular structure.
b. Non-aged = reactivatable Aged = not reactivatable

5. Kinetics of inhibition

a. AChE

The kinetics of inhibition of AChE were measured according to the following procedure: To a 1 ml aliquot of enzyme solution (~5 x $10^{-10}$ M) in buffer solution (for details see Results and Discussion), was added 2-10 µl of a stock solution of the inhibitor in dioxane or acetonitrile to yield final concentrations as specified under Results and Discussion. At time intervals of 0.5-10 min, 10-50 µl of the inhibition mixture was diluted into a cuvette containing 3.2 ml of phosphate buffer (pH 7.0, 0.05 M) and assayed at 25°C as described before (12). The final concentration of the organic solvent in the inhibition mixture was 0.2-1%. Blanks were treated in the same manner, except that the inhibitor solution was replaced by the corresponding organic solvent.

b. α-Cht

I. Inhibition by PBEPF (6)

To 5 ml of α-Cht solution (~5 x $10^{-8}$ M) in 2 mM Tris buffer (pH 7.8, KCl 0.1 M, 25°C) placed in a thermostatted pH-stat titration cell was added 5-25 µl of a stock solution of the inhibitor (0.26 mM) in acetonitrile to give a final inhibitor concentration of 0.26-1.3 µM. At given time intervals, inhibition was terminated by adding 100 µl of substrate (ATEE, 100 mg/ml in dioxane) to produce a final ATEE concentration of 0.016 M.

A control experiment demonstrated that addition of 1.3 µM PBEPF to an α-Cht solution containing 0.016 M ATEE did not cause significant inhibition within the first 2 min. Residual α-Cht activity was measured immediately upon addition of the substrate by the pH-stat procedure mentioned above. Straight lines were obtained for the first 2 min. Blanks were treated in the same manner except that the inhibitor solution was replaced by pure acetonitrile for estimation of 100% α-Cht activity. Under the experimental conditions described above, ~90% of the enzyme was inhibited within 15 min. A separate evaluation of the reversible inhibition constant $K_I$ was carried out as follows: Varying amounts of pyrene-containing ligands were diluted 100-500fold from a stock solution in acetonitrile (~0.1 mM) into 5-10 ml of α-Cht (~0.01 µM) in 2 mM Tris buffer (pH 7.8, 0.1 M KCl, 25°C)

containing 1-8 mM ATEE. Enzyme activity was measured before and immediately after addition of the inhibitor. $K_I$ was calculated according to the Downs-Hunter equation as described elsewhere (10).

6. Kinetics of reactivation

a. AChE

Phosphorylated enzyme was produced by diluting 2-5 µl of a 0.01 M stock solution of the inhibitor in dioxane or acetonitrile into 0.2-0.5 ml of AChE (~0.1 µM) in either phosphate, Tris or carbonate buffer (0.05 M), followed by incubation for 1-30 hrs either in an ice-water bath or at 25°C (for specific details see Results and Discussion section). The reactivation process was initiated by diluting the inhibited enzyme 200-fold into the appropriate reactivation medium. At selected time intervals, 15-50 µl of the reactivation mixture was diluted into 3.2 ml of 0.05 M phosphate buffer (pH 7.0) and assayed as described before at 25°C. Blanks were treated in the same manner except that the inhibitor solution was replaced by the corresponding organic solvent.

b. α-Cht

For reactivation experiments, lyophilized samples of OP-Cht (93-98% inactivated as described above) were dissolved in dd water to yield solutions which were ca. 0.4 mM in catalytic sites. Aliquots of these solutions were diluted 100-fold into a reactivation medium (pH 7.0, 0.1 M Tris, 25°C) containing 0.1 M 3-PAM. At selected time intervals, 20 µl of the reactivation mixture was diluted into 5 ml of Tris buffer (2 mM, pH 7.4) and assayed as described before. Blanks were treated in the same manner except that the inhibited enzyme was replaced by native α-Cht. We note that 0.1 M 3-PAM partially stabilized native α-Cht solutions for periods of 48-72 hrs as compared to controls without 3-PAM.

7. Aging measurements

In order to define the extent of reactivatability of a given OP-enzyme conjugate prior to the $^{31}$P-nmr or fluorescence spectroscopy studies, the corresponding OP-AChE or OP-Cht preparation was incubated at 25°C in the presence of 1 mM 2-PAM or 0.1 M 3-PAM, respectively, for 16-96 hrs, followed by assay of enzyme activity. Blanks were treated in the same manner except that the OP-enzyme conjugate was replaced by an equal concentration of non-inhibited enzyme.

The pH-dependence of the aging reaction was monitored by 100-fold dilution of AChE, inhibited at pH 5-10 (0.05 M phosphate, Tris or carbonate), into 1 mM 2-PAM solution in 0.05 M phosphate buffer at pH 8 and followed by incubation at 25°C for 16 hrs and an assay of enzyme activity. Blanks were treated in the same manner, except that the inhibitor solution was replaced by the same amount of the pure organic solvent.

8. Release of p-nitrophenol

The release of pNP in reactions in which PB(pNP)PC (9) and $PB(pNP)_2P$ (10) were allowed to react with either α-Cht, phosphate buffer or alkali was measured spectrophotometrically at 400 nm. The amount of the liberated pNP was determined from a calibration curve constructed for p-nitrophenol under the same experimental conditions.

9. Hydrolysis of OP ligands

The rate of hydrolysis of the fluorescent OP ligands was determined either by following the rate of loss of their anti-cholinesterase (anti-ChE) activity as described before (17) or by monitoring the rate of release of p-nitrophe-nol as described above.

10. nmr Measurements

$^{31}P$-nmr spectroscopy at 101.3 MHz was performed with a Bruker WM250 spectrometer coupled to a Nicolet Aspect 2000 computer. Twenty to ninety-nine percent $D_2O$ in the same tube (10 mm diameter) served as an internal standard for field frequency locking. A power of 10 W was maintained for the continuous broadband heteronuclear proton decoupling so as to avoid internal build-up of heat. Throughout the run, the temperature was maintained at 23 ± 3°C. Spectral data were accumulated as the Fourier transform by application of 70° pulses with a spectral width of 16000 Hz. A delay time of 0.8 sec was utilized between accumulations.

All chemical shifts were recorded from the built-in absolute crystal frequency and assigned to the internal standard, N,N-hexamethylphosphorotriamidate (HMPA). The $^{31}P$-nmr spectra of the α-Cht conjugates and the model compounds were recorded in a concentration range of 1-4 mM, assuming MW = 25,000 for α-Cht. Five to 100 K scans were accumulated for each run.

11. Optical spectroscopy

Absorption spectra were recorded using a Cary 219 spectrophotometer. Fluorescence spectra were measured with a Perkin-Elmer MPF-44A fluorimeter.

Fluorescence decay measurements were performed with an instrument built at the Weizmann Institute which em-ploys the sampling technique (18). Decay curves were analyzed by the method of non-linear least squares (19), assuming fluorescence decay according to $I(t) = \Sigma_i \alpha_i e^{-t/\tau_i}$ where I(t) is the decay function and $\alpha_i$ and $\tau_i$ are, respectively, the amplitude and lifetime of the $i^{th}$ component.

Measurements of CPL were performed with an instrument built at the Weizmann Institute (20). (CPL relates to the molecular conformation of the chromophore in its emitting excited state in the same way that circular dichroism [CD] relates to the molecular conformation in the ground state.) Thus, the anisotropy factor of the emission, $g_{em}$, is defined as $g_{em} = \Delta I/(I/2)$, where $\Delta I$ is the intensity of the circularly polarized component in the emission, and I is the total luminescence intensity. $\Delta I$ is positive for left-handed circularly polarized emission.

All measurements were performed in 0.1 M NaCl-0.01 M phosphate, pH 7.0, at room temperature (23 ± 1°C). The AChE concentration is expressed in terms of its active-site concentration, assuming MW = 75,000 and $A^{1\%}_{280} = 17.6$.

## RESULTS and DISCUSSION

### 1. Synthesis

The synthetic routes described in Technical Approach were selected on the basis of purity and homogeneity of the final product rather than yield or convenience of starting materials.

The determination of the homogeneity and structure of the newly synthesized fluorescent OP ligands was based on mass spectroscopy, $^{31}$P-nmr and UV spectroscopy, as well as elementary analysis (e.g., C, H, N, P, Cl). For compounds 9, 12, 13 and 16, the elemental analysis deviated from the theoretical value by more than ±0.4%, for one or more elements. Nevertheless, since $^{31}$P-nmr spectroscopy established the presence of one kind of phosphorus-containing compound (Figs. 1 and 2), we assumed that the contamination, if present at all, was caused by non-phosphorus molecules whose origin was presumed to be the crystallizing medium. We note that of these four compounds, only 9 and 12 (Fig. 1) were used for preparation of OP-enzyme conjugates.

In only one case were we unable to obtain the expected OP ligand, dansylaminoethyl-OP(O)(Pin)Cl (DAPinPC). We suggest that the compound isolated, 15, has a cyclic structure as depicted below:

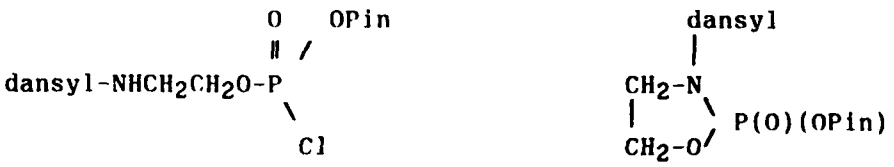

DAPinPC



DPinPO (15)

The cyclic structure assigned to 15 is based on the following findings:

a. Absence of the amidate proton (dansyl-NH-) in the $^1$H-nmr spectrum of 15 as opposed to the open-chain analogs 14 and 16, in which this proton shows up as a triplet (Fig. 3).

b. The multiplicity of the -N-$CH_2CH_2$O- proton resonance for compounds 15 as opposed to the $^1$H-nmr spectra of 14 and 16 (Fig. 3) strongly indicates that these protons are ring-member hydrogens.

c. The C,H analysis is in good agreement with the expected theoretical value calculated for 15:

Clcd. for $C_{20}H_{29}N_2O_5PS$: C=54.55; H=6.55.
Found: C=53.91; H=6.83.

(The calulated values for the open-chain analog DAPinPC are: C=50.37; H=6.3).

d. Although the C,H analysis is also in good agreement with the structure of the pyro-analog [dansyl-$NHCH_2CH_2O$-P(O)(OPin)]$_2$O, this possibility may be ruled out because of the absence of the $^{31}$P-nmr characteristics of the pyrophosphate structure (e.g., an upfield chemical shift relative to $H_3PO_4$ and the complexity of the $^{31}$P-nmr signal due to the four chirality centers). We note that the two $^{31}$P-nmr singlets assigned to 15 are due to the diastereoisomer mixture, (Fig. 4).

The mass spectroscopy ($m^+$, 440) along with the $^{31}$P-nmr spectroscopy and the C,H analysis supports the cyclic structure proposed for 15. It is not unlikely that 15 was obtained from DAPinPC by intramolecular dehydrochlorination.

The stoichiometric release of pNP from PB(pNP)PC (9) and PB(pNP)$_2$P (10) after 6 hrs of reflux in 1 M NaOH pro-vided additional support for the proposed structure of these pNP-containing

ligands. Thus, 9 released 1 ± 0.1 equivalents of pNP and 10 contained 2 ± 0.1 equivalents of bound pNP. Free pNP, if present, accounted for 4% or less of the total pNP. It should be noted here that the same stoichiometries were found for the release of pNP in the reactions of 9 and 10 with α-Cht, when large quantities of conjugates were prepared for $^{31}$P-nmr and optical spectroscopies.

2. Specificity of binding and stoichiometry of OP-enzyme fluorescent conjugates

In order to employ the fluorescent OP ligands as probes for detection of conformational changes which might occur during aging, it was necessary to establish that they interacted specifically and stoichiometrically with the enzyme.

a. AChE

The specificity of binding and stoichiometry of PBEP-AChE and PBP-AChE obtained from the reaction between electric eel 11S AChE and either PBEPC (7) or PBPDC (8) was described by us earlier (2). In both cases, a ca. 1:1 stoichiometry was reported. The stoichiometry of binding of PBPinPC (11) and PBPinPF (12) to AChE was obtained from the corresponding absorption spectra, assuming $\epsilon_{280}=1.4 \times 10^5 M^{-1}cm^{-1}$ and $\epsilon_{347}=4 \times 10^4 M^{-1}cm^{-1}$ for the protein and the fluorescent OP ligand, respectively. The molar ratio of bound fluorescent ligand to catalytic sites was found to be ca 2. Therefore, in contrast to α-Cht (see below), AChE provides at least one additional binding site for both PBPinPC and PBPinPF. It is of interest to note that it takes the combination of the pyrene and the pinacolyl moieties to bring about this additional binding to AChE, since pyrene alone (e.g., PBEPC and PBPDC)(2) or the pinacolyl alone (DPinPO) formed a 1:1 stoichiometric conjugate with AChE.

In order to understand better the nature of this additional binding of the pinacolyl-pyrenebutyl-OP compounds to AChE, we reacted samples of AChE, whose catalytic sites had been blocked by pretreatment with paraoxon, with either PBPinPC or PBPinPF. Such samples were found to bind 1 mole of fluorescent ligand per catalytic subunit. If such preparations were denatured with 8 M urea, > 97% of the fluorescent label was released, suggesting that when the active-site serine is blocked, AChE can still bind 1 mole of PBPinPC or PBPinPF, but non-covalently. Similar dialysis against phosphate buffer did not release the bound fluorophore, suggesting that the OP is bound in a hydrophobic pocket in the native protein. The non-covalent nature of this binding was confirmed as follows: PBPinPC and PBPinPF were incubated in 0.1 M NaOH for 1 hr before their

addition to the inhibition mixture. Such treatment should totally remove the halogen atom and thus completely destroy their ability to react covalently with the active-site serine. After this alkali treatment, the hydrolyzed fluorescent OP compounds still bound to DEP-AChE.

Radic et al. (21) earlier showed the existence of two types of binding of OP's to AChE: a covalent binding to the active site and a non-covalent binding to a site which may be equivalent to the second substrate-binding site, which is believed to be involved in substrate inhibition. In order to further characterize the second site for binding of PBPinPC and PBPinPF, we dialyzed DEP-AChE which had been treated with these compounds against 5 mM acetylcholine. We also tested the possibility that the binding site which we observed corresponded to the trimethyl site (22) by dialysing against 5 mM of either pinacolone (23) or pinacolyl alcohol. In all three cases, dialysis failed to release fluorescent OP ligand from the ternary complex. These observations imply that the additional binding site corresponds neither to the substrate site alone nor to the trimethyl site alone.

The low extinction coefficient of the dansyl fluorophore at wavelengths above 310 nm (~4 x $10^3$ $cm^{-1}M^{-1}$) precluded direct measurement of the stoichiometry of its binding to AChE. However, we could examine the specificity of its binding by using the following technique: The fluorescence of the dansyl-OP-conjugate was compared with that of a control sample of AChE whose active site had been previously blocked by exposure to the non-fluorescent inhibitor paraoxon, followed by the reaction with the dansyl-OP. It was found that exposure of AChE pretreated with paraoxon to either DAEPF (14) or DPinPO (15) yielded a product the fluorescence of which was less than 1% of that of the corresponding dansyl-OP conjugates.

b. α-Cht

The specificity of binding of PB(pNP)PC, $PB(pNP)_2P$ and PBPinPC to α-Cht was demonstrated as had been done previously for both PBPDC and PBEPF (1). Thus, α-Cht was inhibited > 99% with DFP to yield DIP-Cht and this conjugate was exposed to the pyrene-containing OP inhibitors under the same conditions employed for the native enzyme. The reaction mixture was then passed through a Sephadex G-10 column so as to separate the OP-enzyme conjugate from the unbound fluorescent OP.

Pretreatment with DFP was thus shown to prevent almost completely the binding of all the fluorescent OP's to α-Cht, as can be seen from the data for PBEPF and $PB(pNP)_2P$ displayed in Fig. 5. Thus the fluorescent OP's appear to interact specifically

and exclusively with the active-site serine and the Sephadex G-10 column provides an efficient method of separating the fluorescent OP-Cht conjugate from the free fluorophore.

The stoichiometry of binding was determined from the absorption of the bound pyrene at 345 nm, which is the absorption maximum of pyrene in all the pyrene-containing OP-Cht conjugates studied here, and the absorption at 290 nm, where there is a shoulder in the absorption of α-Cht itself (Figs. 5 and 6). Although the protein absorbs maximally at 278 nm, 290 nm was selected for estimation of the protein concentration because the bound pyrene makes only a minor contribution to the total absorbance at this wavelength. The concentration of the enzyme was determined from the absorbance at 290 nm by using $A^{1\%}_{290nm}$ = 14.2 ± 0.7 and a molecular weight of 25,000. The concentration of bound pyrene was determined assuming $\epsilon_{345}$ = 3.5 ± 0.1 x $10^4$ $M^{-1}cm^{-1}$. This value was obtained by measuring the increase in molar absorption from 2.3 x $10^4$ $M^{-1}cm^{-1}$ to 3.5 x $10^4$ $M^{-1}cm^{-1}$ concomitant with a shift in the absorption maximum from 342 to 345 nm upon the addition of excess α-Cht to PBEPF in water-10% acetonitrile and completion of the inhibition reaction. These results are in good agreement with previously published data, in which a similar bathochromic shift and increase in the extinction coefficient was observed [$\epsilon_{349}$ = 3.9 ± 0.1 x $10^4 M^{-1}cm^{-1}$) for analogous pyrene-containing conjugates (23a). From the ratio of $\epsilon_{345}$ to $\epsilon_{290}$, it was calculated that the various conjugates contain 0.85-1.10 molecules of bound pyrene per catalytic site. It should be noted, however, that uncertainties with respect to both the extinction coefficient of the bound pyrene and the amount of catalytically active α-Cht lost as a result of denaturation prior to the phos-phorylation reaction may lead to deviations from 1:1 stoichiometry.

Table 4 summarizes stoichiometry measurements for pyrene-containing OP-Cht conjugates.

Table 4: Stoichiometry of binding of pyrene-containing OP's to α-Cht

| Conjugate | % Inhibit. of α-Cht activity (n=3) | Absorbance-ratio $\epsilon_{345}/\epsilon_{290}$ Measured (n=3) | Corrected[e] | Pyrene/enzyme ratio[f] |
|---|---|---|---|---|
| PBEP-Cht[a] | 97 ± 2 | 0.74±0.1 | 0.76 | 0.90 |
| PBP-Cht[b] | 98 ± 2 | 0.88±0.2 | 0.90 | 1.07 |
| PBP-Cht[c] | 95 ± 2 | 0.67±0.05 | 0.71 | 0.85 |
| PBPinP-Cht[d] | 92 ± 2 | 0.85±0.1 | 0.93 | 1.10 |

a. Prepared from PBEPF. b. Prepared from PBPDC.

c. Prepared from $PB(pNP)_2P$. d. Prepared from PBPinPC.

e. Corrected = measured/% inhibited enzyme.

f. Obtained by dividing the corrected absorbance ratio by the theoretical ratio 0.84, assuming 1:1 binding of pyrene and 100% inhibition of enzyme activity.

In two additional single experiments, in which PBPinPF and PB(pNP)PC were used as the fluorescent OP, pyrene/enzyme ratios in the same range were obtained.

3. Kinetics of inhibition

a. AChE

PB(pNP)PC (9) and $PB(pNP)_2P$ (10)

The pNP esters of the pyrenebutyl phosphate series, PB(pNP)PC and $PB(pNP)_2P$, displayed relatively low potency as AChE inhibitors (Fig. 7). Both inhibitors required relatively high concentrations (>0.1 mM) in order to obtain half-lives for inhibition of AChE of 40 min or less. However, because of their limited solubility, slight turbidity was observed for both OP's; the inhibition profile shown in Fig. 7 should therefore be considered to represent data generated from a non-homogeneous reaction system . The non-linear curves obtained for the plot of log %-residual activity vs. time for both 9 and 10 (Fig. 7) may be ascribed either to the heterogeneous medium, to the removal of the anti-ChE by hydrolysis, or to a combination of both possibilities.

PBPinPC (11) and PBPinPF (12)

Fig. 8 shows the inhibition of electric eel AChE in phosphate solution (pH 7.0) at 25°C by PBPinPC (11) and PBPinPF (12). In several experiments turbidity was observed and the solutions became clear after several hours. Since the inhibited enzyme did not hydrolyze spontaneously, we assume that the non-linearity observed for inhibition by 11 (Fig. 8) is due to hydrolysis of the P-Cl bond leading to a decrease in the effective PBPinPC concentration. Conversely, the inhibition of AChE by 12 displayed first-order kinetics, the lines passed through the origin and the rate constants were not linearly related to the concentration of the inhibitor. These results indicate that a Michaelis complex (or a similar complex) between the enzyme and the inhibitor is present, and the kinetic pathway may thus be represented by the following scheme:

$$E + I \underset{K_I}{\rightleftharpoons} EI \xrightarrow{k'} E_i$$

Scheme VI

where E, EI and $E_i$ are the free enzyme, the Michaelis complex and the phosphorylated enzyme, respectively, and I is the corresponding inhibitor. $K_I$ and k' are the reversible Michaelis constant and the phosphorylation rate constant, respectively. The mathematical solution for Scheme VI is given in eqns. 1 and 2 (10):

$$k_{obs} = \frac{[I]k'}{K_I+[I]} \qquad (1)$$

$$\frac{1}{k_{obs}} = \frac{K_I}{k'}\frac{1}{I} + \frac{1}{k'} \qquad (2)$$

Indeed, a plot of $1/k_{obs}$ vs. $1/I$ provided a straight line (Fig. 9) and the individual constants $K_I$ and k' were extracted from the corresponding slope and intercept. $K_I$ and k' values are shown in Table 5, along with $k_i$, the bimolecular rate constant for the inhibition reaction ($k_i = k'/K_I$).

PBPinPF was found to be ca. 1000 times less potent than its ethyl analog, PBEPF (2), presumably because the simultaneous presence of two bulky substituents, i.e., pyrenebutyl and pinacolyl, does not permit proper binding and orientation at

the active-site. As discussed before, both PBPinPC and PBPinPF bind to AChE with a 2:1 stoichiometry; the effect of the binding of the second molecule on the kinetic mechanism is not, however, clear at this point.

DAEPF (14) and DPinPO (15)

The first-order plots for inhibition of AChE by DAEPF (14) display straight lines (Fig. 10) up to at least 50% inhibition. Since DAEPF was found to hydrolyze quite rapidly in phosphate buffer (0.05M, pH 7.0, 25°C, see below), and since the inhibited enzyme, DAEP-AChE, did not hydrolyze spontaneously to a significant extent during the time period of the inhibition, we assume that the non-linearity observed in several runs is due to loss of anti-ChE potency of the inhibitor. Whenever log %-residual activity vs time did not produce straight lines, the first-order rate constants were estimated from the initial velocity. We also note that in order to obtain straight lines, DAEPF had to be pre-incubated for 2 min in phosphate buffer (0.05 M, pH 7.0, 25°C) prior to its dilution into the enzyme mixture. This finding raises the possibility of the presence of highly active anti-ChE impurities which are removed by hydrolysis. These impurities were not detected by the analytical procedures described above for determination of the purity and homogeneity of DAEPF. The first order rate constant for inhibition of AChE by DAEPF could not be linearly related to the concentration of the inhibitor, presumably because of a saturation phenomenon. The kinetic results were therefore treated as described for PBPinPF (eqns. 1 and 2), and indeed the double-reciprocal plot resulted in a straight line (Fig. 9), from which $K_I$, k' and the bimolecular rate constants for the inhibition of AChE were calculated (see Table 5).

The inhibition profile of AChE by DPinPO (15) is shown in Fig. 11. Since the activity of the inhibited enzyme was not restored spontaneously, we assumed, as before, that the reason for the non-linear plot is hydrolysis of the anti-ChE compound. Indeed, pre-incubation of the inhibitor at 25°C in phosphate buffer (0.05 M, pH 7) prior to its dilution into the enzyme solution significantly decreased the rate of inhibition of AChE. It is worth mentioning that DPinPO lacks a conventional leaving group (e.g., F, pNP, S-CC-NR'R) and it is not therefore clear which is the leaving group in this case. One may assume that the strain in the five-membered ring (25), along with possible anchimeric assistance of the dimethylamino residue at the dansyl moiety, is responsible for both the relatively rapid hydrolysis and for the inhibition of AChE.

If this assumption is correct, the following Scheme (VII) should depict the mechanism of inhibition of AChE by DPinPO:

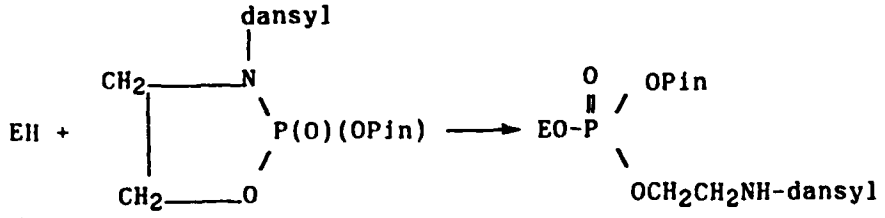


Scheme VII

where EH: AChE dansyl: 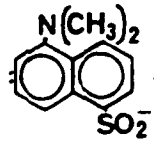 Pin: $CHC(CH_3)C(CH_3)_3$

The inhibited enzyme may subsequently undergo aging by dealkylation of the pinacolyl residue. Aging was, indeed, observed (see below). We cannot completely rule out the possibility that contamination by dansyl$NHCH_2CH_2OP(O)(OPin)Cl$ or by the corresponding "pyro" derivative is responsible for the observed inhibition (see Subsection Synthesis, Results and Discussion). Nevertheless, all these inhibitors should produce the same inhibited enzyme, namely, dansyl-$NHCH_2$-$CH_2OP(O)$-(OPin)-AChE.

The potency of DPinPO (15) as an AChE inhibitor was evaluated by the method developed earlier for measurement of the rate constant for inhibition of enzymes by covalent inhibitors which hydrolyze rapidly (17). The mathematical solution of such a kinetic scheme (VIII) is given in eqn. 3:

$$I + E \xrightarrow{k_i} E' \text{ (inhibited enzyme)}$$

$$k_h \downarrow$$

hydrolysis products

Scheme VIII

$$\ln \frac{E_\infty}{E_o} = -I_o \frac{k_i}{k_h} \qquad (3)$$

In eqn. 3, $E_o$ is the activity of the enzyme at t=o, $E_\infty$ is the activity of the enzyme at $t\to\infty$, $I_o$ is the inhibitor concentration at zero time and $k_i$ and $k_h$ are the inhibition and hydro-

lysis rate constants, respectively. The constant $k_h$ (0.0096 $min^{-1}$) was evaluated by using the same enzymic technique (see below) and $k_i$ was calculated from eqn. 3 by using different values of $I_o$ and the limiting value ln $E_\infty/E_o$. The results are summarized in Table 5.

Table 5: Kinetic constants for inhibition of AChE by fluorescent OP's at pH 7.0 (0.05 M phosphate, 25°C)

| INHIBITOR | $K_I$[a] (M) | $k'$[a] ($min^{-1}$) | $k_i$[b] $M^{-1}min^{-1}$ |
|---|---|---|---|
| PBEPF | -c | -c | $5.0 \times 10^5$[d] |
| PBPinPF | $1.15 \times 10^{-5}$ | 0.0076 | $6.6 \times 10^2$ |
| DAEPF | $3.6 \times 10^{-4}$ | 0.55 | $1.5 \times 10^3$ |
| DPinPO | -c | -c | $6 \times 10^2$[e] |

a. Clcd from eq. 2 and Fig. 9.

b. $k_i = k'/K_I$. c. Not measured. d. See Ref. 2.

e. Clcd from eqn. 3.

b. α-Cht

PBEPF (6)

The rate of inhibition of α-Cht by PBEPF was found to be first-order, but the rate constant was not linearly related to the concentration of inhibitor (Fig. 12A). Since the line passed through the origin, we assume that a Michaelis complex (or another complex) is formed which is readily dissociated by addition of substrate. This kinetic behavior implies that the inhibition of α-Cht follows the kinetic pathway depicted in Scheme VI. The double-reciprocal plot (Fig. 12B), in accordance with eqn. 2, provided a straight line from which $K_I$ and $k'$ were calculated to be $7.5 \times 10^{-7}$ M and 0.44 $min^{-1}$, respectively. The bimolecular rate con-stant, $k_i$, was calculated to be $5.8 \times 10^5$ $M^{-1}min^{-1}$. The value obtained for $K_I$ shows that PBEPF exhibits high affinity for α-Cht. In order to verify this value, the dissociation constant for the reversible Michaelis complex, $K_I$, was measured by the Hunter-Downs method, as described by Aldridge and Reiner (10). This method examines the effect of the substrate ATEE on the reversible inhibition of a given inhibitor, and the mathematical expression for the effect of the substrate is shown in eqn. 4, derived on the basis of Scheme IX:

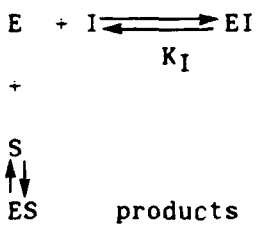


Scheme IX

$$\frac{[I]E}{E_o - E} = K_I + \frac{K_I}{K_m}[S] \qquad (4)$$

In eqn. 4, I and S are the concentrations of inhibitor and substrate, respectively; $E_o$ is the enzyme activity in the absence of inhibitor; and E is the enzyme activity in the presence of inhibitor. $K_I$ and $K_m$, are, respectively, the dissociation constants for the reversible inhibitor-Cht complex and the Michaelis complex. After the addition of PBEPF to the enzyme-substrate mixture, there was an immediate decrease in enzymatic activity which could be monitored for 0.5-1 min with no significant progressive decrease in enzyme activity. The results of plotting $[I]E/(E_o-E)$ vs. [S] are shown in Fig. 13. $K_I$ and $K_m$ were calculated from the intercepts on the vertical axis and horizontal axis, respectively. Thus $K_I$ was found to be $5 \times 10^{-7}$ M, in good agreement with the value obtained from the kinetic measurements. The value of $K_m$ obtained from the Downs-Hunter plot (1.3 mM) was found to be in good agreement with the value obtained by the standard Lineweaver-Burk plot (1.2 mM, not shown). These results imply that PBEPF binds competitively to the substrate-binding site at the active center of the enzyme. The high affinity of PBEPF, as reflected both in $K_I$ and in the bimolecular rate constant, is considerably higher than the values reported for DFP and tetraethyl pyrophosphate (TEPP), is similar to ethyl-p-nitrophenyl phenylpropylphosphonite (10) and lower than the values recently reported for alanine and phenylalanine phosphonate analogs ($k_i = 1.1 \times 10^7$ $M^{-1}min^{-1}$) (26). The high affinity of PBEPF for α-Cht may be ascribed to the hydrophobic pyrene moiety.

4. Reactivation and aging

a. AChE

PBPinP-AChE

AChE inhibited by either PBPinPC (11) or PBPinPF (12) at pH 7.0 (0.05 M phosphate, 25°C) aged quite rapidly, as illustrated in Table 6.

Table 6: Aging of PBPinP-AChE obtained by the inhibition of AChE by PBPinPC (11)[a] at pH 7.0 (phosphate 0.05 M, 25°C).

| Incubation time (min)[b] | % - AChE Activity After 10 min[c] | | After 16 hrs[c] | |
|---|---|---|---|---|
| | buffer[d] | 1 mM 2-PAM[d] | buffer[d] | 1 mM 2-PAM[d] |
| 10 | 68 | 73 | 75 | 81 |
| 30 | 64 | 69 | 67 | 71 |
| 60 | 62 | 61 | 63 | 60 |
| 120 | 48 | 48 | 44 | 48 |

a. AChE inhibited by 0.43 mM 11 and diluted 100 times into the reactivation medium.
b. Time of incubation prior to dilution into the reactivation medium.
c. Time of reactivation.
d. Phosphate buffer, pH 7.0 (0.05 M, 25°C).

Table 6 suggests that the percentage of reactivatable enzyme depends on the time of incubation with the inhibitor prior to the dilution into the reactivation medium. These results support the hypothesis of gradual aging (Scheme I), presumably by dealkylation, which removes the pinacolyl substituent (10).

PBP-AChE conjugates prepared on a large scale from PBPinPC and PBPinPF, as described before, could not be reactivated. It should be noted, however, that a DEP-AChE conjugate which had bound 1 equivalent of either PBPinPC or PBPinPF at a second site (see above) could be reactivated by 1 mM 2-PAM. These results suggest that in future experiments, the catalytic center of the enzyme may be studied while a second fluorescent ligand is attached to the protein non-covalently at a site distinct from the catalytic site.

AChE inhibited by DAEPF could not be reactivated completely. Twenty to thirty percent of the inhibited enzyme was resistant to reactivation. This degree of aging was independent of the

time of incubation with the inhibitor prior to dilution into the reactivation medium. The results are summarized in Table 7. The maximum reactivation obtained in the presence of 2-PAM was calculated by using eqn. 5.

$$\% \text{ - max. reactivation} = 100 \frac{E_\infty - E_i}{E_o - E_i} \qquad (5)$$

where $E_o$ is the enzymic activity without inhibitor, $E_\infty$ is the enzymic activity after 16 hrs of reactivation with 2-PAM and $E_i$ is the enzymic activity immediately before reactivation was initiated. The results displayed in Table 7 indicate that the amount of unreactivatable enzyme is constant and is not a function either of the time of incubation in the presence of the inhibitor or of the rate of reactivation in the presence of 2-PAM. The reactivation was found to be first-order (Fig. 14), the lines passed through the origin and the rate constants were not linearly related to the oxime concentration. These findings strongly indicate that the reactivatable por-

Table 7: %-Max reactivation of DAEP-AChE obtained by incubating AChE and DAEPF (0.015 mM) in phosphate buffer (0.05 M, pH 7.0, 25°)

| Time of incubation with inhibitor (min)[a] | 2-PAM concentration (mM) | %-max reactivation[b] | $k_{obs}$ ($min^{-1}$) |
|---|---|---|---|
| 15 | 0.010 | 67 | 0.29 |
| 30 | 0.125 | 82 | 0.72 |
| 60 | 0.025 | 71 | 0.55 |
| 120 | 0.075 | 77 | 0.81 |
| 210 | 0.100 | 71 | 0.73 |
| 220 | 0.050 | 69 | 0.37 |
| 325 | 0.250 | 75 | 1.06 |
| | | Average: 73 ± 2 (SEM) | |

a. Prior to dilution into the reactivation medium.
b. Calculated according to eqn. 5.

tion of the inhibited enzyme (ca. ~70-75%) is a homogeneous species. Preincubation of the inhibitor in phosphate buffer (0.05 M, pH 7.0, 25°C) for 150-300 min prior to initiation of the inhibition reaction permitted reactivation of 85-90% of the inhibited enzyme. One possible explanation for these observations is that one isomer of the racemic mixture of DAEPF inhibits the enzyme at a rate which is 25% of the rate of inhibition by the other isomer, and produces an instantaneously non-reactivatable form. Such an explanation suggests that aging is not caused by dealkylation and is probably of steric origin because, a priori, there is no reason why the phosphoryl residue should lose alkyl groups such as the $C_2H_5$ or dansylaminoethyl residues. More work will be required to clarify these results. Spontaneous reactivation of DAEP-AChE was negligible at pH 7.0 (phosphate 0.05 M, 25°C). In order to measure the bimolecular rate constant for the reactivation of DAEP-AChE by 2-PAM, we applied the reactivation results to the kinetic pathway shown in Scheme VI. Thus the inhibited enzyme forms a reversible complex ($K_{ox}$) with the oxime prior to the unimolecular reactivation step (k'). Indeed, the double-reciprocal plot (Fig. 15) provided a straight line and the corresponding $K_{ox}$ and k' were found to be $1.45 \times 10^{-5}$M and 0.99 $min^{-1}$, respectively. The bimolecular rate constant for the reactivation was calculated to be $4.05 \times 10^4$ $M^{-1}min^{-1}$ ($k_r = k'/K$). This value is in the range reported for the reactivation of electric eel DEP-AChE by 2-PAM (16), suggesting that the phosphoryl moiety is readily available to nucleophilic displacement.

AChE inhibited in the presence of DPinPO at pH 10.3 (0.05 M carbonate buffer, 4°C), followed by dilution into 1 mM 2-PAM (0.05 M phosphate buffer pH 8.0, 25°C) could be reactivated up to 80-90% (Fig. 16) at a relatively slow rate. The first-order plot did not produce a straight line (not shown). Spontaneous reactivation occurred at a rate of 10-20% per 16 hrs. The percentage of unreactivatable enzyme was independent of the time of incubation at pH 10.3 prior to dilution into the reactivation medium. In order to test the effect of pH on the rate of aging, the inhibited enzyme was prepared at pH 10.3 (carbonate buffer, 0.05 M, 4°C) and diluted 200-fold into the appropriate aging medium. At selected time intervals, an aliquot of the aging medium was further diluted 10-fold into the reactivation mixture (1 mM 2-PAM, 0.05 M phosphate buffer, pH 8.0, 25°C), and incubated for 16 hrs. The first-order plot for the aging reaction did not produce a straight line (Fig. 17). The reactivation and aging results obtained for the DAP-AChE conjugate indicate that the inhibited enzyme is not a homogeneous species, and it is not unlikely that the racemic mixture DPinPO also leads to the formation of two enzyme conjugates which differ in their optical configuration around the phosphorus. Nevertheless, it should be pointed out that the conjugate used for the optical spectroscopy measurements was completely aged under the experimental conditions described for the large-scale preparation of DAP-AChE.

b. α-Cht

The reactivation of lyophilized OP-Cht conjugates was performed with 0.1 M 3-PAM (27) in 2 mM Tris buffer at pH 7.0 (25°C). The activity of the regenerated enzyme was compared to that of a control sample of unmo-dified α-Cht similarly incubated in the presence of 0.1 M 3-PAM. 3-PAM stabilized the activity of α-Cht to some extent for periods of 20-30 hrs. Fig. 18 illustrates the reactivation profile for PBEP-Cht (obtained from PBEPF), PBPinP-Cht (obtained from PBPinPC) and PBP-Cht [obtained by use of either $PB(pNP)_2P$ or PBPDC]. As expected, PBP-Cht could not be reactivated, irres-pective of the inhibitor employed. Thus aged enzyme was formed either instantaneously (PBPDC, Scheme II), or gradually [$PB(pNP)_2P$], as depicted in Scheme I. This aging was expected by analogy with a previous study, in which α-Cht inhibited by Tris(pNP) phosphate was demonstrated to undergo aging concomitantly with release of a stoichiometric amount of p-nitrophenol (8). PBEP-Cht and PBPinP-Cht could be only partially reactivated. Since the reactivation of the OP-Cht conjugates proceeds very slowly, one has to assume that several side reactions may occur, such as denaturation of both the inhibited and free α-Cht as well as dealkylation to form the aged conjugate of the enzyme, as was observed from $^{31}P$-nmr measurements with respect to both PBPinP-Cht and DIP-Cht (4). In one case, PBPinP-Cht could be reactivated only up to 10%, and we assume that in this preparation aging was accelerated as a result of the experimental conditions employed, which included prolonged dialysis at pH 4.0. This particular preparation was also found to be aged on the basis of the optical spectroscopy measurements.

In order to substantiate the reactivation results, the progressive changes in the reaction mixture PBEP-Cht/0.1 M 3-PAM were also monitored by $^{31}P$-nmr spectroscopy. The main signal, which showed up at -29.15 ppm (Fig. 19), was assigned to the expected reactivation product, namely, $PBOP(O)(OC_2H_5)OH$, which stems from the nucleophilic displacement at the P atom of the phosphorylated enzyme. This assignment was based on comparison of the chemical shift obtained for the hydro-lysis product of $PB\text{-}OP(O)(OC_2H_5)F$ (PBEPF) in the pre-sence of 0.1 M 3-PAM (-29.15 ppm) with the signal shown in Fig. 19.

5. Hydrolysis of fluorescent OP ligands

During the studies of inhibition of AChE by DAEPF (14) and DPinPO (15), it was noticed that both inhibitors lose their anti-ChE potency upon incubation in phosphate buffer. Their stability in aqueous solution was measured by a previously published procedure (17), in which the rate constants for the hydrolysis of

AChE inhibitors were evaluated from the rate of loss of their anti-ChE activity. The concentration of labile inhibitor during the inhibition reaction, as shown in Scheme VIII, is given by eqn. 6:

$$I_t = I_o e^{-k_h t} \qquad (6)$$

where $I_o$ is the concentration of the inhibitor at zero time and $I_t$ is its concentration at time t. The rate of hydrolysis of the inhibitor can be measured as follows: A small volume of a dioxane solution of the inhibitor is diluted into the buffer (phosphate 0.05 M, pH 7.0, 25°C). At selected time intervals, an aliquot of the inhibitor-buffer solution is injected into an AChE solution and the value $I_t$ can be determined by use of eqn. 3, since $I_o$ (as indicated in eqn. 3) becomes a function of the time of prior hydrolysis. The value $I_t$ is then inserted into eqn. 6 to evaluate $k_h$, as demonstrated in Fig. 20. The hydrolysis rate constants in phosphate buffer (0.05 M, pH 7.0, 25°C) were found to be 0.038 $min^{-1}$ and 0.0096 $min^{-1}$ for DAEPF and DPinPO, respectively. We assume that the anchimeric effect of the aromatic dimethylamino group is responsible for the accelerated hydrolysis of the dansyl containing OP ligands in phosphate buffer solutions.

6. $^{31}$P-nmr spectroscopy

α-Cht

In our previous report (1), we presented $^{31}$P-nmr spectroscopy results supporting the hypothesis that the aged form of phosphorylated Cht prepared from the dihalide PBPDC contains a $P\text{-}O^-$ bond. Thus, by correlating the chemical shifts of the OP-Cht conjugates with the $^{31}$P-nmr chemical shift of known model compounds, we were able to demonstrate a significant downfield shift in the $^{31}$P-nmr signal of the conjugate PBP-Cht, relative to the corre-sponding non-aged form, PBEP-Cht. Such a downfield shift was predicted from the chemical shift of the model compounds. In order to verify the nature of the P atom in the newly prepared OP-Cht conjugates, we measured the $^{31}$P chemical shift under the experimental conditions described before (1), with HMPA serving as internal standard. Table 8 summarizes the chemical shifts for the various OP conjugates in their native and denatured forms.

The relative chemical shifts of the various PBP-Cht conjugates obtained from either PBPDC, PB(pNP)PC or $PB(pNP)_2P$ were found to be practically the same (Table 8 and Fig. 21), suggesting that the same non-reactivatable conjugate is formed, irrespective of the mechanism of aging (Schemes I and II).

The $^{31}P$ chemical shifts of the triesters, PBPinP-Cht and DIP-Cht, were found to be upfield relative to DEP-Cht and PBEP-Cht ($\Delta\delta$, ca. 1.3 ppm), as expected from similar changes observed in the chemical shifts of branched vs. unbranched trialkylphosphates (26). No pH-chemical shift dependence was observed in the pH range 3-7 except for DEP-Cht (1). After denaturation, the chemical shifts for both aged and non-aged conjugates moved upfield and became close to the reported values for the tri- and diester model compounds (1,4). This shift is also accompanied by a considerable decrease in line width (Fig. 22).

Table 8.: $^{31}P$-nmr chemical shifts[a] ($\delta$,ppm relative to HMPA) of OP-Cht conjugates at pH 3-7 (25°C).

| Conjugate | OP used | $\delta$, ppm (from HMPA)[b] | |
|---|---|---|---|
| | | Native | Denatured[c] |
| DEP-Cht | DEPF | -28.65 | -31.02 |
| DEP-Cht | Paraoxon | -28.74 | -31.05 |
| DIP-Cht | DFP | -30.13(28.6)[d] | NM[e] |
| PBEP-Cht | PBEPF | -28.68 | -30.97 |
| EP-Cht | EPDC | -27.60 | -29.38 |
| PBP-Cht | PBPDC | -27.50 | -29.38 |
| PBP-Cht | PB(pNP)PC | -27.55[f] | -29.50[f] |
| PBP-Cht | $PB(pNP)_2P$ | -27.50 | -29.40 |
| PBPinP-Cht | PBPinPC | -29.80(-28.00)[d] | -31.56(-29.41)[d] |
| PBPinP-Cht | PBPinPF | -29.95[f](-28.10)[d] | NM |

a. Results are the average of at least three measurements. Estimated errors <0.05 ppm.

b. Negative signs indicate an upfield shift relative to HMPA.

c. Denatured with 6 M guanidine hydrochloride.

d. Figures in parentheses are chemical shifts of a second $^{31}P$-nmr signal with a relatively high intensity.

e. Not measured.

f. Single measurement.

The OP-Cht conjugates obtained by using either PBPinPC or PBPinPF displayed similar $^{31}P$ chemical shifts (Table 8). However, it should be noted that incubation in aqueous solutions (pH 3-4) for long periods (48-96 hrs) resulted in the gradual appearance of a second $^{31}P$-nmr signal (Fig. 23). A similar observation was reported by Van der Drift with respect to the $^{31}P$-nmr signals of (DIP-Cht (4); the most likely explanation is that the pinacolyl residue is removed, presumably with concomitant formation of a P-O$^-$ function, to produce PBP-Cht. These dynamic changes are in good agreement with the optical spectroscopy data (see below), in which it was demonstrated that the spectra of the aged conjugates obtained from either PBPDC, PBPinPC, PB(pNP)PC or PB(pNP)$_2$P corresponded to the same product, namely, PBP-Cht. It should be noted that although the $^{31}P$-nmr chemical shift of the time-dependent signal, shown in Fig. 23, is consistent with the formation of a P-O$^-$ bond (Scheme X), the chemical shift observed ($\delta$, -28.1 ppm, Table 8, Fig. 23) is ~0.5 ppm upfield relative to the chemical shift obtained for native

PB-O-P(O)(OPinacolyl)-Cht → PB-OP(O)(OH)-Cht

PBPinP-Cht PBP-Cht

PB = Pyrenebutyl

Scheme X.

PBP-Cht prepared from either PBPDC, PB(pNP)PC or PB(pNP)$_2$P. Although the reason for this difference is not yet clear, it may be speculated that the aging of PBPin-Cht is accompanied by chemical changes at or near the active site of the inhibited enzyme which affect the $^{31}P$-nmr chemical shift of the assumed product, PBP-Cht. For example, if aging proceeds via the formation of a carbonium ion (i.e., an $S_N1$ mechanism), we cannot rule out possible alkylation of a neighboring amino acid residue which might, in turn, influence the $^{31}P$-nmr chemical shift. The following observations support this hypothesis:

a. Reactivation of PBEP-Cht was monitored in parallel by $^{31}P$-nmr spectroscopy. In addition to the strong signal at $\delta$, -29.15 ppm, which was assigned to PB-O-P(O)-(OC$_2$H$_5$)OH, two peaks showed up at -27.50 and -28.08 ppm after long periods of incubation at room temperature (Fig. 19). These findings indicate that PBEP-Cht indeed aged partially, as indicated by the appearance of a signal at -27.50 ppm. The signal at -28.08 ppm might result from aging and concomitant alkylation of the same residue that was suggested to be undergoing alkylation during aging of PBPinP-Cht. Thus the fact that two different OP conjugates, namely, PBPinP-Cht and PBEP-Cht, produce upon

aging the same $^{31}$P-nmr signal at -28.08 ppm favors a common chemical process, such as alkylation. Indeed dialkylphosphate esters have been reported to be alkylating agents (28).

b. Denaturation in 6 M guanidine·HCl moved the chemical shift of the aged PBPinP-Cht (Fig. 22) upfield to the same position obtained for denatured PBP-Cht conjugates which were obtained by use of PBPDC, PB(pNP)PC and PB(pNP)$_2$P.

c. The pH-chemical shift profile for DEP-Cht (1) and DIP-Cht (4) showed an upfield shift in the $^{31}$P-nmr signal with increasing pH ($\Delta\delta$ ca 0.5 ppm at pH 3-9). If alkylation prevents hydrogen bond formation with the phosphoryl center, one should expect an upfield shift of ca 0.5 ppm, which is in good agreement with the trend reported here (28.08-27.5 ≅ 0.5 ppm).

d. The aged conjugates formed by inhibition of α-Cht with PBPDC, PB(pNP)PC and PB(pNP)$_2$P would not be expected to generate an alkylated enzyme concomitantly with aging; indeed, no trace of a peak at -28.08 ppm is observed in any of these three conjugates.

Further experimentation will be needed in order to substantiate this interesting possibility.

7. Optical spectroscopy

a. AChE

The fluorescence spectra of DAEP-AChE and of DAP-AChE are presented in Fig. 24. The emission maximum lies at 505 nm for both conjugates, and the relaxation of the excited fluorophore in the two conjugates must therefore be similar. This implies that the polarity and rigidity of the environment of the dansyl group are similar. The quantum yield of DAP-AChE is, however, only 55 ± 5% of that of DAEP-AChE. Neither of these spectra is affected by the presence of positively charged ligands such as gallamine triethiodide (29) or acetylcholine. Thus, even if a conformational change occurs as a result of the binding of these ligands, it does not affect the conformation at the active site.

Fluorescence decay measurements of the non-aged conjugate, DAEP-AChE, and of the aged form, DAP-AChE, are shown in Fig. 25. The fluorescence decay of both conjugates can be described by a biexponential function. The long component is ca. 20 nsec, and the short component is ca. 3 nsec. However, whereas the ratio of the amplitudes in the non-aged conjugate is ca. 2:1, it is ca. 1:1 in the aged AChE, leading to a different quantum yield for the two conjugates. Calculation of

the relative quantum yields, according to eqn. 7, re-veals that the fluorescence intensity of the aged conjugate is 65 ± 5% of that of the non-aged conjugate, in agreement with the

$$q_r = \frac{\sum \alpha_i \tau_i}{\sum \alpha_i} \qquad (7)$$

steady-state measurements. Quenching of the dansyl moiety is therefore dynamic rather than static. Based on their relative quantum yields, we may also conclude that the interaction between the dansyl moiety and the polypeptide chain is stronger in the aged OP conjugate than in the non-aged conjugate.

It is of interest to compare the results obtained for the dansyl-OP conjugates of AChE with those obtained for the corresponding pyrene-OP conjugates (2). In both cases the emission maximum does not change upon aging. However, the fluorescence intensity of the aged dansyl conjugate is ca. 60% of that of the non-aged form, whereas the reverse situation occurs with the pyrene-OP conjugates, for which the intensity of the non-aged conjugate is ca. 40% of that of the aged form. Thus, the interaction of the fluorophore with the polypeptide chain of AChE is stronger for the aged conjugate when the probe is dansyl, while it appears to be stronger for the non-aged conjugate when the probe is pyrene. It should be noted, however, that earlier collisional quenching experiments with the pyrene-OP conjugates of AChE indicated that the non-aged conjugate is more accessible to external quenchers (2); the possibility of preferential oxygen quenching of the non-aged conjugate cannot therefore be excluded. It should also be noted that whereas upon aging of the pyrene-OP conjugate, the change in quantum yield is largely due to a change in the magnitude of the fluorescence lifetimes, in the case of the dansyl-OP conjugates, the fluorescence lifetimes do not change and the change in quantum yield is due solely to a change in the relative contributions of the two components. Since the two fluorescent probes may be interacting with different sites on the enzyme surface, it is not yet possible to offer interpretations of these observations.

b. <u>α-Cht</u>

During the previous year (1), we presented optical spectroscopic results for two conjugates, namely, the non-aged conjugate, PBEP-Cht, and the aged conjugate, PBP-Cht. During the period covered by this report, we used various organophosphates designed to form the same putative aged conjugate, in order to show that the end product obtained is the same by the criteria of optical spectroscopy. The OP inhibitors used were: PB(pNP)PC, $PB(pNP)_2P$, PBPinPF and PBPinPC.

In order to obtain a comprehensive overview of the results, we first present a short summary of our previous results (1):

The absorption spectra of the various conjugates are similar, and exhibit only small differences in intensity within the protein absorption band (250-310 nm); the pyrene absorption band is structured, with maxima at 315, 329 and 345 nm. The CD spectra of PBEP-Cht (non-aged) and of PBP-Cht (aged) conjugates in the tryptophan absorption region are similar. However, the absorption anisotropy factor in the pyrene absorption region (ca. 350 nm) is markedly more negative for the non-aged than for the aged form of Cht ($g_{ab}$ being $-5.0 \cdot 10^{-4}$ and $-0.5 \cdot 10^{-4}$, respectively). This implies that the conformation of the protein in the vicinity of the organophosphate, namely, at the active site, is different for the two conju-gates. Similar results were obtained from CPL measurements. The emission anisotropy factor, $g_{em}$, of the aged conjugate is different in both magnitude and sign from that of the non-aged conjugate, implying that the excited-state active-site asymmetry of the aged and non-aged conjugates is of opposite screw sense. Steady-state fluorescence measurements of the conjugates reveal a similar fluorescence profile, the quantum yield of the aged conjugate PBP-Cht being ca. 20% lower than that of PBEP-Cht (the non-aged form). Fluorescence decay measurements proved this quenching to be dynamic. All the fluorescence decay data of the conjugates could be described by a biexponential decay function. The short component, ca. 5 nsec, was found to be equal for the aged and the non-aged Cht, while the long component assumed values of ca. 88 nsec and 98 nsec, respectively. These results imply that the orientation of the pyrene fluorophore relative to the polypeptide chain is different in the two conjugates, resulting in a stronger interaction of the OP residue with the protein in the case of the aged conjugate.

The fluorescent label used in all the measurements carried out with α-Cht conjugates was pyrene. Pyrene is known to have a tendency to form excimers (5). We therefore examined the possibility of formation of eximers by the OP-Cht conjugates.

Steady-state fluorescence spectra of PBEP-Cht and of PBP-Cht, as a function of concentration, are presented in Fig. 26. The spectrum of each conjugate is normalized at the peak to the intensity of the most dilute sample in order to facilitate comparison. The dependence of the emission spectra on concentration is obvious. Concomitantly with the increase in concentration, there appears a new emission band, which lies at the red edge of the spectrum of the dilute OP conjugate. This concentration dependence can be explained only by the occurrence of a bimolecular process. Further support for the

presence of excimers was obtained from fluorescence decay and CPL measurements, to be described below. The existence of OP-Cht photo-dimers is interesting in itself, since the formation of protein excimers is not a common phenomenon.

Fluorescence decay measurements, performed at different concentrations and collecting various parts of the emission band, are shown in Table 9. The decay function of all the OP conjugates could be described by a bi-exponential function. At a concentration of 0.025 mg/ml, no excimer formation could be detected, as determined by the decay parameters of the emission above 500 nm. Under these conditions, the non-aged conjugate PBEP-Cht exhibits a mean value (n=3) for the short-lived component of 5 ± 1 nsec and a mean value for the long-lived one of 97.5 ± 1.5 nsec, while the corresponding mean life times of the aged PBP-Cht conjugate are 4.5 ± 1.5 nsec and 86 ± 3 nsec (n=3). The orientation of the pyrene label relative to the polypeptide chain must therefore be different in the two conjugates, the interaction between the fluorophore and the protein being stronger in the aged conformation.

The aforementioned decay parameters of the aged OP conjugate were invariably obtained regardless of the origin of the conjugate. Thus PBP-Cht conjugates formed by PBPDC, PB(pNP)PC, $PB(pNP)_2P$ and PBPinPC gave similar results, implying that the OP conjugate obtained was the same. The dependence on concentration of the fluorescence decay parameter can be ascribed to the bimolecular process of excimer formation, discussed above. When the concentration is high (>0.6 mg/ml) and detection is focused on the red part of the emission spectra where the excimers emit, the decay functions of both PBP-Cht and PBEP-Cht exhibit a negative amplitude (see Figs. 27 and 28). Negative amplitudes are characteristic of a process in which the emitting species is formed from an excited species rather than directly by the excitation light (30). It is worth noting that the tendency of the conjugates obtained by either PBPDC or PB(pNP)PC to form excimers is not identical, even though their lifetimes in dilute solutions are the same. This implies a subtle difference in the orientation of the pyrene in these two aged conjugates, so that it is more available for photo dimerization in one of the conformations. By comparing the ratio of the amplitudes obtained while collecting the whole emission spectrum with that obtained collecting a bandwidth between 370 and 400 nm, one may conclude that the emission of the short-lived component is shifted to the red with respect to the long-lived component.

Table 9: Fluorescence decay parameters of the aged and non-aged OP-Cht conjugates

| Conjugate | OP used | Protein concentration mg/ml | Emission-band observed (nm) | $\alpha_1$ | $\tau_1$(nsec) | $\alpha_2$ | $\tau_2$(nsec) | RMS |
|---|---|---|---|---|---|---|---|---|
| PBEP-Cht | PBEPF | 0.025 | > 370 | 0.105±0.001 | 98.6±0.4 | 0.018±0.001 | 6.2±0.6 | 0.0039 |
| PBP-Cht | PBPDC | 0.025 | > 370 | 0.116±0.001 | 87.7±0.3 | 0.023±0.001 | 6.1±0.5 | 0.0035 |
| PBP-Cht | PB(pNP)PC | 0.025 | > 370 | 0.110±0.001 | 88.6±0.3 | 0.032±0.001 | 4.8±0.4 | 0.0039 |
| PBP-Cht | PB(pNP)$_2$P | 0.025 | > 370 | 0.128±0.001 | 82.3±0.5 | 0.048±0.001 | 3.3±0.4 | 0.0064 |
| PBP-Cht | PBPinPC | 0.025 | > 370 | 0.136±0.001 | 84.4±0.8 | 0.078±0.002 | 3.8±0.2 | 0.0064 |
| PBEP-Cht | PBEPF | 0.6 | > 500 | 0.114±0.001 | 99.0±0.3 | (-)0.028±0.003 | 3.1±0.4 | 0.0042 |
| PBP-Cht | PBPDC | 0.6 | > 500 | 0.129±0.001 | 55.5±0.2 | (-)0.043±0.007 | 1.7±0.3 | 0.0038 |
| PBP-Cht | PB(pNP)$_2$P | 0.8 | > 500 | 0.080±0.038 | 59.4±7.0 | 0.064±0.038 | 35.6±6.0 | 0.0028 |
| PBP-Cht | PB(pNP)PC | 0.15 | 370-400 | 0.129±0.001 | 84.1±0.3 | 0.050±0.001 | 5.4±0.2 | 0.0034 |
| PBP-Cht | PB(pNP)PC | 0.15 | > 370 | 0.088±0.001 | 84.8±0.3 | 0.072±0.002 | 6.0±0.3 | 0.0046 |

The results shown for each conjugate present data obtained in a single experiment which is, in each case, representative of at least three separate, experiments all of which yielded similar results. Excitation was performed using a combination of filters which transmits a narrow band whose maximum lies at 315 nm (a glass filter Schott UG11 + a chemical filter composed of 0.027 gr $K_2C_rO_4$ + 0.1 gr $Na_2CO3$ in 100 ml water).

CPL measurements of the OP conjugates are shown in Fig. 29. The spectra of the aged conjugates derived from PBPDC and PB(pNP)PC are the same, within experimental error, and differ from the spectrum of the non-aged PBEP-Cht in both magnitude and sign. Several conclusions may be drawn: 1) The aged conjugate, PBP-Cht, prepared from two different organophosphates, is the same, demonstrating that the two different aging processes (Schemes I and II) indeed produce the same end product. 2) The excited active-site conformation of the aged and non-aged conjugates is different. The asymmetry induced in the pyrene fluorophore by its environment in the two conformations is of opposite screw sense. 3) The value of the emission anisotropy factor is not constant across the emission band. To a first approximation, $g_{em}$ of a homogeneous population of fluorophores is constant across the emission band if their emission originates in a single allowed electronic transition (31,32). Pyrene emission ($\tau$~100 nsec) does not stem from a fully allowed transition. Moreover, $g_{em}$, which is an inherent property of the emitting species, is concentration-dependent (see Fig. 28). The latter observation implies that another emitting species is formed by a bimolecular process. Thus the total emission spectrum is composed of monomer emission, which prevails at the blue edge of the spectrum, and of photodimer emission, which prevails at the red edge of the spectrum. It is worth noting that the absolute value of the emission anisotropy factor of the excimers is markedly greater than that of the monomers.

## CONCLUSIONS

1. The newly synthesized pyrenebutyl and dansylaminoethyl OP inhibitors were found to be suitable for the preparation of homologous pairs of aged and non-aged conjugates of AChE and α-Cht. $^{31}$P-nmr and optical spectroscopy, together with inhibition and reactivation studies, permitted detection of chemical and conformational differences between the homologous aged and non-aged conjugates of both AChE and α-Cht.

2. The same aged OP-Cht conjugate is obtained irrespective of the leaving group which is responsible for the phosphorylation or of the residue which is detached concomitantly with aging:

| | | |
|---|---|---|
| 8 + Cht | PB-O-P(O)(Cht)Cl | |
| 9 or 10 + Cht | PB-O-P(O)(Cht)pNP | PB-O-P(O)(Cht)O$^-$ |
| 11 or 12 + Cht | PB-O-P(O)(Cht)OPin | Aged enzyme |

PB: pyrenebutyl  pNP: p-nitrophenoxy  Pin: pinacolyl

The formation of the same aged conjugate by use of different inhibitors provides strong evidence for the presence of a P-O$^-$ bond in the corresponding OP-Cht conjugate, since only this product is to be expected as a common end-product of the reactions depicted above.

3. The optical spectroscopy data indicate significant differences in the orientation of the fluorophore with respect to the polypeptide backbone on comparison of the aged and non-aged forms of pyrenebutyl-OP-Cht, of pyrenebutyl-OP-AChE and of dansyl-OP-AChE. In the case of pyrenebutyl-OP-Cht and dansyl-OP-AChE, the fluorescence intensities of the aged conjugates are lower than those of the corresponding non-aged conjugates, suggesting a stronger interaction of fluorophore with the polypeptide in the latter. In the case of the pyrenebutyl-OP-AChE conjugates, the aged conjugate displays a higher fluorescence intensity than the non-aged conjugate. This may be interpreted as indicating a stronger interaction with the polypeptide backbone of the fluorophore in the non-aged, relative to the aged, pyrenebutyl-OP-AChE conjugate. However, the possibility of preferential oxygen quenching of the pyrene fluorophore in the non-aged OP-AChE conjugate cannot be excluded.

4. The resistance of the aged conjugates to reactivation may be ascribed either to the electrostatic repulsion of a nucleophile reactivator by the P-O$^-$ bond, to the conformational changes around the phosphoryl residue, which make it less accessible to the nucleophile reactivator, or to a combination of the two mechanisms.

5. Preliminary evidence indicates that when aging involves removal of an alkyl group, this process may be accompanied by concomitant alkylation of an adjacent amino acid residue. This alkylation may provide an additional barrier to reactivation of the aged enzyme.

6. During the period of research covered by this report, two unexpected observations were made which are worth mentioning:

   a. In contrast to α-Cht, AChE was found to possess a second binding site (in addition to the catalytic site) for pyrenebutyl inhibitors which also contain a pinacolyl substituent. Binding to this second site is non-covalent.

   b. Concentrated solutions of pyrenebutyl-OP-Cht conjugates (>0.1 mg/ml) form photo-dimers (excimers).

## REFERENCES


1) Characterization by nmr and fluorescence spectroscopy of differences in the conformation of non-aged and aged organophosphoryl conjugates of AChE, (1984) Ashani, Y. and Silman, I. Annual Summary Report 1 - 1 September 1983-31 August 1984, for Grant No. DAMD17-83-G-9548. Submitted to USAMRD, Fort Detrick, Frederick, MD.

2) Novel pyrene-containing organophosphates as fluorescent probes for studying aging-induced conformational changes in organophosphate-inhibited acetylcholinesterase, (1982) Amitai, G., Ashani, Y., Gafni, A. and Silman, I., Biochemistry 21, 2060-2069.

3) The inhibition of acetylcholinesterase by organophosphorus compounds containing a P-Cl bond, (1974) Wins, P. and Wilson, I.B., Biochim. Biophys. Acta 334, 137-145.

4) Physico-chemical characterization of atropinesterase from Pseudomonas putida: A comparison with other serine hydrolases, (1983) Van der Drift, A.C.M., Ph.D. Thesis, Univ. of Utrecht.

5) "Photophysics of Aromatic Molecules", (1970) Birks, J.B., Wiley Interscience, 128-129.

6) Fluorescent organophosphates: Novel probes for studying aging-induced conformational changes in inhibited acetyl-cholinesterase and for localization of cholinesterase in nervous tissue, (1980) Amitai, G., Ashani, Y., Shahar, A., Gafni, A. and Silman, I., Monogr. Neurol. Science 7, 70-84.

7) Ligand-induced conformational changes in AChE investigated with fluorescent phosphonates, (1979) Epstein, D.J., Berman, H.A. and Taylor, P., Biochemistry 18, 4749-4754.

8) Phosphate and carbonate esters: "Aging" reactions with αCht. Kinetics and Mechanism, (1972) Bender, M.L. and Wedler, F.C., J. Amer. Chem. Soc. 94, 2101-2109.

9) Reactivation and aging of diphenyl phosphoryl acetylcholinesterase, (1975) Maglothin, J.A., Wins, P. and Wilson, I.B., Biochim. Biophys. Acta 403, 370-387.

10) "Enzyme Inhibitors as Substrates", (1972) Aldridge, W.N. and Reiner, E., North-Holland Pub. Co.

11) Novel fluorescent organophosphates as probes for studying aging-induced conformational changes in inhibited AChE, (1980) Amitai, G., Ph.D. Thesis, Weizmann Institute of Science, Israel.

12) A new and rapid colorimetric determination of AChE activity, (1961) Ellman, G.L., Courtney, K.D., Andres, V. and Featherstone, R.M., Biochem. Pharmacol. 7, 88-95.

13) The influence of pH on the kinetic constants of α-Cht-catalysed hydrolysis, (1956) Cunningham, L.W. and Brown, C.S., J. Biol. Chem. 221, 287-299.

14) Acetylcholinesterase, (1974) Dudai, Y. and Silman, I. Methods in Enzymology 34, 571-580.

15) The spectrophotometric determination of the operational normality of an α-Cht solution, (1961) Schonbaum, G.R., Zerner, B. and Bender, M.L., J. Biol. Chem. 236, 2930-2935.

16) The design of reactivators for irreversibly blocked AChE, (1971) Wilson, I.B. and Froede, H.C. in Drug Design (Ariens, E.J., ed.), Vol. 2, 213-229, Academic Press, N.Y.

17) The inhibition of cholinesterase by diethyl phosphorochloridate, (1972) Ashani, Y., Wins, P. and Wilson, I.B., Biochim. Biophys. Acta, 284, 427-434.

18) An improvement of nanosecond fluorimeters to overcome drift problems, (1974) Hazan, G., Grinvald, A., Maytal, M. and Steinberg, I.Z., Rev. Sci. Instrum 45, 1602-1604.

19) On the analysis of fluorescence decay kinetics by the method of least-squares, (1974) Grinvald, A. and Steinberg, I.Z., Anal. Biochem. 59, 583-598.

20) Sensitive instrument for the study of circular polarization of luminescence, (1972) Steinberg, I.Z. and Gafni, A., Rev. Sci. Instrum. 43, 409-413.

21) Binding sites on AChE for reversible ligands and phosphorylating agents, (1984) Radic, Z., Reiner, E. and Simeon, V., Biochem. Pharmacol. 33, 671-677.

22) Hydrolysis by acetylcholinesterase, (1980) Hassan, F.B., Cohen, S.G. and Cohen, J.B. J. Biol. Chem. 255, 3898-3904.

23) 1-Bromopinacolone, an active-site-directed covalent inhibitor for AChE, (1982), Cohen, S.G., Leiberman, D.L., Hassan, F.B. and Cohen, J.B., J. Biol. Chem. 257, 1408714092.

24) Fluorescent phosphonate label for serine hydrolases, pyrenbutyl methylphosphonofluoridate, reaction with AChE, (1978) Berman, H.A. and Taylor, P., Biochemistry 17, 1704-1713.

25) Mechanisms of nucleophilic substitution in phosphate esters, (1964), Cox, J.R. and Ramsay, O.B., Chem. Rev. 64, 317-352.

26) Aminoalkylphosphonofluoridate derivatives: Rapid and potentially selective inactivators of serine peptidases, (1983) Lamden, L.A. and Bartlett, P.A., Biochem. Biophys. Res. Comm. 1085-1090.

27) Studies on the reactivation of diethylphosphorylchymotrypsin, (1960) Cohen, W. and Erlanger, B.F. J. Amer. Chem. Soc. 82, 3928-3934.

28) Alkylation reaction of organophosphorus pesticides: Its chemical and biochemical significance, (1970) Eto, M. and Ohkawa, H. in "Biochemical Toxicology of Insecticides", 93-104, Pergamon Press, N.Y.

29) Responses of acetylcholinesterase from Torpedo Marmorata to salts and curarizing drugs, (1966) Changeux, J.-P. Mol. Pharmacol. 2, 369-392.

30) "Photoluminoscence of Solutions", (1968) Parker, C.A., Elsevier.

31) Circularly polarized luminescence, (1978) Steinberg, I.Z., Methods in Enzymology 49, 179-198.

32) Fluorescence polarization: Some trends and problems, (1975) Steinberg, I.Z. in "Concepts in Biochemical Fluorescence" (Chen, R.F. and Edelhoch, H. eds.), Vol. I, 79-113, Marcel Dekker, N.Y.

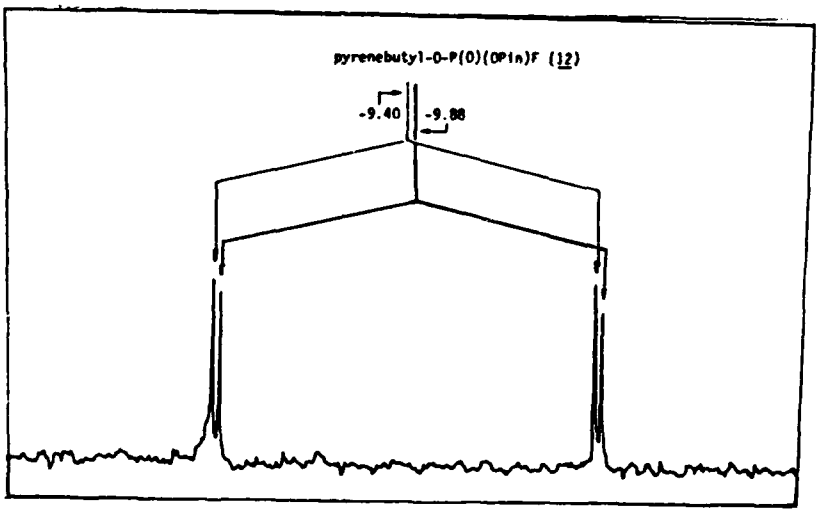


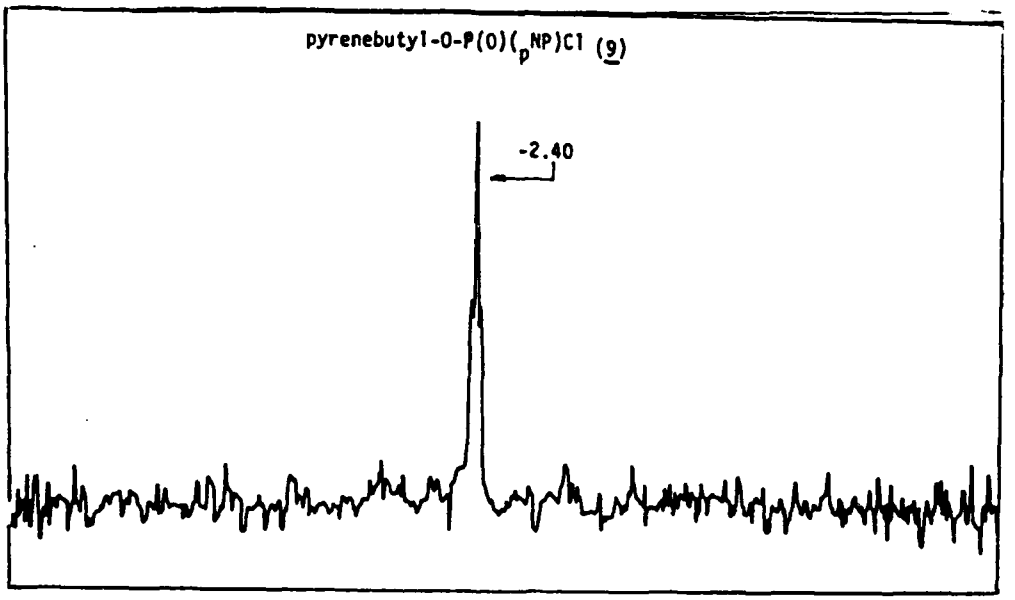


Fig. 1: $^{31}P$-nmr spectra of the pyrenebutyl-containing OP's 9 (in $C_6H_6$) and 12 (in diethylether-$CH_2Cl_2$). The negative signs for chemical shifts indicate an upfield shift relative to $H_3PO_4$. The triplet in the spectrum of 9 is due to $CH_2O$ ($^1H$-undecoupled). $J_{P-F}$ for 12: 974 Hz. The doubling of the resonance is due to the presence of two chirality centers.

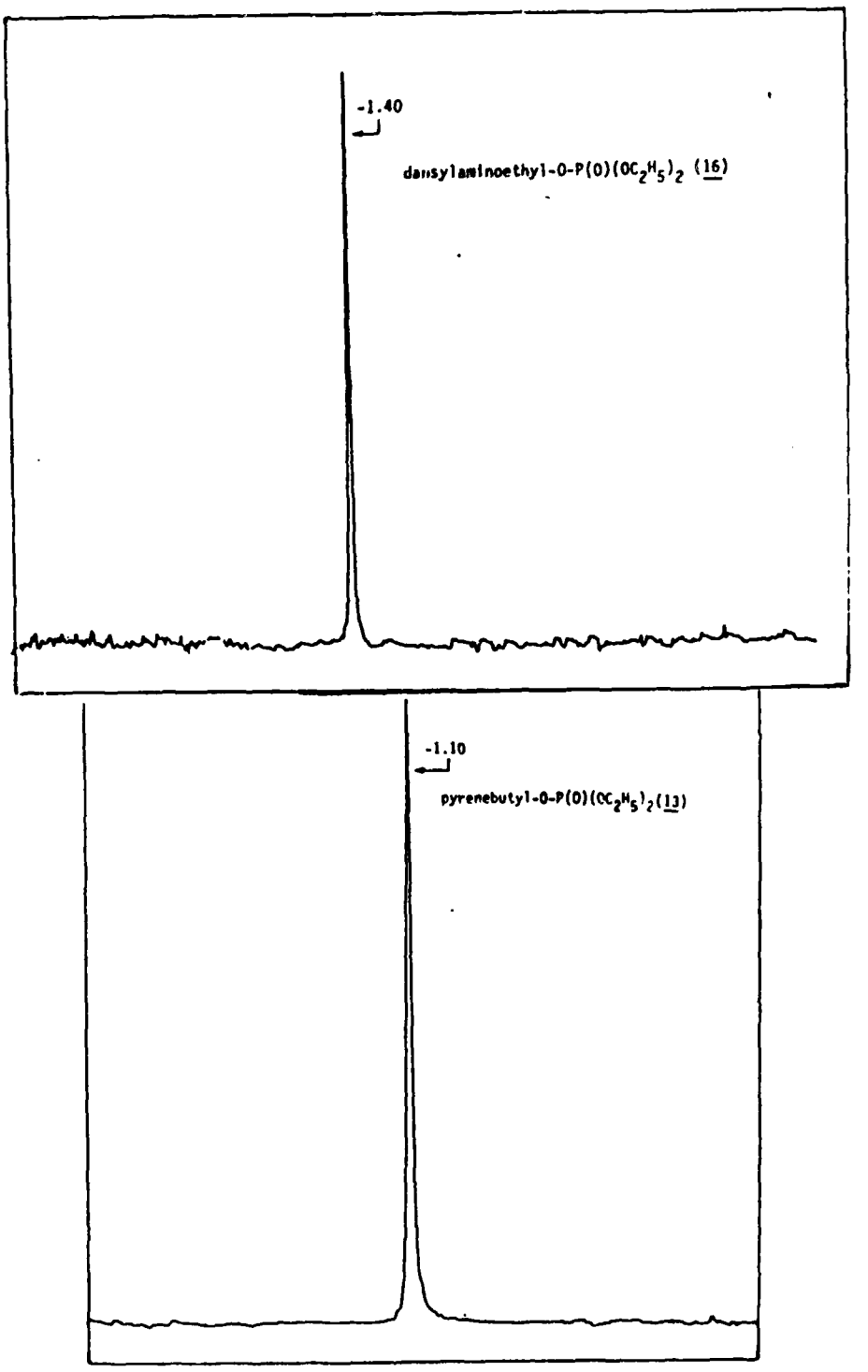


Fig. 2: $^{31}$P-nmr spectra (in diethylether) of diethylphosphates containing either pyrenebutyl (13) or dansylaminoethyl (16) residues. The negative signs for the chemical shifts indicate upfield shifts relative to $H_3PO_4$.

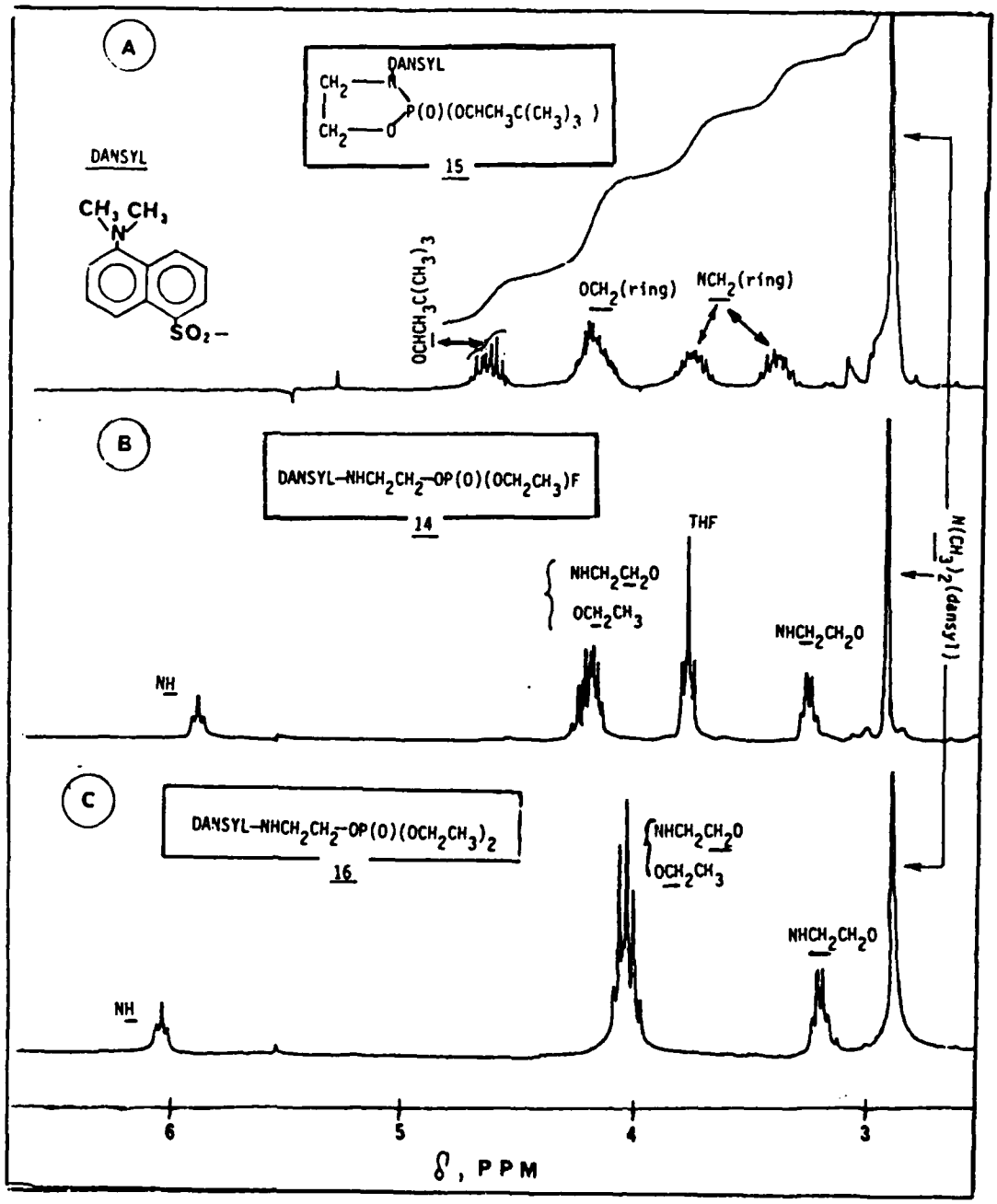


Fig. 3: $^1$H-nmr spectra of dansyl-containing OP ligands. Chemical shifts are relative to TMS. The tetrahydrofuran (THF) signal (B) stems from the solvent which was not removed.

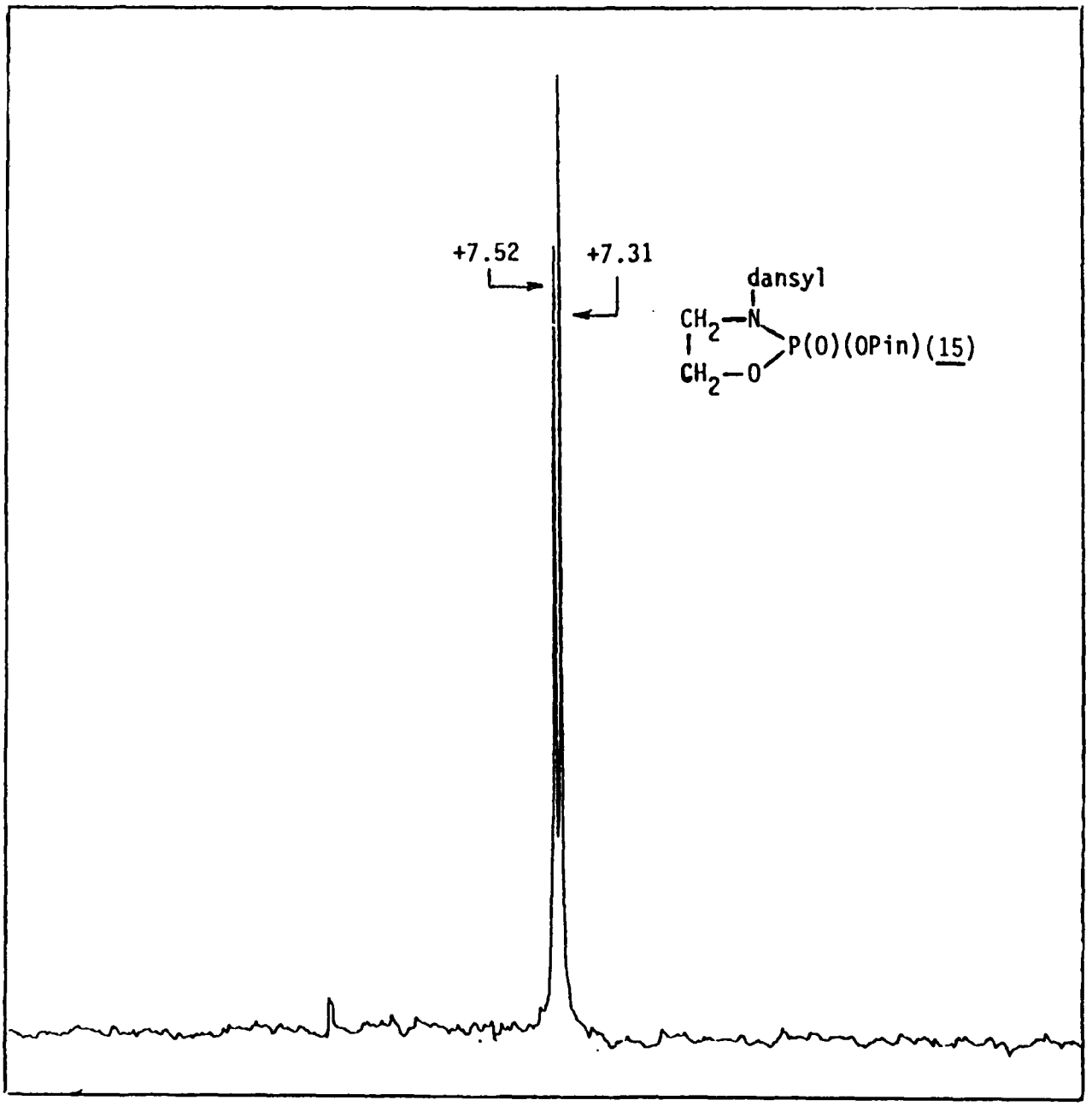


Fig. 4: $^{31}P$-nmr spectrum (in $CDCl_3$) of the dansyl-containing DPinPO (15). The doubling of the resonance stems from the diasteroisomeric mixture. The positive chemical shifts indicate a downfield shift relative to $H_3PO_4$.

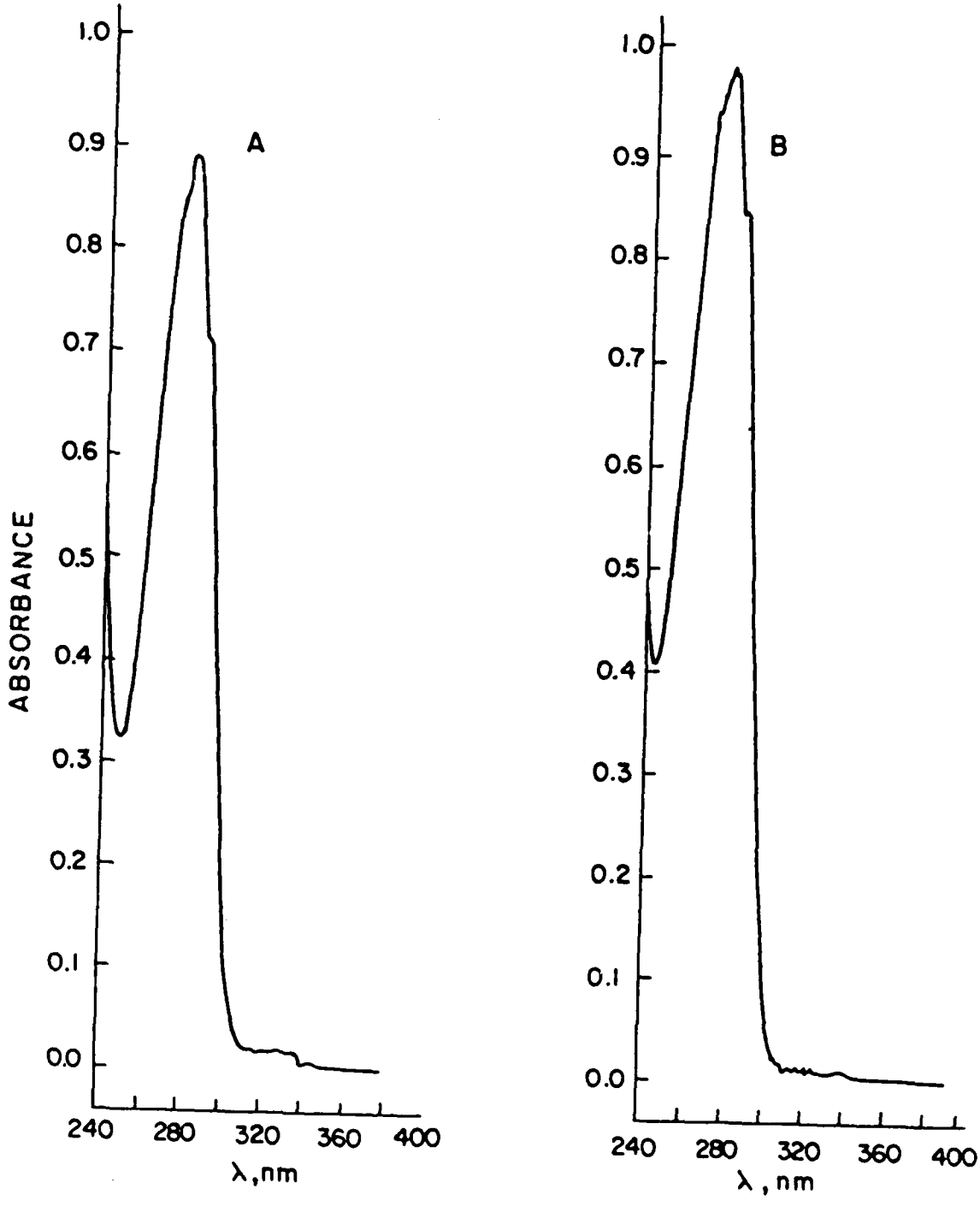


Fig. 5: Absorbance spectra of samples of α-Cht which were pretreated with DFP (5) prior to incubation with either PBEPF (6, A) or $PB(pNP)_2P$ (10, B), followed by separation of unbound fluorescent ligand by gel filtration on a Sephadex G-10 column.

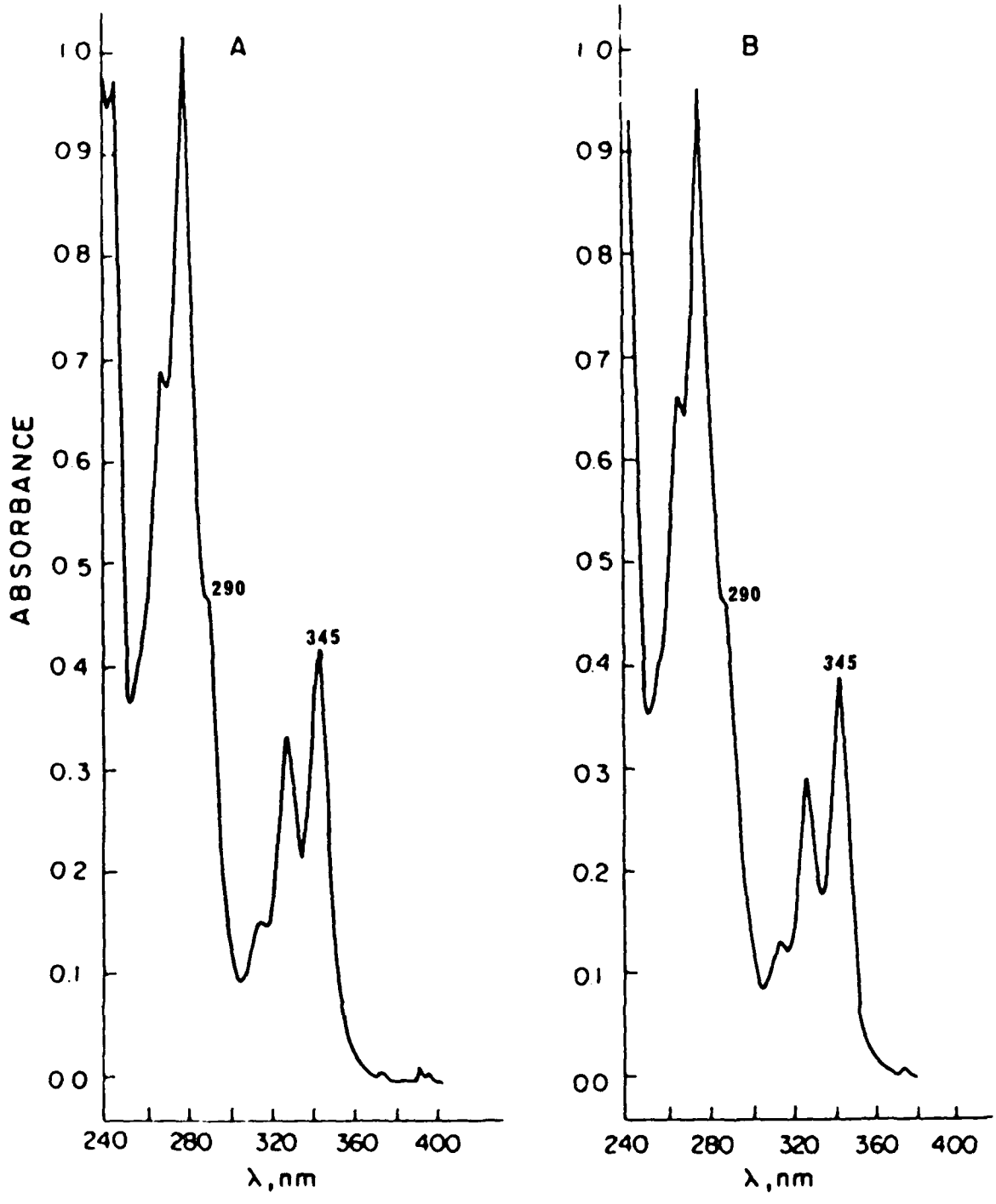


Fig. 6: Absorbance spectra of fluorescent OP-Cht conjugates after unbound fluorophore had been removed by gel filtration on Sephadex G-10 followed by lyophilization.
A: PBP-Cht prepared from PBPinPC (11).
B: PBP-Cht prepared from PBPDC (8).

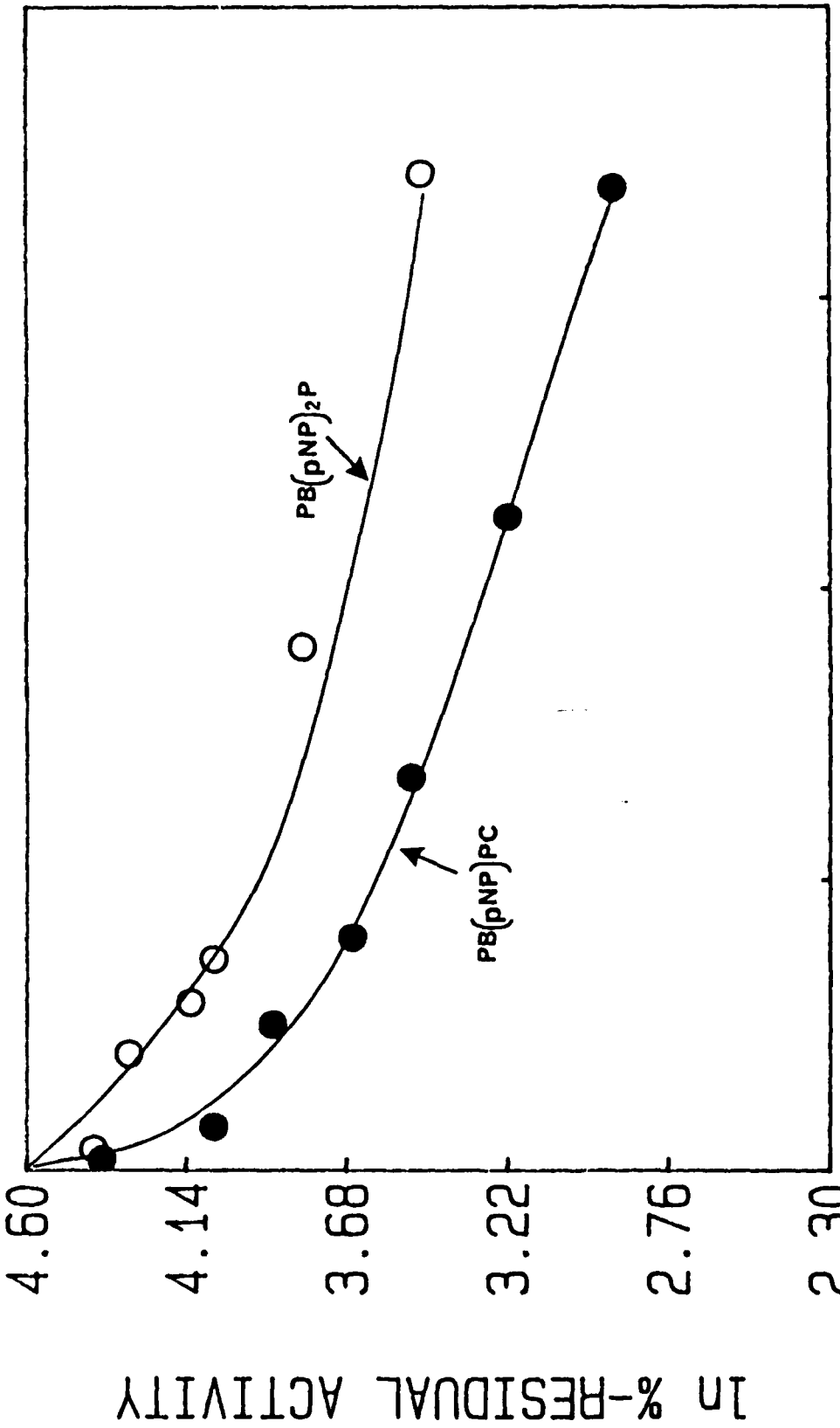


Fig. 7: First-order plots for the inhibition of AChE by 0.12 mM PB(pNP)PC (9) and 0.27 mM $PB(pNP)_2P$ (10) in 0.05 M phosphate, pH 7.0, 25°C, 1% dioxane.

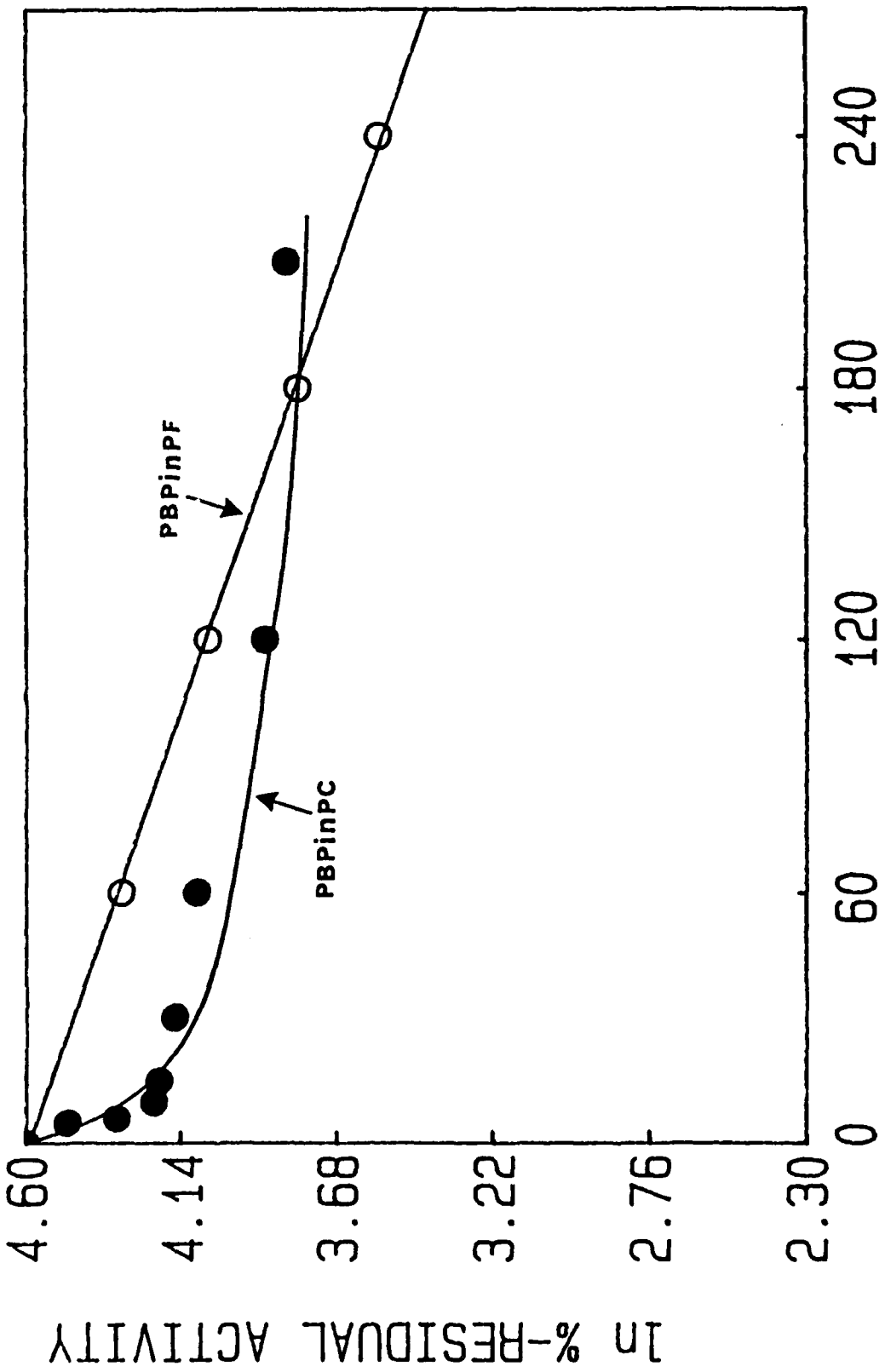


Fig. 8. First-order plot for the inhibition of AChE in the presence of 0.43 mM PBPinPC (11) and 0.017 mM PBPinPF (12) (0.05 M phosphate, pH 7.0, 25°C, 1% dioxane).

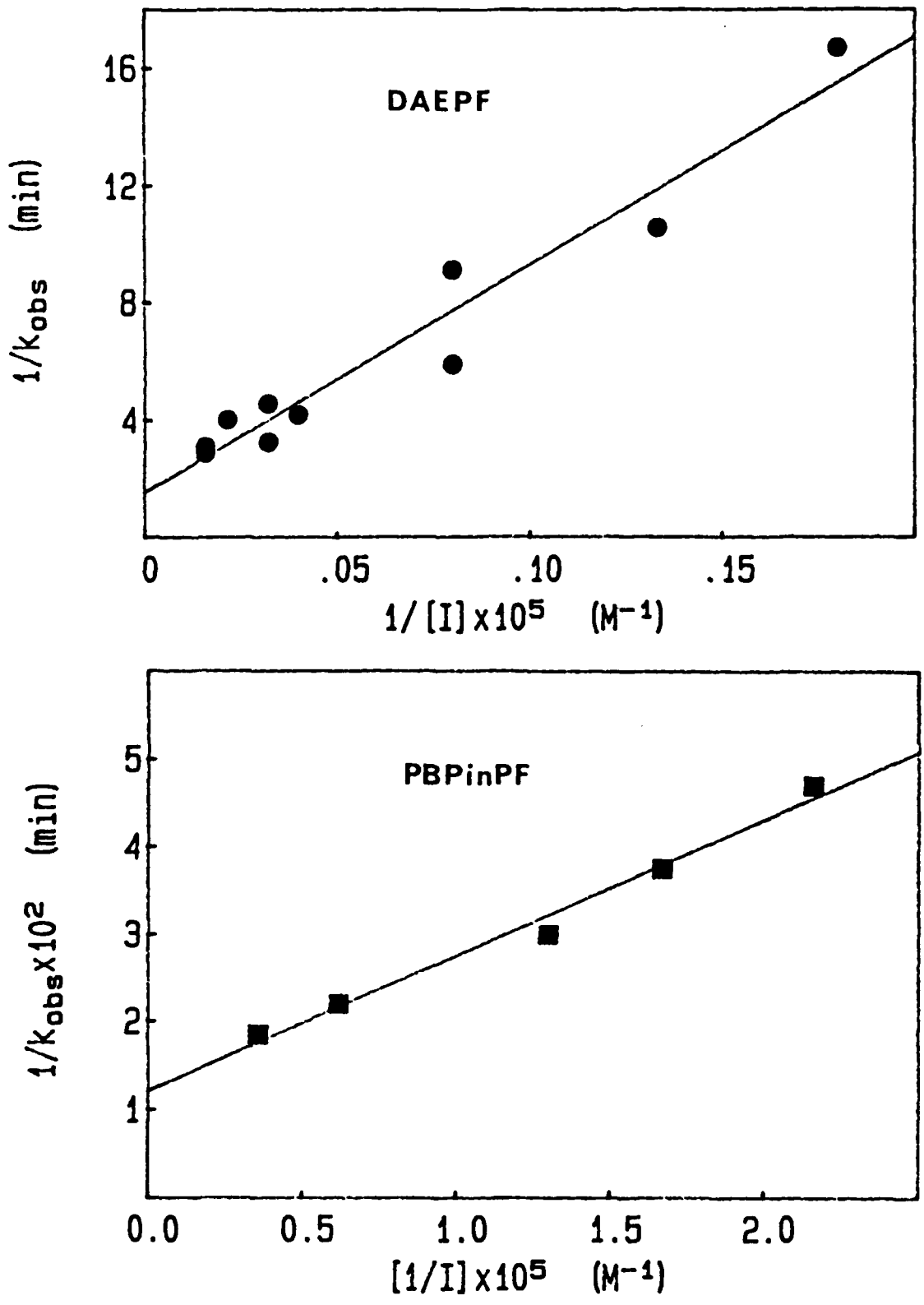


Fig. 9: The evaluation of $K_I$, k' and $k_i$ for the inhibition of AChE by PBPinPF (12) and DAEPF (14) according to eqn. 2 (0.05 M phosphate, pH 7.0, 25°C).

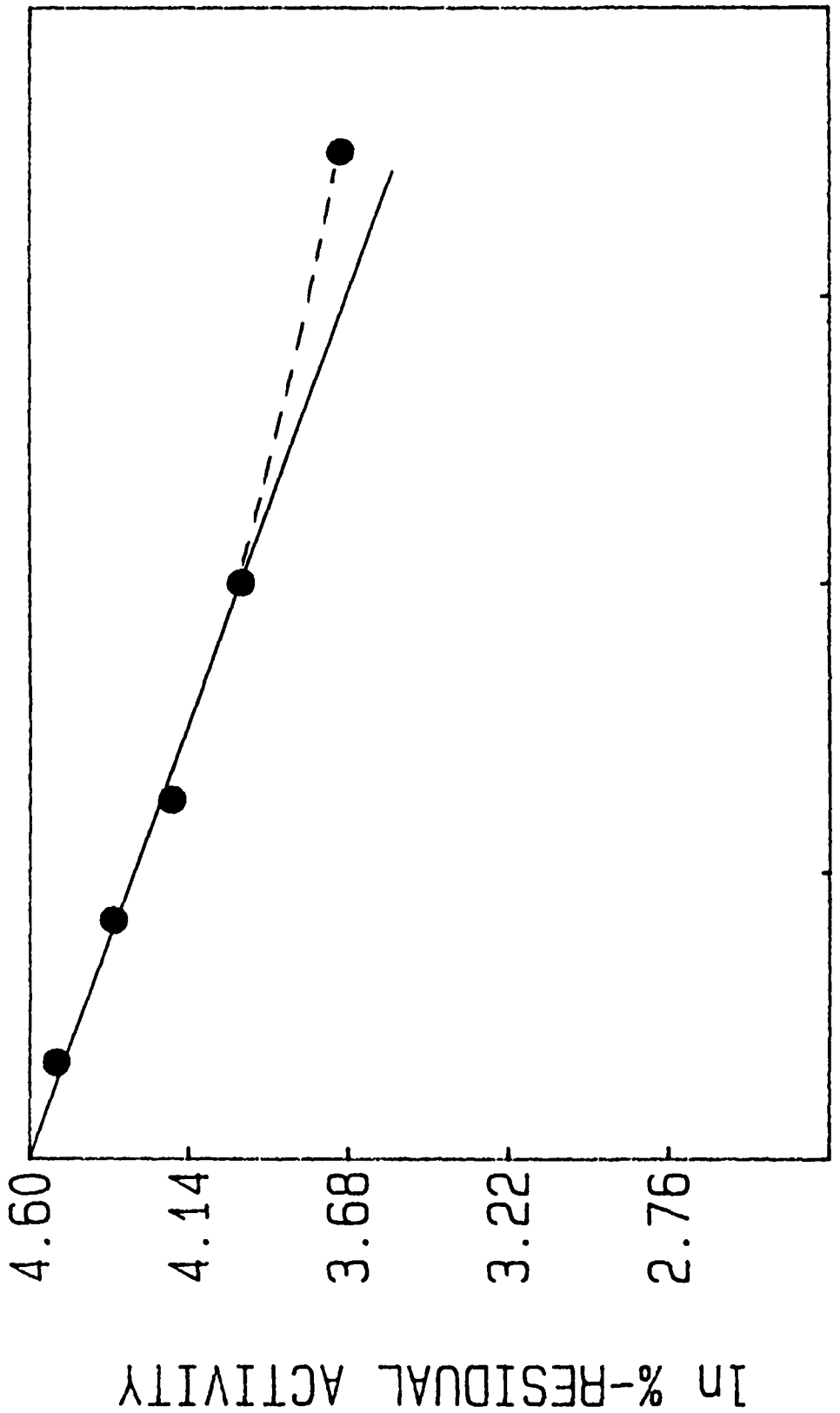


Fig. 10: First-order plot for the inhibition of AChE by 0.072 mM DAEPF (14) in phosphate buffer (0.05 M, pH 7.0, 25°C). The deviation from linearity results from loss of anti-ChE potency due to hydrolysis of the inhibitor.

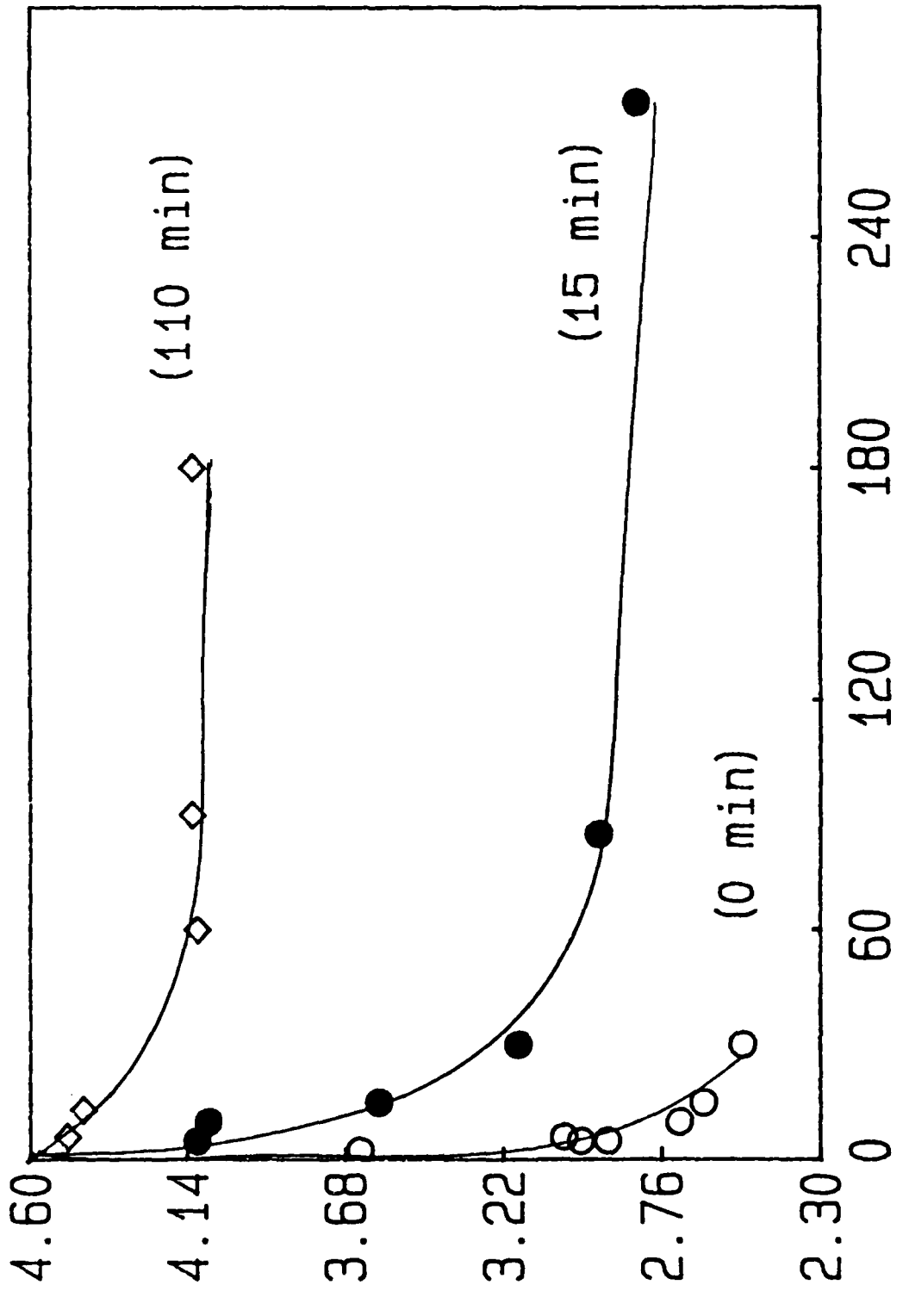


Fig. 11: First-order plot for the inhibition of AChE by 0.068 mM DPinPO (15) in 0.05 M phosphate, pH 7.0, 25°C. Prior to dilution into the AChE solution at the final concentration (0.068 mM), the DPinPO was pre-incubated in the same buffer (0.05 M phosphate, pH 7.0) at 6.8 mM for the times indicated in parentheses for each trace.

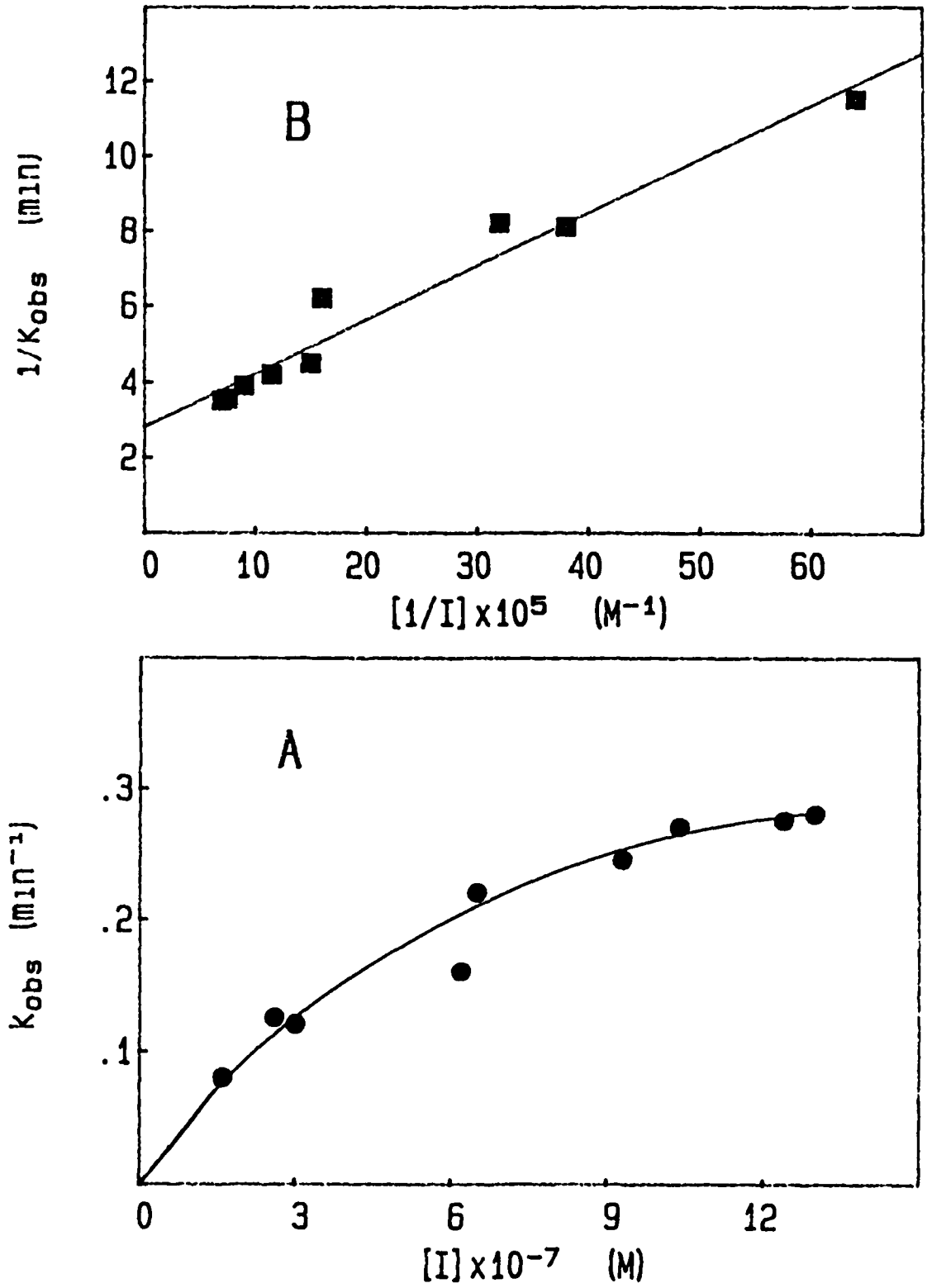


Fig. 12: The evaluation of $K_I$, k' and $k_i$ for inhibition of α-Cht by PBEPF (6) (2 mM Tris-0.1 M KCl pH 7.8, 25°C, $CH_3CN$ < 2%). A: Plot of $k_{obs}$ vs. PBEPF concentration. B: Double-reciprocal plot according to eqn. 2.

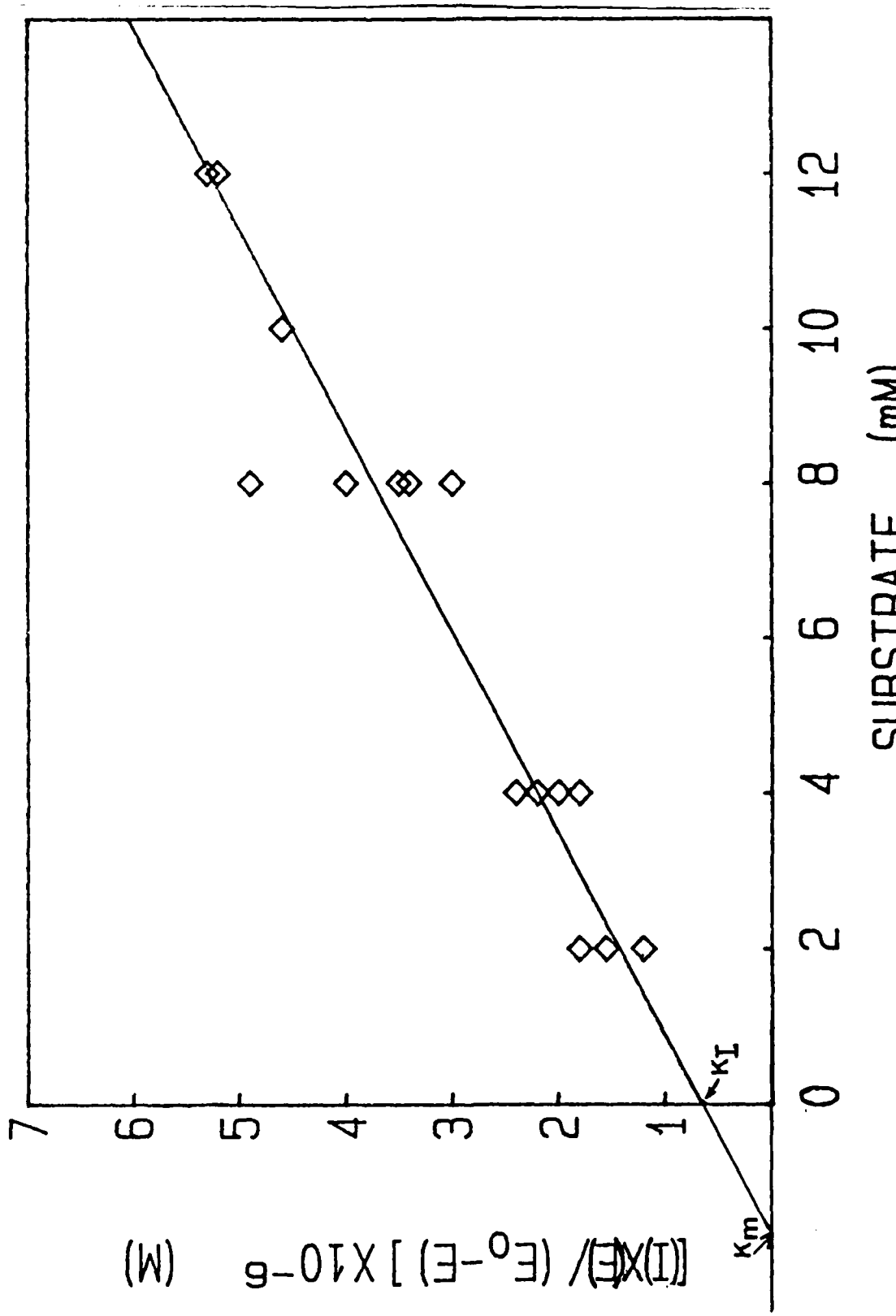


Fig. 13: The effect of substrate (ATEE) on the reversible inhibition of α-Cht by PBEPF (6) according to eqn. 4 (2 mM Tris-0.1 M KCl, pH 7.8, 25°C).

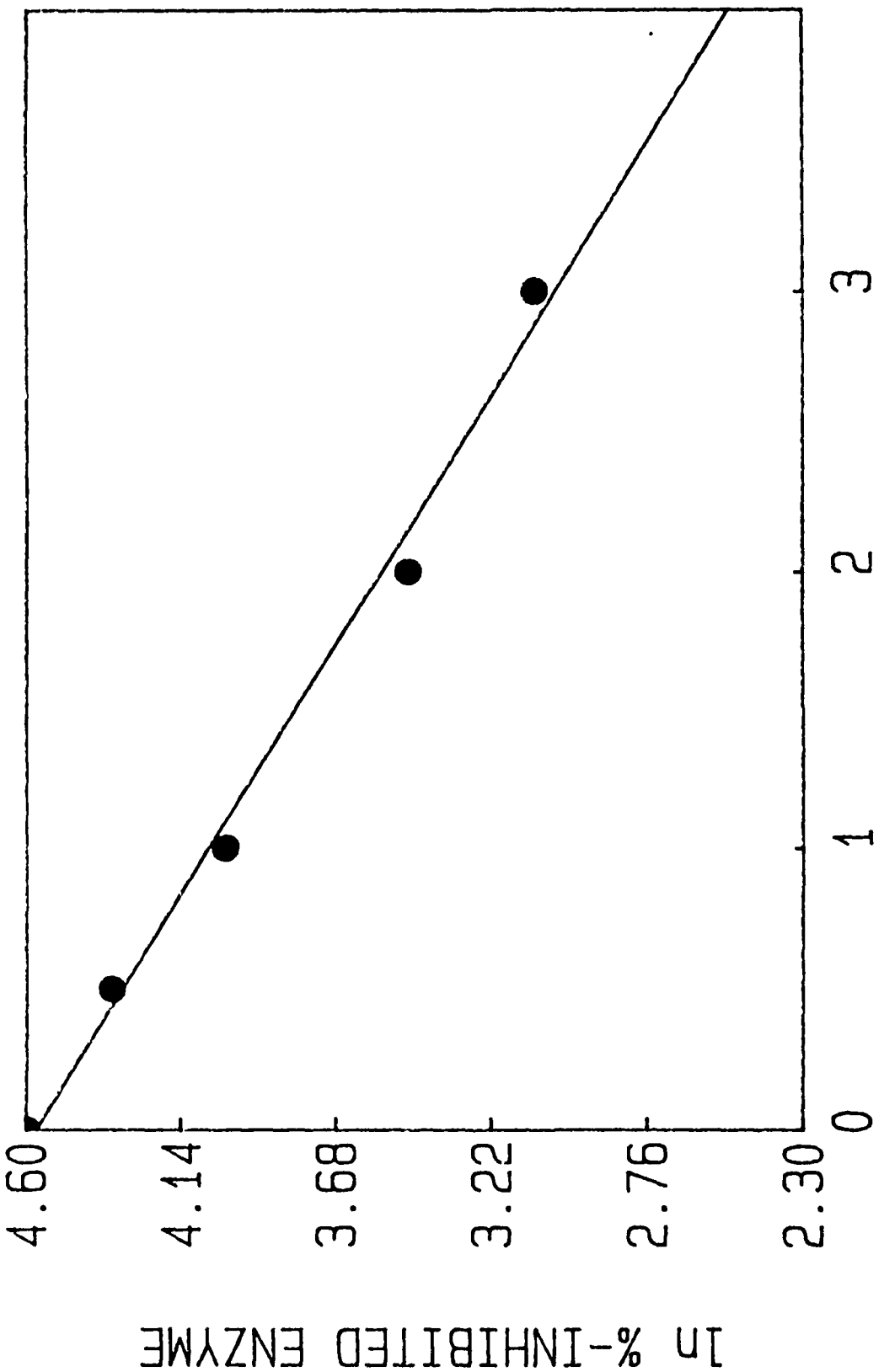


Fig. 14: First-order plot for the reactivation of DAEP-AChE by 0.025 mM 2-PAM (0.05 M phosphate, pH 7.0, 25°C).

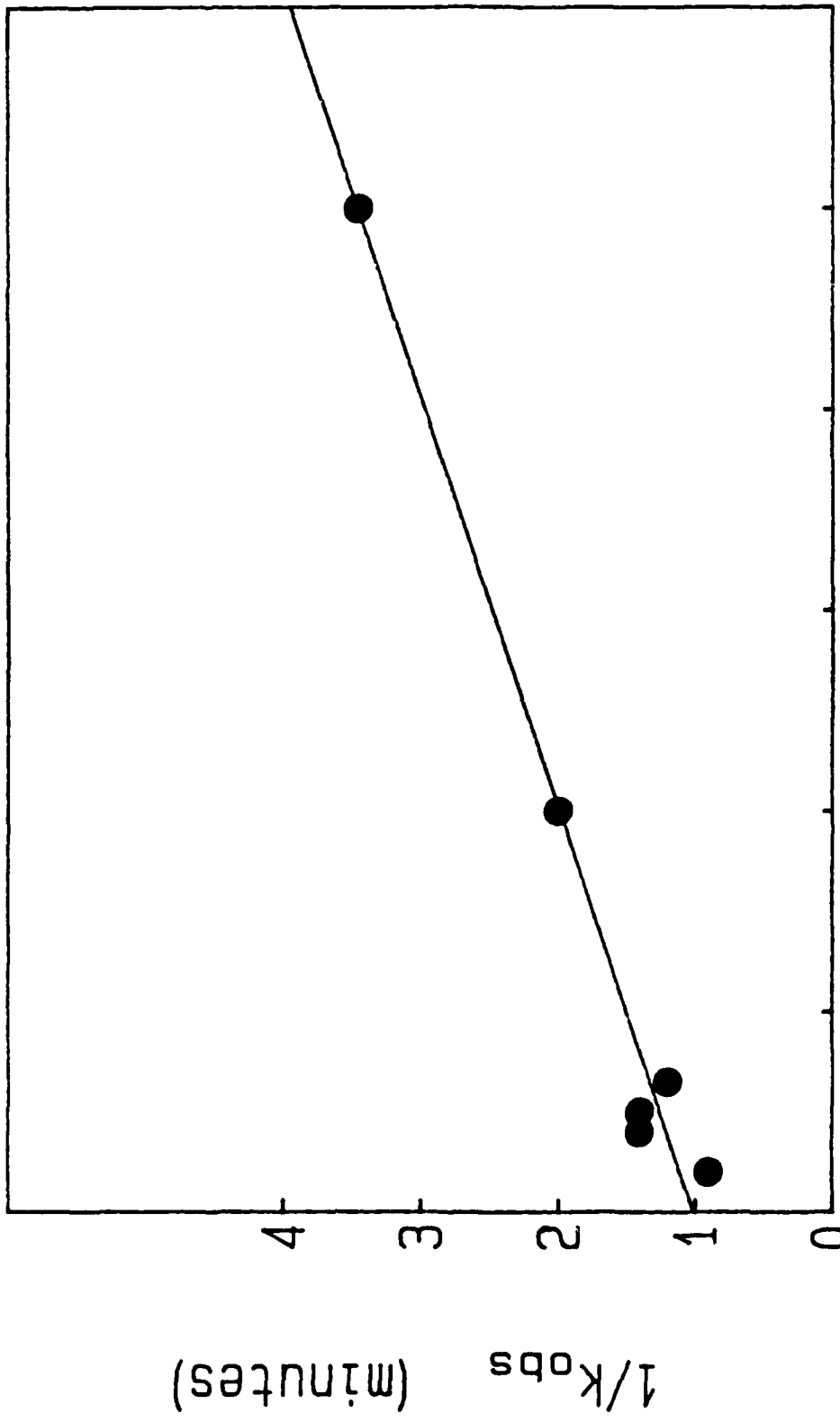


Fig. 15: Double-reciprocal plot, according to eqn. 2, for the reactivation of DAEP-AChE by 2-PAM in phosphate buffer (0.05 M, pH 7.0, 25°C)

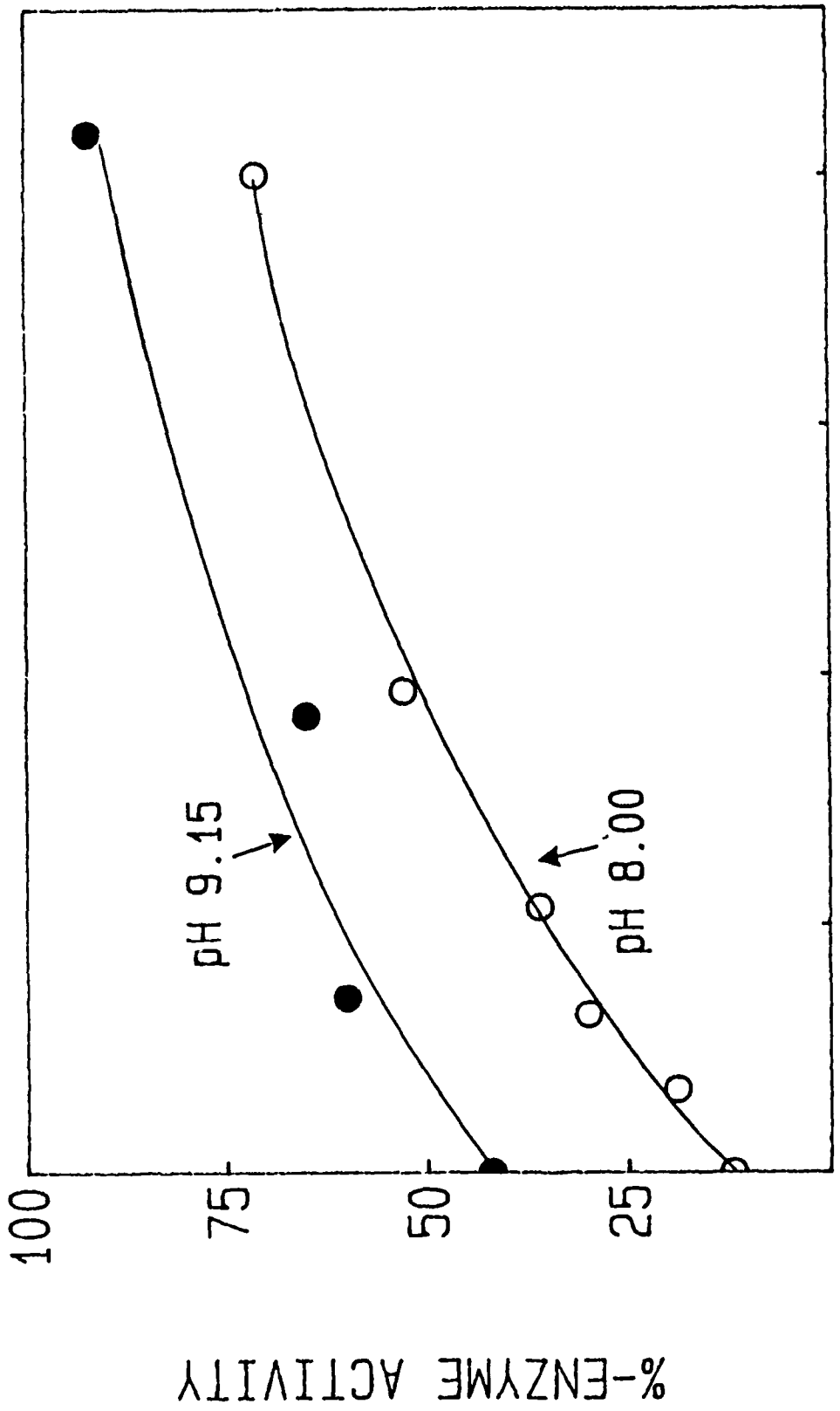


Fig. 16: Reactivation profile of AChE inhibited by 0.15 mM DPinPO (15) at pH 10.3 (0.05 M carbonate, 4°C) followed by 200-2000-fold dilution into 1 mM 2-PAM solution at pH 8.0 or 9.15 (0.05 M Tris, 25°C).

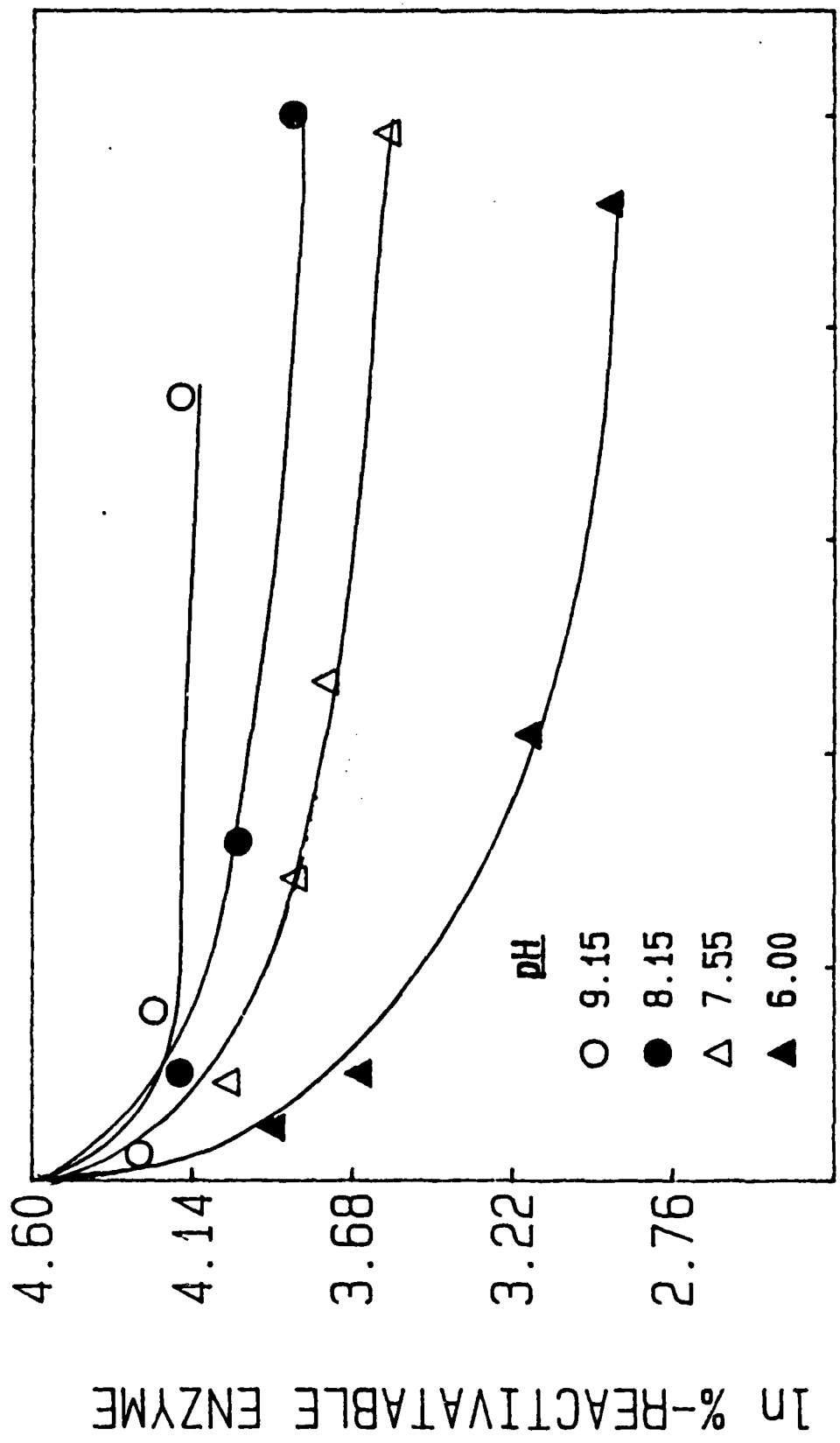


Fig. 17: The effect of pH on the rate of aging of DAP-AChE. AChE was inhibited by DPInPO (15) in carbonate buffer (0.05 M, pH 10.3) prior to dilution into the aging medium. At appropriate time intervals samples were further diluted into 1 mM 2-PAM (in 0.05 M phosphate, pH 8.0, 25°C) and incubated for 16 hours prior to assay.

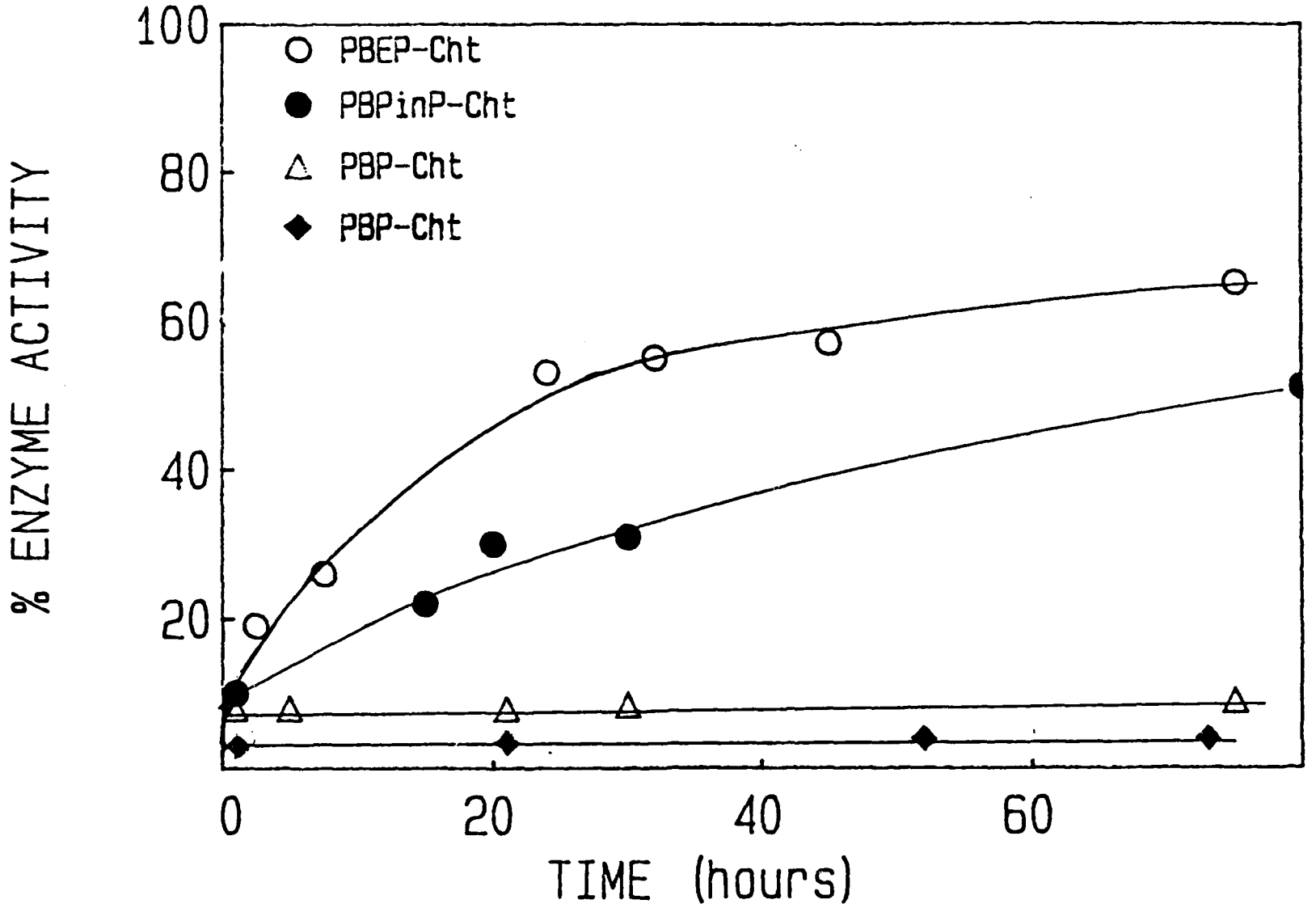


Fig. 18: Reactivation profiles of OP-Cht conjugates in the presence of 0.1 M 3-PAM in 2 mM Tris, pH 7.0, 25°C. The OP-Cht conjugates were prepared from: O——O, PBEPF (16); ●——● , PBPinPC (11); Δ——Δ, $PB(pNP)_2P$ (10); ◆——◆ , PBPDC (8).

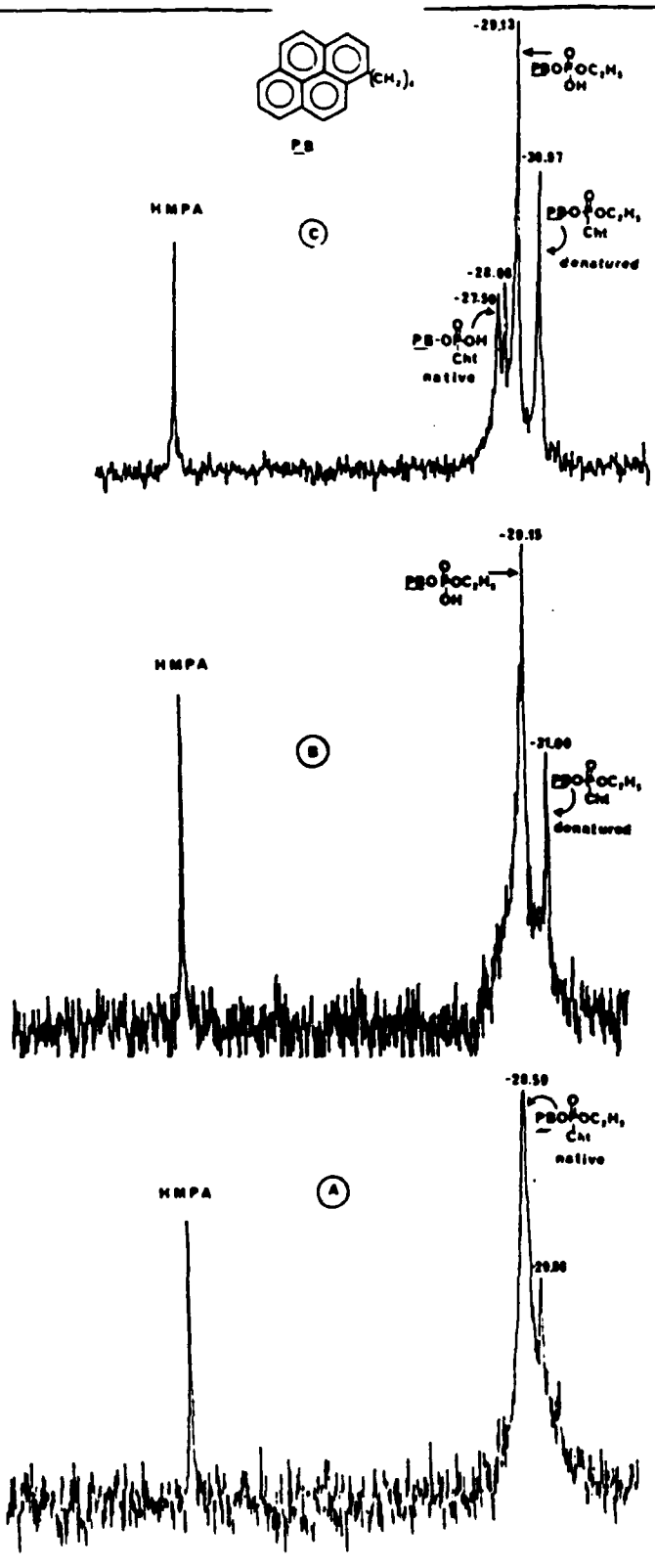


Fig. 19: $^{31}$P-nmr spectra of pyrenebutyl-OP(O)($OC_2H_5$)Cht in the presence of 0.1 M 3-PAM (2 mM Tris, pH 7.0, 25°C)
A. Before initiation of reactivation.
B. After 48 hr incubation with 3-PAM.
C. After 5 days incubation with 3-PAM.

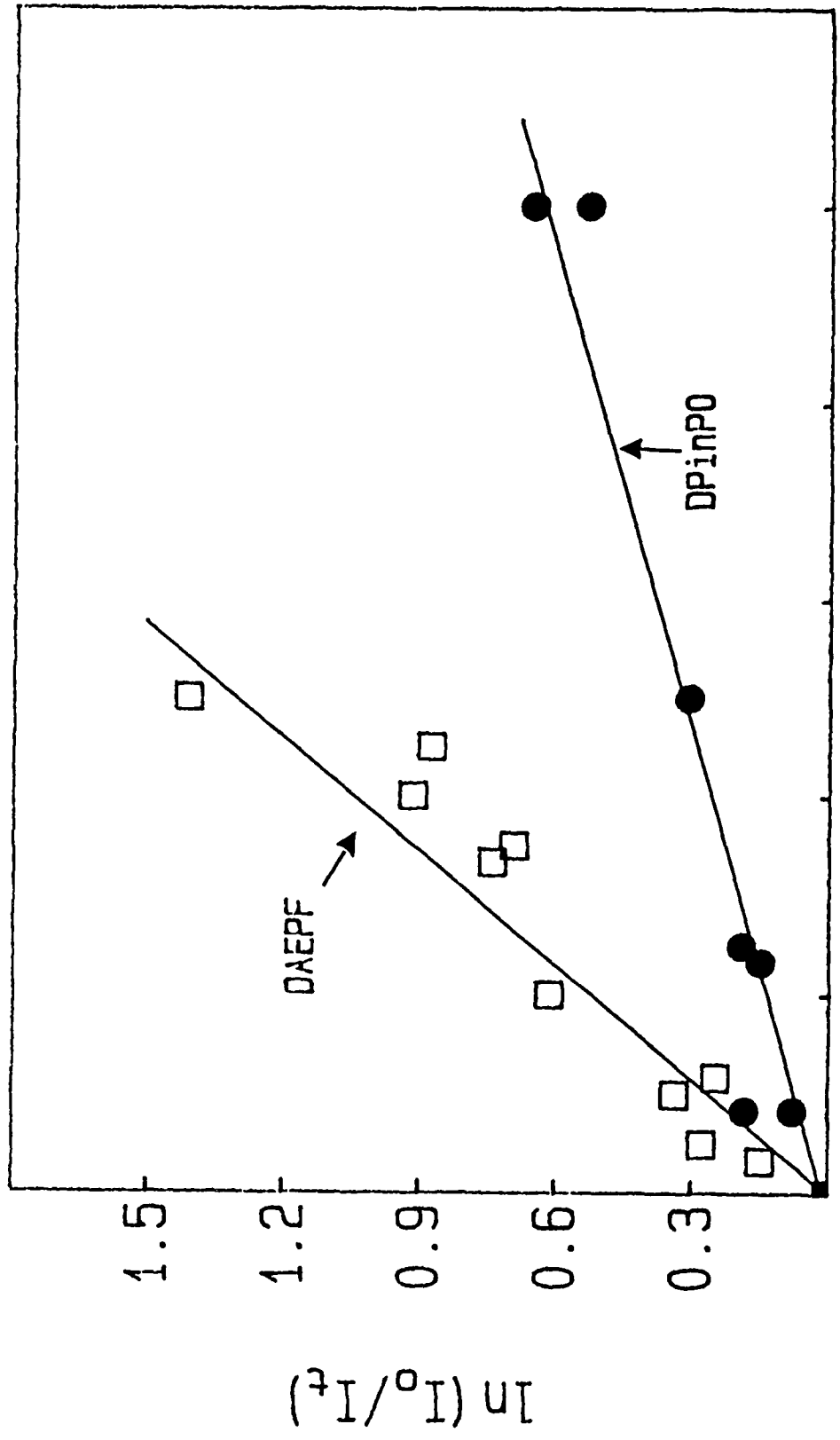


Fig. 20 Determination of the rate constants for the hydrolysis of DAEPF (14) and DPinPO (15) in phosphate buffer (0.05 M, pH 7.0, 25°C) by determination of the rate of loss of anti-ChE activity according to eqn. 5.

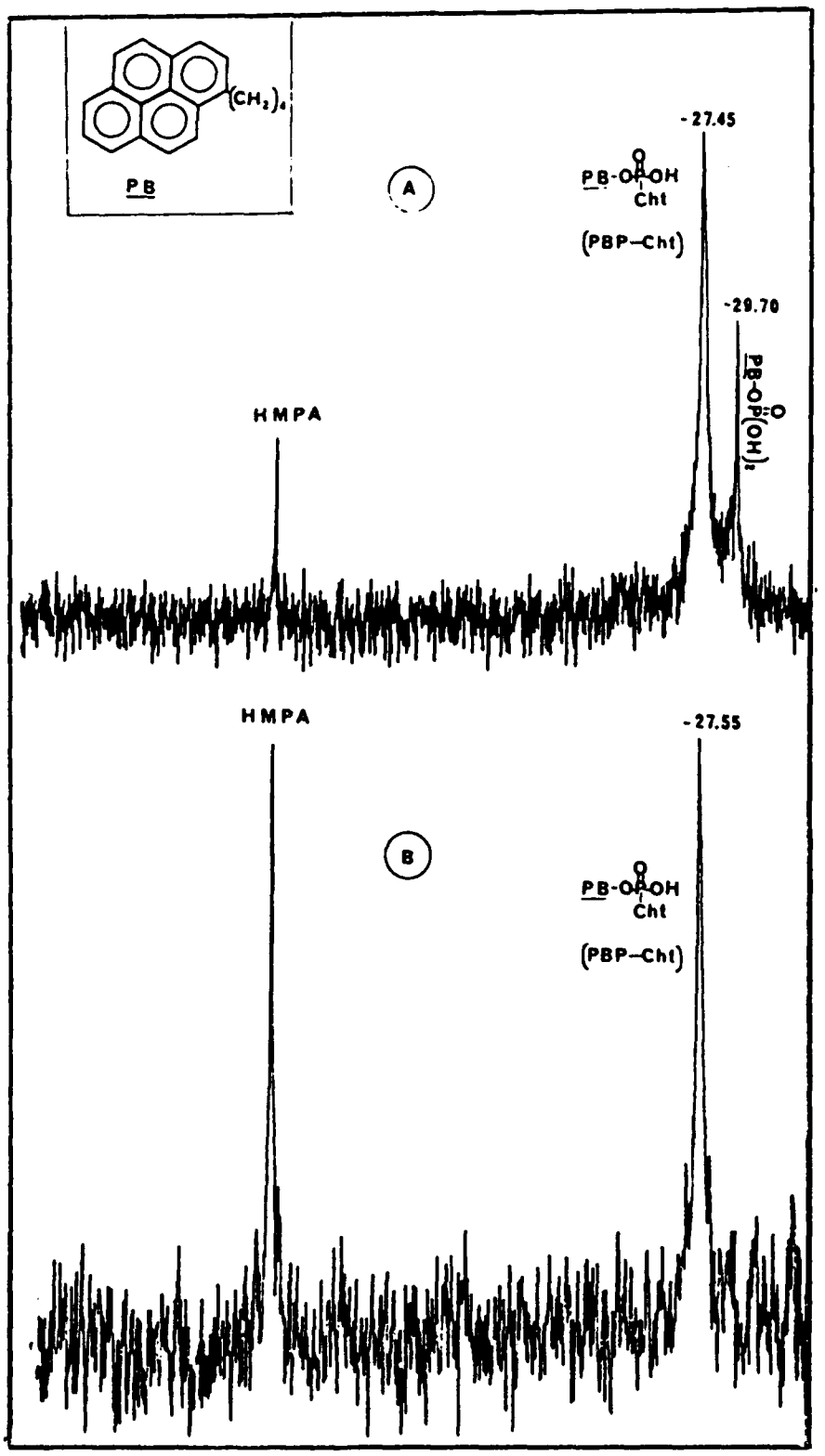


Fig. 21: $^{31}$P-nmr spectra of aged OP conjugates of Cht obtained with either PBPDC (8, A) or PB(pNP)$_2$P (10, B). Negative signs indicate an upfield chemical shift relative to HMPA. The diacid signal (A) stems from unremoved hydrolyzed inhibitor.

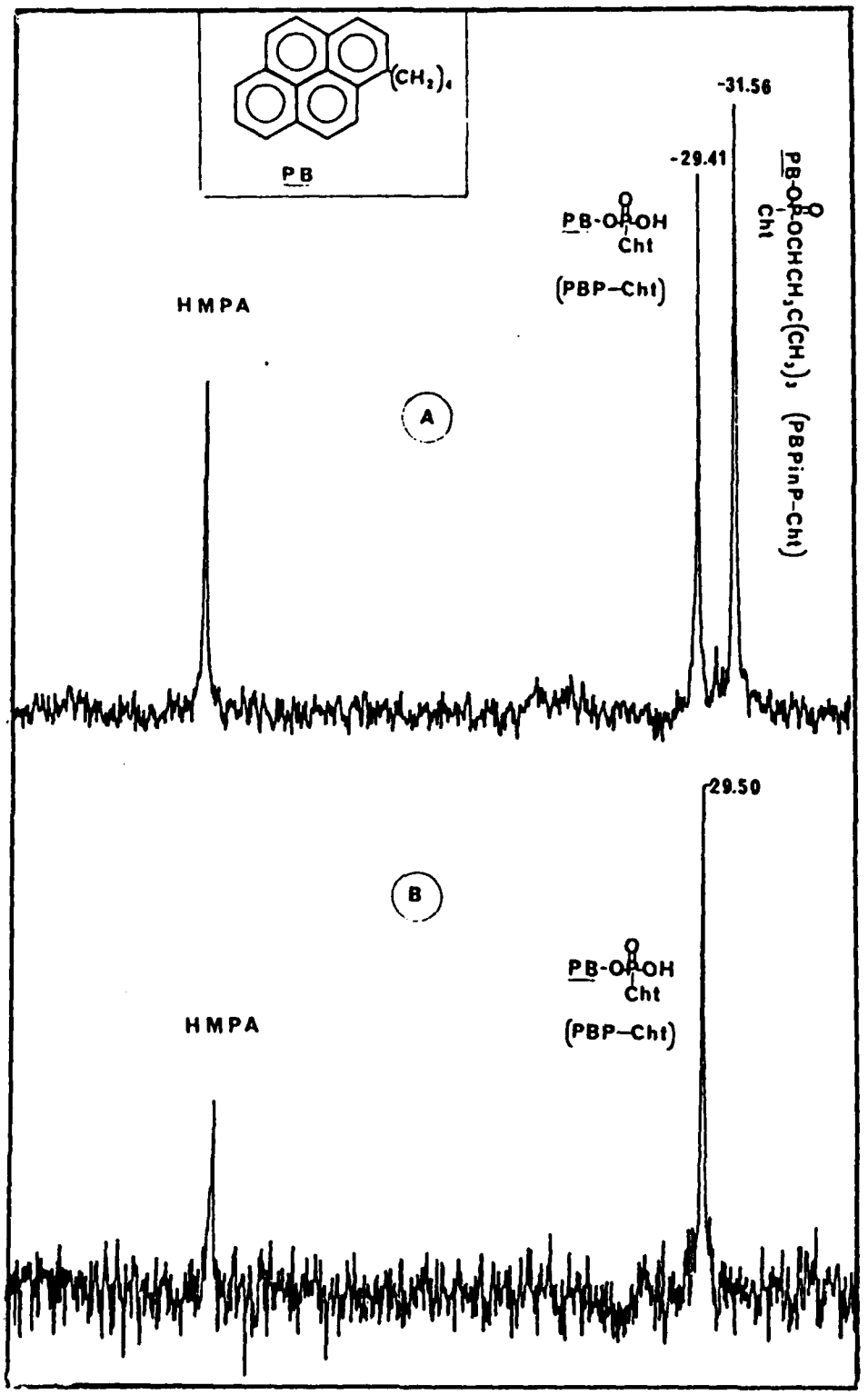


Fig. 22: $^{31}$P-nmr spectra of OP-Cht conjugates after denaturation with 6 M guanidine·HCl.
A: Mixture of aged and non-aged PBPinP-Cht obtained from PBPinPC (11).
B: Aged PBP-Cht obtained from PB(pNP)PC (9).
Negative signs indicate an upfield chemical shift relative to HMPA.

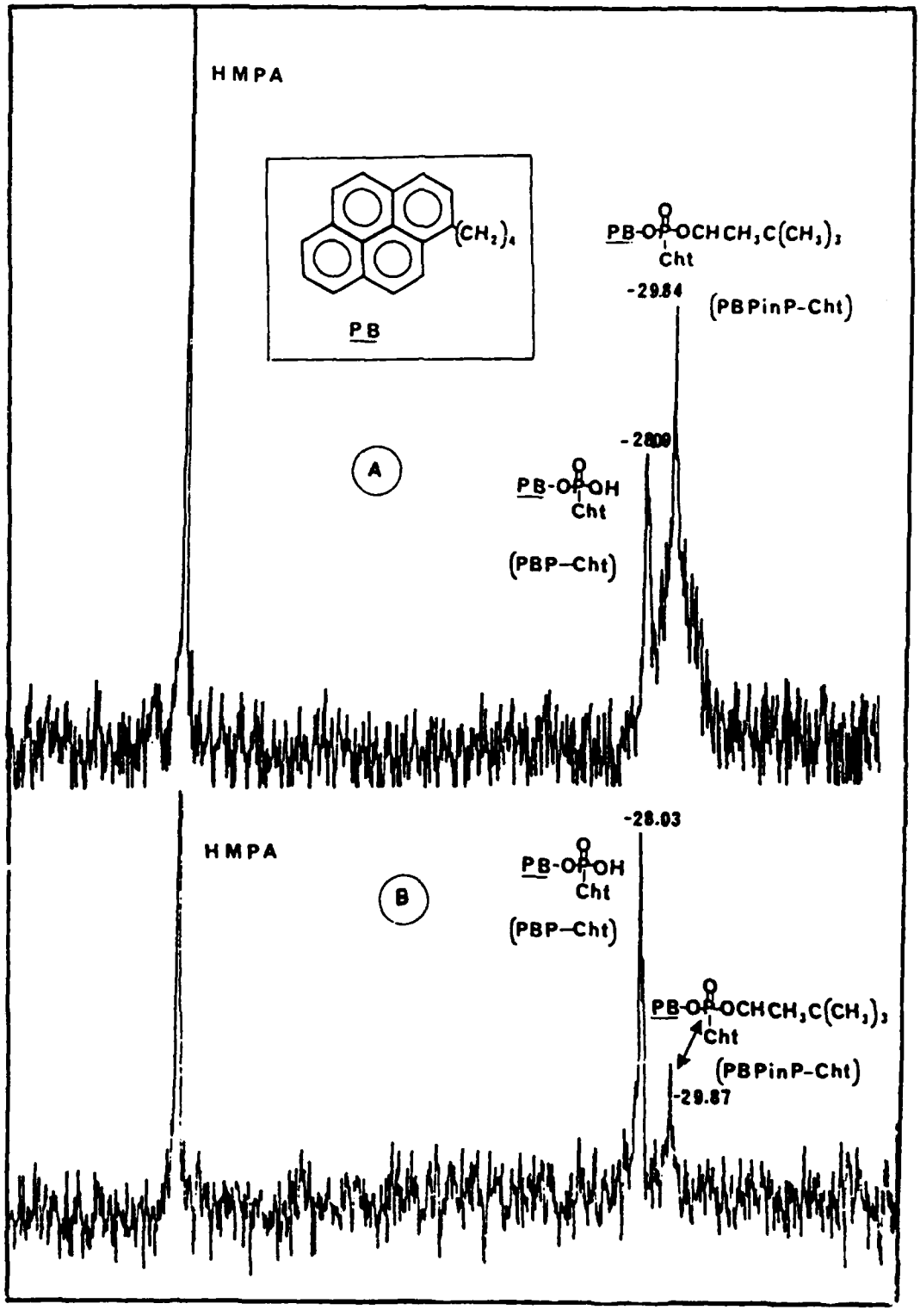


Fig. 23: $^{31}$P-nmr spectra of PBPinP-Cht.
A. Dialyzed for 24 hrs at pH 4.0.
B. Dialyzed for 48 hrs at pH 3.0.
Negative signs indicate an upfield chemical shift relative to HMPA.

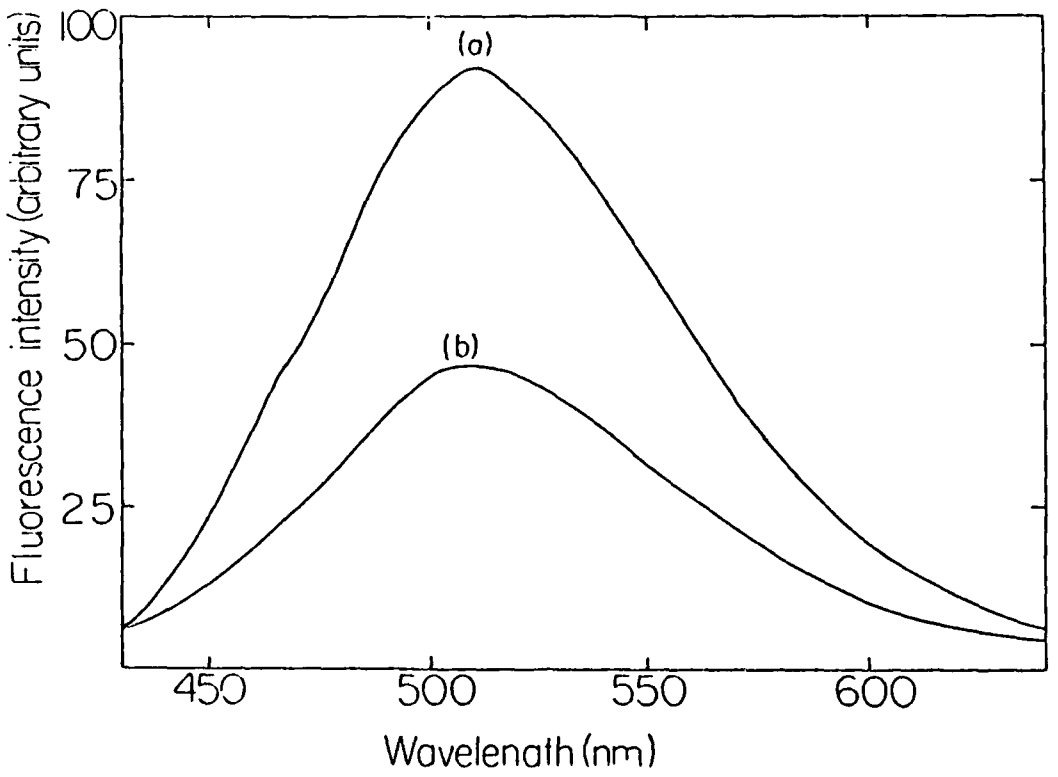


Fig. 24: Fluorescence spectra of DAEP-AChE (a) and of DAP-AChE (b) in 0.1 M NaCl-0.01 M phosphate, pH 7.0. The concentration of the conjugates was 0.3 mg/ml and the excitation wavelength was 345 nm.

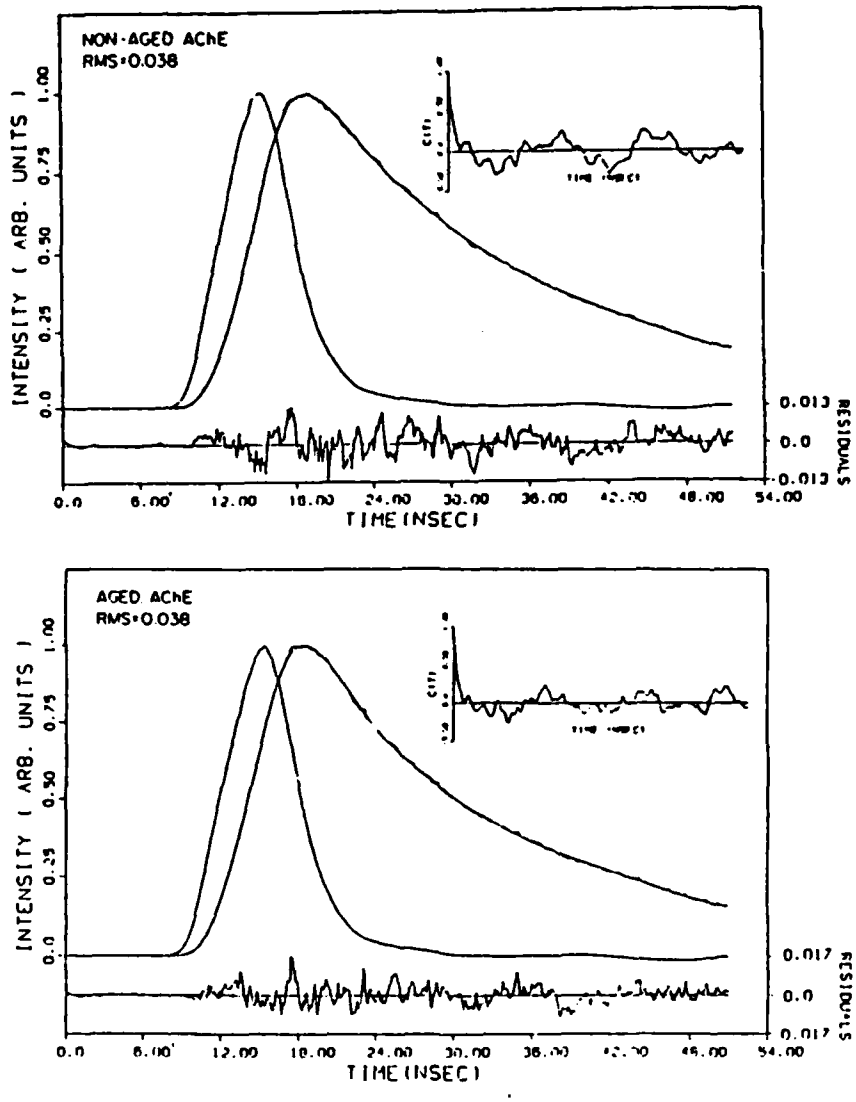


Fig. 25: Fluorescence decay of DAEP-AChE (non-aged) and of DAP-AChE (aged) in 0.1 M NaCl-0.01 M phosphate, pH 7.0. The concentration of the OP conjugates was ca. 0.02 mg/ml. The decay parameters obtained for the non-aged conjugate are: $\tau_1$=19.9±0.2 nsec, $\tau_2$=3.3±0.1 nsec, $\alpha_1$=0.166±0.002, $\alpha_2$=0.086±0.002; and those obtained for the corresponding aged conjugate are: $\tau_1$=19.5±0.2 nsec, $\tau_2$=3.1±0.1 nsec, $\alpha_1$=0.146±0.002, $\alpha_2$=0.143±0.001. The traces of the deviations between the theoretical and experimental decay curves are shown below each curve, and the autocorrelation functions of the deviations are shown in the inset at the upper right. $\lambda_{ex}$=315 nm and $\lambda_{em}$ > 370 nm.

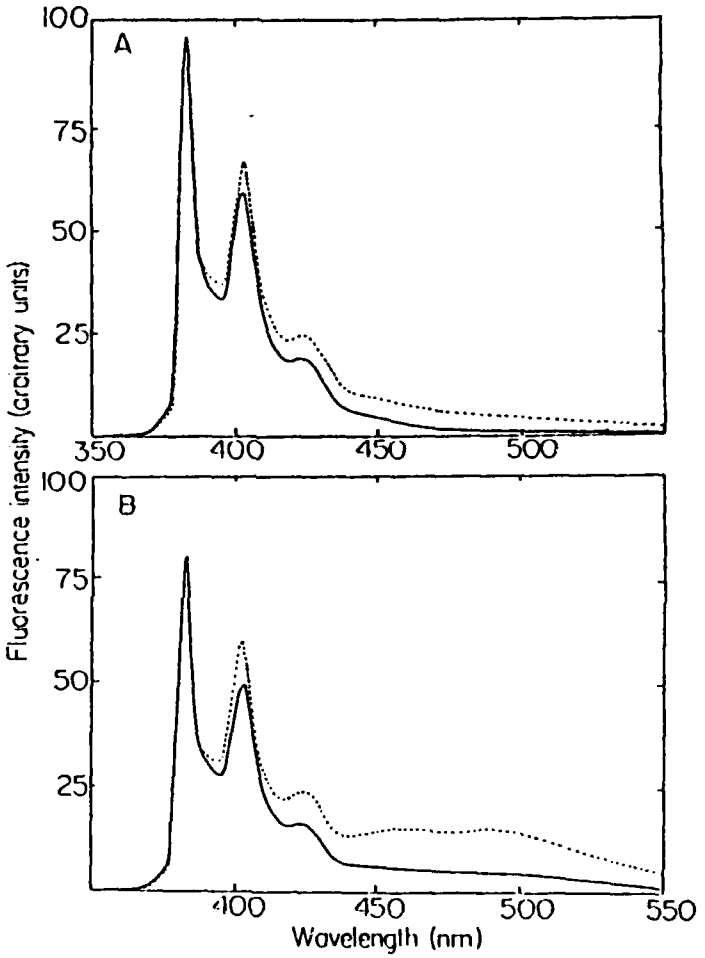


Fig. 26: Fluorescence spectra of PBEP-Cht (prepared from PBEPF, A) and PBP-Cht (prepared from PBPDC, B) at two different concentrations. —— , 0.025 mg/ml ---, 1.0 mg/ml. The spectra were recorded in 0.1 M NaCl-0.01 M phosphate, pH 7.0, and the excitation wavelength was 345 nm. The spectrum of each conjugate is normalized at the peak to the intensity of the more dilute sample, so as to facilitate comparison.

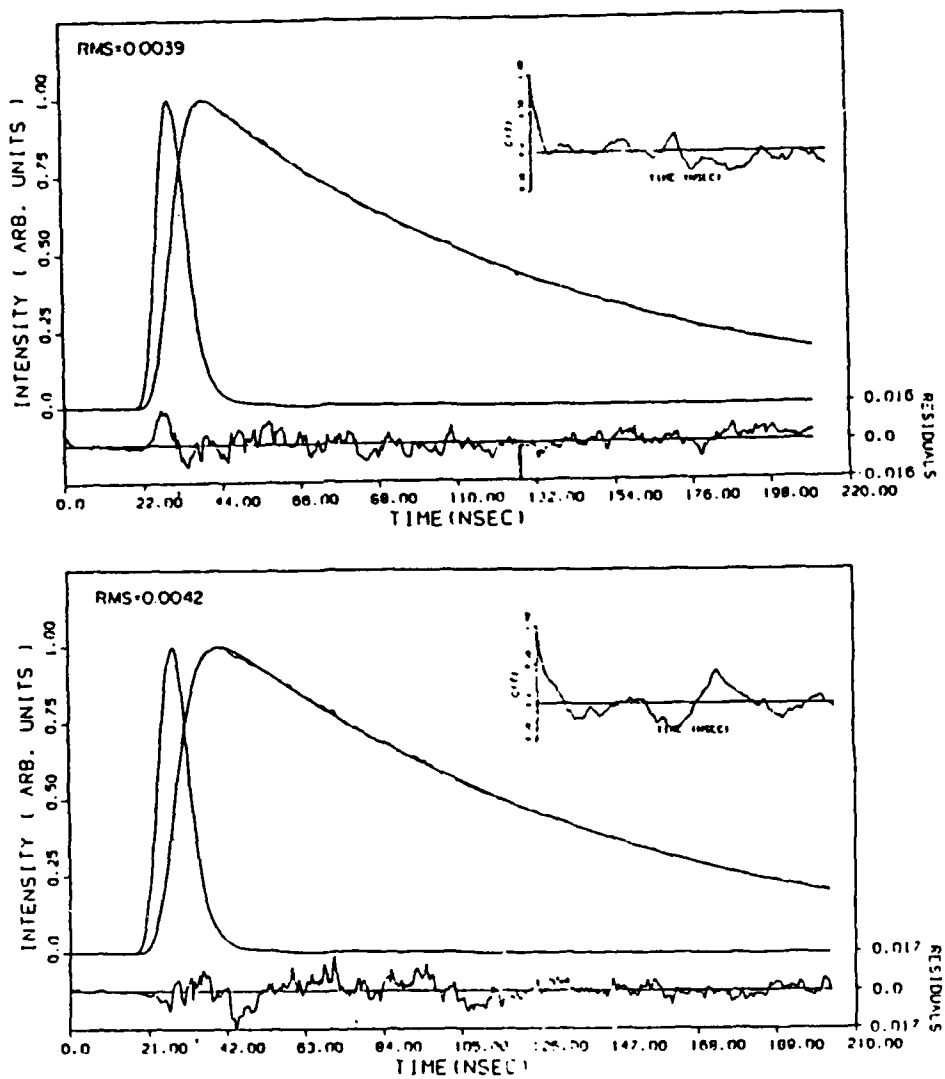


Fig. 27: Fluorescence decay of PBEP-Cht (prepared from PBEPF) in 0.1 M NaCl-0.01 M phosphate, pH 7.0. Top: At a concentration of 0.025 mg/ml, $\lambda_{ex}$=315 nm, $\lambda_{em}$ > 370 nm. The decay parameters obtained are: $\tau_1$=98.6±0.4 nsec, $\tau_2$=6.2±0.6 nsec, $\alpha_1$=0.105±0.001, $\alpha_2$=0.018± 0.001. Bottom: At a concentration of 0.6 mg/ml, $\lambda_{ex}$=315 nm, $\lambda_{em}$ > 500 nm. The decay parameters obtained are: $\tau_1$=99.9±0.3 nsec, $\tau_2$=3.1±0.4 nsec, $\alpha_1$=0.114±0.001 nsec, $\alpha_2$=(-0.028)±0.003. The traces of the deviations between the theoretical and experimental decay curves are shown below each curve, and the autocorrelation functions of the deviations are shown in the inset at the upper right.

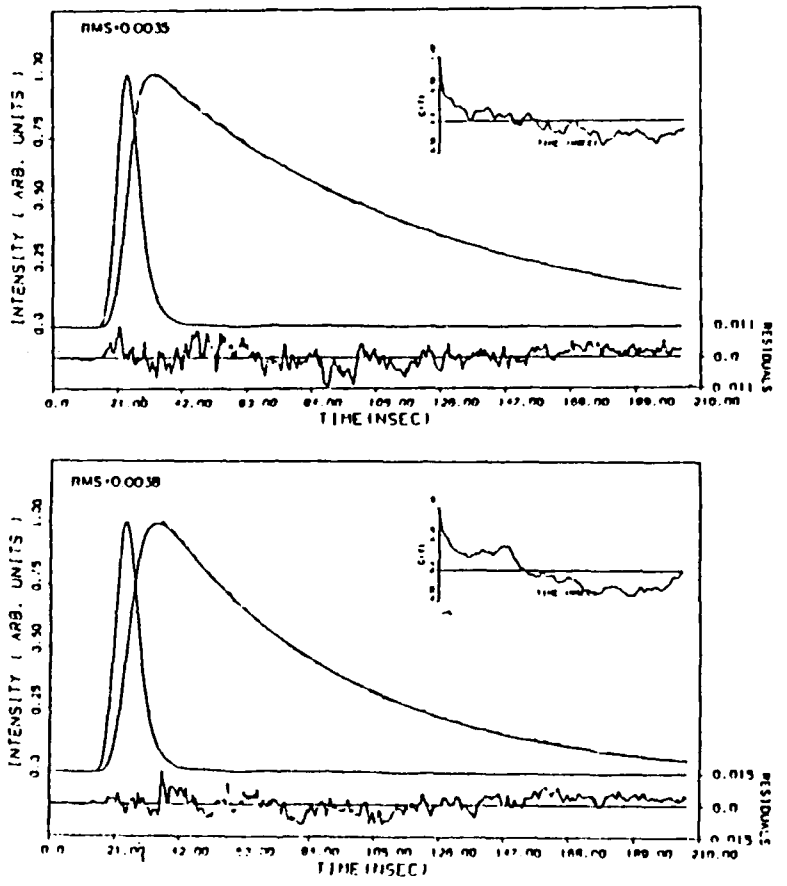


Fig. 28: Fluorescence decay of PBP-Cht (prepared from PBPDC) in 0.1 M NaCl-0.01 M phosphate, pH 7.0. Top: At a concentration of 0.025 mg/ml, $\lambda_{ex}$=315 nm, $\lambda_{em}$ > 370 nm. The decay parameters obtained are: $\tau_1$=87.7±0.3 nsec, $\tau_2$=6.1±0.5 nsec, $\alpha_1$=0.116± 0.001, $\alpha_2$=0.023± 0.001. Bottom: At a concentration of 0.6 mg/ml, $\lambda_{ex}$=315 nm, $\lambda_{em}$ > 500 nm. The decay parameters obtained are: $\tau_1$=55.5±0.2 nsec, $\tau_2$=1.7±0.3 nsec, $\alpha_1$=0.129± 0.001 nsec, $\alpha_2$=(-0.043)±0.007. The traces of the deviations between the theoretical and experimental decay curves are shown below each curve, and the autocorrelation functions of the deviations are shown ir the inset at the upper right.

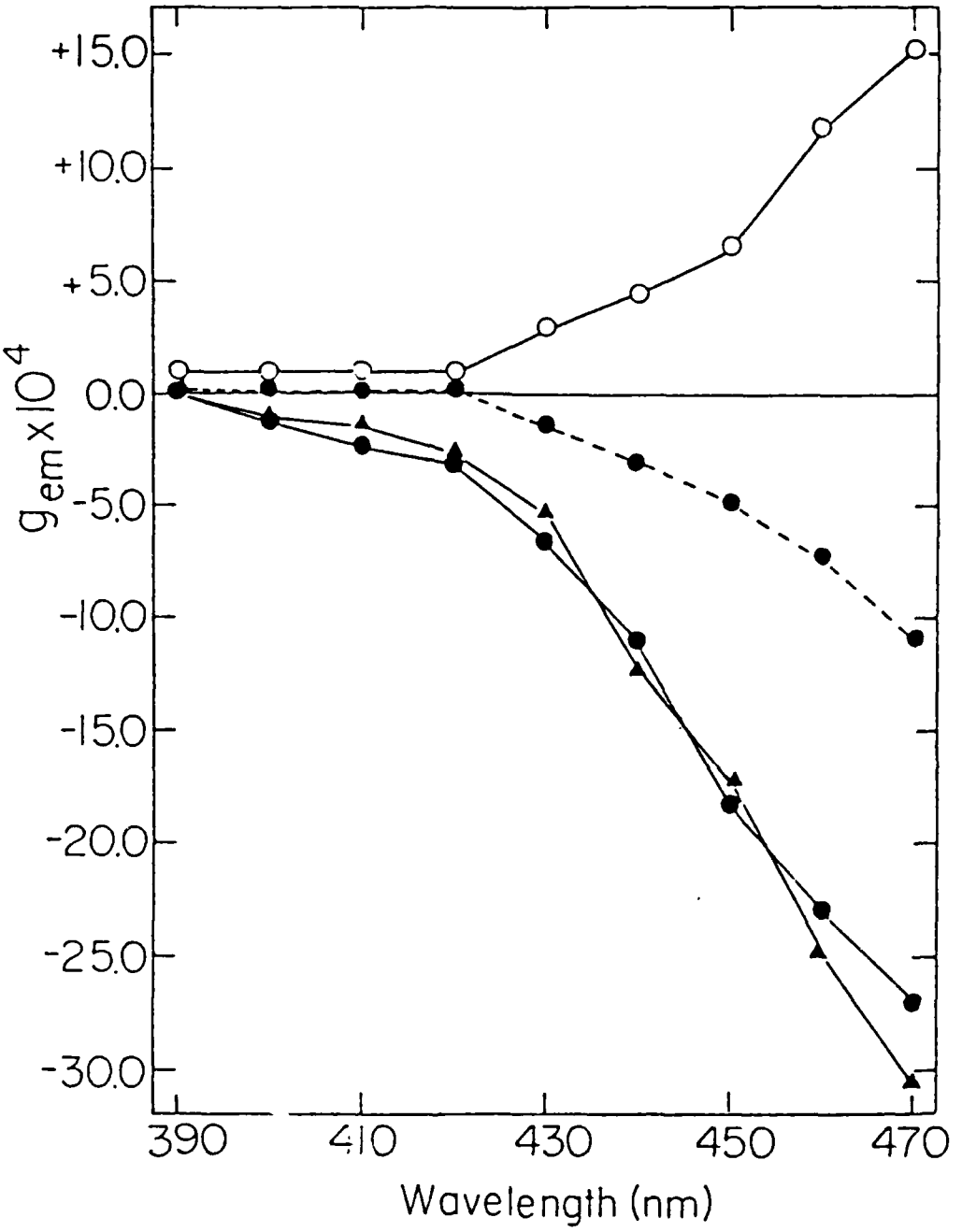


Fig. 29: Circularly polarized luminescence spectra of PBEP-Cht, prepared using PBEPF (O), and of PBP-Cht, prepared using either PBPDC (•) or PB(pNP)PC (Δ) at a concentration of either 1.0 mg/ml (——) or 0.3 mg/ml (----). The spectra were measured in 0.1 M NaCl-0.01 M phosphate, pH 7.0, and the excitation wavelength was 335 nm. The experimental error in $g_{em}$ is $\pm 0.5 \cdot 10^{-4}$.

DISTRIBUTION LIST

1 copy: Commander
US Army Medical Research
ATTN: SGRD-RMI-S
Fort Detrick, Frederick, MD 21701-5012

2 copies: Administrator
Defense Technical Information Center
ATTN: DTIC-DDA
Cameron Station
Alexandria, VA 22314

1 copy: Commandant
Academy of Health Sciences, US Army
Fort Sam Houston, TX 78234

1 copy: Dean, School of Medicine
Uniformed Services University
of the Health Sciences
4301 Jones Bridge Road
Bethesda, MD 20014